EPFL

Thèse n° 10 521

Functional characterization of *Drosophila melanogaster* immune effectors

Présentée le 26 octobre 2023

Faculté des sciences de la vie
Unité du Prof. Lemaitre
Programme doctoral en approches moléculaires du vivant

pour l'obtention du grade de Docteur ès Sciences

par

Alexia Laurie CARBONI

Acceptée sur proposition du jury

Prof. J. Lingner, président du jury
Prof. B. Lemaitre, directeur de thèse
Prof. C. Rhiner, rapporteuse
Prof. L. Neukomm, rapporteur
Dr H. Stocker, rapporteur

École
polytechnique
fédérale
de Lausanne

2023

Acknowledgements

There are many people without whom I would not have been able to complete this incredible journey. First and foremost, I would like to thank Bruno Lemaitre for giving me the opportunity to accomplish my PhD in his laboratory. You were aware that my background was in mammalian immunology, but trusted my ability to learn a completely new research field, and promised me that I would someday love *Drosophila*. Today, I can tell you that you were right. Thank you for your guidance and support. I would also like to express my gratitude to the members of my PhD jury, Prof. Joachim Lingner, Dr. Hugo Stocker, Prof. Lukas Neukomm and Prof. Christa Rhiner, for evaluating my work.

I would like to thank all my present and former colleagues of the Lemaitre Lab, who enlightened this journey at EPFL. One person without whom I would have never been able to complete this thesis is Samuel. Sam, thank you for being the best scientific mentor and personal psychotherapist I could have asked for. Thank you for always pushing me to go beyond my personal limitations and make me reach my full potential. Thank you for always being there for me when life has been more challenging. I feel privileged to have been mentored by you, but also to count you as one of my friends. Florent and Thomas, I also count you as one of the best things the Lemaitre lab has brought me. Flo, believe it or not, you always made me remember how fun science is. Either by sharing random biology facts, presenting weird papers in lab meetings, or pipetting like a crazy machine next to me. Thomas, thank you for being my daily geopolitical newspaper in the lab. Thank you for always being available to discuss and give me good advice, in my scientific projects but also in personal situations. Also, thank you both for always being here to drink beers after work. Fanny, JP and Christophe, thank you for all the technical help and advice, but also for always being here for me in the lab. Thank you, Hannah, for all the cakes, for being so funny, and for becoming a true friend. Thank you, Manon, Bianca, Alice, Mark, Li, Léna, Asya, Ana, Faustine for your precious company in the Lab. Thank you Véronique, Mercedes and Carole for your support and organization during my 4 years at UPLEM.

I would also like to thank all my friends, from Genève, Lausanne, and more exotic places, for always being here for me, supporting me through this journey, but also taking my mind off things during my free time. Thank you Juls, Cam, Ophe, Matt, Pauline, Céline, Henri, Fabrice, Kyllian, Maxence, Amael, Tiia, Anaïs, Garance, Julien, Lucyle.

Most importantly, none if this could have happened without my family. Thank you, mom, for always being my number 1 fan, for your eternal faith in me, and for your unconditional love. Thank you, Dad, for checking up on my mental health during this journey and always giving me precious advice. Thank you, Laeti, for being unconditionally proud of me.

Last but not least, I would like to thank the closest person to my heart, my life and adventure partner, Robin. Thank you for your eternal support, through the good and the bad. For your ability to turn the most difficult times into something positive and hopeful. For showing me that anything is possible as long as we do it together. I will be forever grateful to have you in my life.

Table of Contents

Summary

Drosophila melanogaster, commonly known as the "fruit fly", is a genetically tractable model organism widely used to study biological processes, notably the innate immune system. The advent of novel genome editing technologies, such as the CRISPR-Cas9 system, has allowed researchers to overcome technical challenges associated with conventional genetical approaches. This advancement has opened up novel opportunities to delete short genes and generate multiple knockouts, allowing the functional study of numerous uncharacterized genes. In this thesis, we take advantage of this biotechnological breakthrough to investigate three novel classes of immune-related genes.

The first part of this thesis focuses on the functional characterization of a family of antimicrobial peptides named the Cecropins. We generated a fly line lacking the four *Cecropin* genes, named ΔCec^{A-C}. Using the ΔCec^{A-C} deficiency alone or in combination with other antimicrobial peptide mutations, we showed that Cecropins contribute to defense against certain Gram-negative bacteria and fungi. Our work provides the first genetic demonstration of a role for Cecropins *in vivo*.

The second part of this thesis aims at characterizing the molecular function of a family of stress-induced peptides named the Turandots. We generated a mutant fly line lacking 6 *Turandots* (A,B,C,Z,M and X) and showed that this deletion increases fly susceptibility to environmental stresses due to tracheal apoptosis. The high exposure of phosphatidylserines, a negatively charged phospholipid, on the surface of tracheal cells sensitizes them to antimicrobial peptide activity. Turandots are secreted into the hemolymph of flies and subsequently bind to host cells exposing high levels of phosphatidylserines, masking them from cationic pore forming AMPs. This study provides the first demonstration of a role for Turandots in immune resilience by mitigating antimicrobial peptide toxicity to host tissues.

The third part of this PhD thesis aims at functional characterization of the role of *Drosophila* immune-induced Dnases. To investigate this, we generated a null mutant line for *Dnase II* gene. Dnase II seems to play a role in disease tolerance, as *Dnase II* mutant flies are susceptible to systemic bacterial infection, without any increase in pathogen load. Our preliminary results suggest a role for Dnase II in the cellular immune response. Hemocytes of *DNAse II* deficient larvae are unable to digest phagocytosed apoptotic DNA after injury,

leading to immune activation. This activation can be abolished by *STING* knock-out, suggesting that immunity is activated through STING following detection by a yet-unidentified cytosolic DNA sensor.

Collectively, this thesis provides new insights on key innate immune effectors of *Drosophila melanogaster*, revealing their roles in fighting pathogens and increasing resilience, by protecting the host from deleterious effects of the immune system.

Keywords

Drosophila melanogaster, innate immunity, antimicrobial peptides, immune resilience, disease tolerance, stress response, sterile inflammation

Résumé

Drosophila melanogaster, plus connue sous le nom de « mouche du vinaigre », est un organisme modèle génétiquement manipulable et largement utilisé pour étudier les processus biologiques, notamment le système immunitaire inné. L'avènement de nouvelles technologies d'édition du génome, telles que le système CRISPR-Cas9, a permis aux chercheurs de surmonter les défis techniques associés aux approches génétiques conventionnelles. Cette avancée a ouvert de nouvelles opportunités pour supprimer des gènes courts et générer simultanément des délétions de plusieurs gènes, permettant l'étude fonctionnelle de nombreux gènes jusqu'alors non caractérisés. Dans cette thèse, nous tirons parti de cette avancée biotechnologique pour étudier trois nouvelles classes de gènes impliqués dans la réponse immunitaire.

La première partie de cette thèse se concentre sur la caractérisation fonctionnelle d'une famille de peptides antimicrobiens appelés « Cecropins ». Nous avons généré une lignée de mouches dépourvue des quatre gènes codant pour les Cecropins, appelée $\Delta Cec^{A\text{-}C}$. En utilisant la déficience $\Delta Cec^{A\text{-}C}$ seule ou en combinaison avec d'autres mutations de peptides antimicrobiens, nous avons montré que les Cecropins contribuent à la défense contre certaines bactéries Gram-négatives et certains champignons. Notre travail fournit la première démonstration génétique d'un rôle pour les Cecropins *in vivo*.

La deuxième partie de cette thèse vise à caractériser la fonction moléculaire d'une famille de peptides induits par le stress, nommés les « Turandots ». Nous avons généré une lignée de mouches mutantes dépourvues de 6 Turandots (A,B,C,Z,M et X) et avons montré que cette délétion augmente la susceptibilité aux stress environnementaux en raison de l'apoptose des trachées. La forte exposition des phosphatidylsérines, un phospholipide chargé négativement, à la surface des cellules trachéales les sensibilise à la destruction par les peptides antimicrobiens. Les Turandots sont secrétés dans l'hémolymphe des mouches et s'attachent ensuite aux cellules de l'hôte qui exposent de hauts niveaux de phosphatidylserines, les masquant ainsi des peptides antimicrobiens, qui sont cationiques et qui forment des pores.

Cette étude démontre pour la première fois que les Turandots jouent un rôle dans la résilience immunitaire, ceci en atténuant la toxicité des peptides antimicrobiens contre les tissus de l'hôte.

La troisième partie de cette thèse de doctorat vise à caractériser fonctionnellement le rôle des Dnases induites par le système immunitaire de la drosophile. Pour ce faire, nous avons généré une lignée de mutants nuls pour le gène *Dnase II*. La Dnase II semble jouer un rôle dans la tolérance à la maladie, car les mouches mutantes Dnase II sont sensibles à l'infection systémique bactérienne sans avoir d'augmentation de charge pathogène. Nos résultats préliminaires suggèrent un rôle de la Dnase II dans la réponse immunitaire cellulaire. Les cellules sanguines de larves déficientes en *Dnase II* montrent une incapacité à digérer les corps apoptotiques phagocytés après une blessure, ce qui entraîne une activation immunitaire. Cette immunité activée peut être abolie par la délétion du gène STING, ce qui suggère qu'il existe une détection de l'ADN par un senseur cytosolique encore non-identifié.

En résumé, cette thèse offre de nouvelles perspectives sur les effecteurs clés de l'immunité innée chez la Drosophile, révélant leurs rôles dans la défense contre les pathogènes et dans l'augmentation de la résilience, ceci en protégeant l'hôte contre les effets délétères du système immunitaire.

Mots clés

Drosophila melanogaster, immunité innée, peptides antimicrobiens, résilience immunitaire, tolérance à la maladie, réponse au stress, inflammation stérile

List of Figures

Chapter 1: Introduction

Drosophila melanogaster has been extensively used as a model organism to study innate immunity. Its genetic tractability and the use of powerful genetic resources have enabled researchers to selectively manipulate gene expression, contributing to pioneer discoveries in the comprehension of innate immune mechanisms. In Chapter 1, we review key immune concepts in Drosophila melanogaster and their underlying molecular mechanisms.

1.1. Drosophila melanogaster defense mechanisms

1.1.1. Behavioral immunity

Drosophila melanogaster live in a microbe-rich environment. As mounting an immune response against pathogens is costly, the first line of defense against microbes is characterized by proactive behavioral mechanisms which aim to inhibit contact with pathogens in the first place. As a first mechanism, grooming allows *Drosophila* to remove dust particles, but also harmful environmental pathogens (Szebenyi 1969). Antennal cleaning can maintain acute olfactory senses responsible for protective functions, such as sensing danger (Böröczky *et al.* 2013). A recent study showed that *Drosophila melanogaster* cannot innately avoid contaminated food. However, *Drosophila* is able to adapt its feeding behavior after initial ingestion of pathogens, in order to avoid re-ingestion of harmful food (Kobler *et al.* 2020). Novel findings also suggest that the peptidoglycan recognition protein LB (*PGRP-LB)*, expressed in bitter gustatory neurons of the proboscis, senses bacteria-derived peptidoglycans and triggers behavioral changes (Masuzzo *et al.* 2022). Finally, *Drosophila* oral infection with *Pseudomonas entomophila* has been shown to induce a food uptake blockage in the host, which could also represent a physiological adaptation to counteract infection (Vodovar *et al.* 2005).

1.1.2. Immune Resistance

Disease avoidance behaviors are not always sufficient to resist pathogens. Therefore, *Drosophila melanogaster* has the ability to mount an immune response against microbes in order to resist infection. In contrast with vertebrates, which developed a second line of

defense called the “adaptative immune system” during evolution, insects only have an innate immune system. The innate immune system is the first line of defense against pathogens, and relies on different mechanisms from adaptive immunity. Firstly, it prevents physical entry of pathogens into the body cavity with epithelial barriers, such as the cuticle and epidermis of the tracheas, gastrointestinal tract and genital organs (Davis and Engström 2012). If pathogens manage to overcome epithelial barriers and enter the body cavity, the innate immune response relies on the detection of Pathogen-Associated Molecular Patterns (PAMPs) present on microbes, which are recognized by specific host Pattern Recognition Receptors (PRRs) (Lemaitre and Hoffmann 2007). Molecular patterns are motifs which are conserved and specific to microbes, which allow the distinction between self and infectious non-self (Janeway and Medzhitov 2002). They include bacterial peptidoglycan and lipopolysaccharide, fungal β-glucans and viral nucleic acids. This recognition then initiates activation of downstream signaling pathways in the host, mounting an immune response to fight the detected pathogen. Altogether, immune resistance is defined as the ability of the immune system to respond and decrease/eliminate a pathogen burden present in an infected host. However, these immunological processes can be deleterious for the host, as they are metabolically costly and tissue-damaging (Soares *et al.* 2017). Therefore, another defense mechanism, called “disease tolerance”, aims at maintaining host health while having a neutral (or even positive) effect on pathogen virulence (McCarville and Ayres 2018).

1.1.3. Disease Tolerance

Immune resistance always works in tandem with disease tolerance. This defense mechanism represents the ability of an organism to limit detrimental effects to homeostatic functions and host structures (Caldwell *et al.* 1958) that comes with or follows an infection, in order to maintain host health without interfering with pathogen load (Soares *et al.* 2017). This defense mechanism is usually triggered by specific sensors which monitor homeostatic parameters such as the osmolarity, oxygen concentration, pH, temperature and circulating metabolites. When these physiological parameters change beyond optimal levels, these sensors activate downstream stress responses to signal disrupted homeostasis. One very well characterized stress response to exposure to abnormally high temperature, the heat shock response, was been discovered in *Drosophila melanogaster* (Ritossa 1962). This study led to the

identification of Heat Shock Proteins (HSPs), which are transcriptionally induced by a heat stress (Ritossa 1996), but also by other stresses such as cold (Matz *et al.* 1995), UV exposure (Cao *et al.* 1999), and infection (Bolhassani and Agi 2019). They are characterized by the ability to stabilize newly formed proteins and ensure proper folding of proteins in cells damaged by stress. Infection leads to the accumulation of toxic and damaging molecules such as Reactive Oxygen Species (ROS), which are essential to fight infection but also cause tissue damage and dysfunction (Lambeth and Neish 2014). Therefore, organisms have evolved several detoxification mechanisms to reduce ROS (D'Autréaux and Toledano 2007), such as the production of antioxidants. The presence of ROS also acts on specific macromolecules which are particularly vulnerable, such as lipids, leading to the accumulation of inflammatory oxidized lipids (Ayala *et al.* 2014). Therefore, the fruit fly has evolved a detoxification mechanism mediated by the lipid binding protein Materazzi, which flushes free lipids from circulation into secretory organs, the Malpighian tubules, to protect host tissues during the immune response (Li *et al.* 2020).

Another stress response mechanism relies on the molecular activation of the JAK/STAT pathway in response to various stresses, which induces the production of stress response proteins. One famous family of stress-induced proteins are the Turandots, which act as readouts for activation of the JAK/STAT pathway (Agaisse and Perrimon 2004). However, their molecular function remains unknown.

In response to stress, organisms undergo metabolic adaptations in order to adapt physiologically and ensure survival. One key regulator of the metabolic stress response is the conserved transcription factor Forkhead Box-O (*FOXO*). Studies have described the importance of FOXO in regulating metabolic genes to maintain homeostasis in response to environmental stressors (Dionne *et al.* 2006; Karpac *et al.* 2011; Borch Jensen *et al.* 2017).

1.1.4. Trade-off

In biology, the concept of a trade-off defines the process through which a trait increases in fitness at the expense of decrease in fitness in another trait (Garland 2014). The interconnection between immune resistance and disease tolerance can be defined as a trade-off, as an organism's investment in one usually comes at the expense of the other (**Fig.1.1.**) (Råberg *et al.* 2007). Investment in immune resistance is essential in eliminating pathogens,

but it is a process which is costly in terms of energy and tissue damage. In contrast, investment in disease tolerance is necessary to cope with consequences of the infection itself and the immune response, which maintains an overall healthy state of the organism. Usually, the trade-off shifts over the course of an infection from immune resistance to disease tolerance. In the early stages of infection, a strong investment in mounting an immune response is essential to prevent pathogen spread. The resources then shift towards disease tolerance to promote tissue repair and organism recovery.

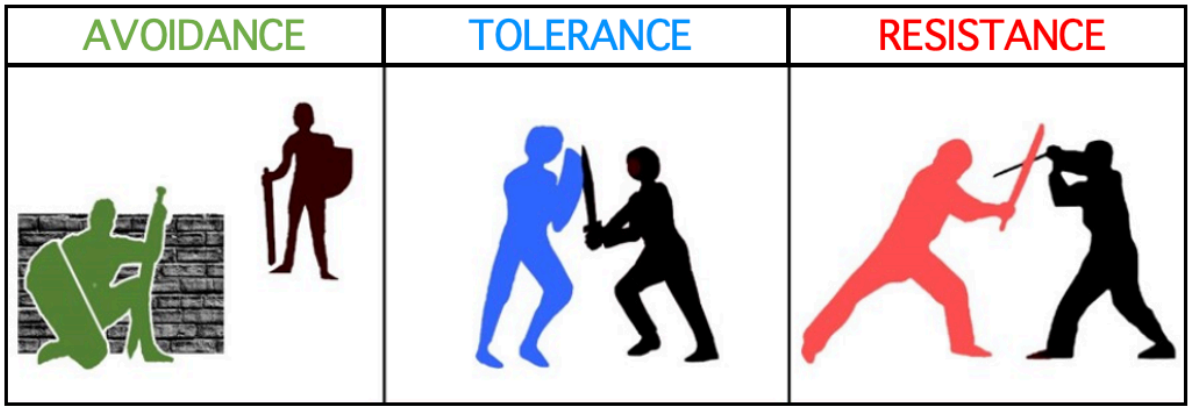

Figure 1.1. : The three complementary defense mechanisms shaping the innate immune response. First avoidance, which limits exposure to pathogens, relies on behaviours to avoid diseased animals and contaminated food. Second, tolerance which limits damage caused by the infection relies on the protection of tissues and damage repair. Finally resistance, which limits the number of pathogens, relies on the activation of immune responses to eliminate pathogens (adapted from (Sheldon *et al.* 2020))

1.2. Overview of the *Drosophila melanogaster* immune response

1.2.1. The epithelial immune response

1.2.1.1. Physical barriers and local AMP expression

Physical barriers are the first fundamental component of the *Drosophila* innate immune system. They represent the very first line of defense against infectious agents as they provide an immediate, nonspecific defense mechanism. First, they are essential in preventing the invasion and spread of pathogens inside the body cavity. *Drosophila melanogaster* possesses

various physical barriers essential to prevent pathogen invasion. First, the outer cuticle, which is composed of chitin, lipids and proteins, provides an impermeable and robust barrier for microorganisms (Chihara *et al.* 1982). Secondly, some internal tissues, such as the gastro-intestinal tract or the respiratory system, are also exposed to external environment but are not always covered by cuticle. Therefore, these tissues are protected by additional defensive barriers. For example, the *Drosophila* midgut lumen is protected by a chitinous barrier named the peritrophic matrix. Underneath, a secreted carbohydrate-rich mucus layer provides an additional protective barrier (Capo *et al.* 2019). This secreted mucus is composed of mucins, which are glycoproteins with potent anti-bacterial properties (Johansson *et al.* 2011). The *Drosophila* respiratory system represents another potential entry route for pathogens. It is composed of a network of epithelial tubes, the tracheae, which ramifies throughout the body cavity (Ghabrial *et al.* 2003). The tracheal system is made of an epithelial monolayer that comprises primary, secondary and tertiary branches (Wagner *et al.* 2008), and allows transport of gases (supply of oxygen, elimination of carbon dioxide) between the external environment and the tissues. This epithelium needs to ensure its role in gas transportation and cannot bear additional layers of protection, and is therefore an entry route for pathogens. Transcriptional profiling of tracheae has uncovered significant expression of antimicrobial genes, indicating local activation of an effective defense mechanism against microbial invasion (Basset *et al.* 2000; Tzou *et al.* 2000; Gendrin *et al.* 2013). This local antimicrobial expression is both constitutive and inducible. Several antimicrobial peptide genes are expressed in a constitutive manner in specific tissues, meaning that their expression is not regulated by the two central NF-κB pathways, but by tissue-specific transcription factors (Lemaitre and Hoffmann 2007). Indeed, a pioneer study using a GFP reporter gene revealed that *Drosomycin* is constitutively expressed in several epithelial tissues such as the respiratory and digestive tracts (Ferrandon *et al.* 1998). Another form of local antimicrobial expression is inducible, meaning that it is triggered in response to pathogen exposure. Local expression of AMPs induced after infection in different tissues has been demonstrated, such as *Drosomycin* and *Drosocin* in the tracheas, or *Diptericin* and *Attacin* in the midgut (Tzou *et al.* 2000).

1.2.1.2. Reactive Oxygen Species (ROS)

The epithelial immune response involves an additional mechanism: the local generation of Reactive Oxygen Species (ROS). When pathogens are detected in the gut, the epithelium

rapidly produces significant amounts of ROS to directly eliminate microbes. These ROS primarily originate from two enzymes: Dual Oxidase (Duox), responsible for generating hydrogen peroxide (H2O2) and hypochlorous acid (HOCl), and NADPH oxidase (Nox), which specifically produces H2O2 (Ha *et al.* 2005; Jones *et al.* 2013; Iatsenko *et al.* 2018). Knocking down *Duox* has been shown to increase the susceptibility of flies to oral infection with *Pectobacterium carotovorum carotovorum 15 (Ecc15)*, and was associated with an elevated bacterial load (Benguettat *et al.* 2018). While ROS production is vital for combating infection, excessive ROS levels can be detrimental to the host. For example, overactivation of *Duox* or *Nox* can cause severe damage to the gut epithelium and lead to dysbiosis. Therefore, excessive ROS production is counteracted by specific catalases (Radyuk *et al.* 2009; Lee *et al.* 2009). Overall, maintaining a balanced redox state is crucial for controlling both pathogen invasion and minimizing host tissue damage.

1.2.2. The humoral immune response

Upon systemic infection, the fat body, an organ analogous to the mammalian liver, synthesizes and secretes significant quantities of peptides and proteins into the hemolymph (Uttenweiler-Joseph *et al.* 1998; Liu *et al.* 2006). This arm of the innate immune response is referred to as the humoral immune response, as it relies on the secretion of effectors into the hemolymph. These molecules released into the hemolymph play a crucial role in host defense against infection. They can directly combat microbes through antimicrobial activity, indirectly limit pathogen growth by sequestering nutrients, fulfill the host's metabolic requirements to withstand the infection, or promote disease tolerance (Lemaitre and Hoffmann 2007)

1.2.2.1. Host defense peptides

Drosophila immune effectors refer to molecules that are synthesized in response to systemic infection, and subsequently released into the circulation, in order to cope with the infection. Host defense peptides will be addressed in detail in Chapter 1.3.3.

1.2.2.2. Iron sequestration

Nutritional immunity defines the process by which an organism sequesters and restricts nutrient minerals in order to limit pathogen proliferation during infection. As pathogens

require iron for fundamental physiological processes such as cell replication, respiration and metabolism (Zughaier and Cornelis 2018), hosts have developed strategies to sequester free iron from circulation in order to limit pathogen growth. Iron sequestration relies on the presence iron-binding proteins, the most prominent ones being transferrins. A recent study showed that Transferrin 1 (Tsf1) plays a key role in *Drosophila* host defense (Iatsenko *et al.* 2020), by relocating free iron from the hemolymph into the fat body after infection. Using a genetic approach, this study shows that flies mutated for *Tsf1* have increased susceptibility to bacterial and fungal infection, supporting a role for transferrins in innate immunity.

1.2.3. The cellular immune response

The third component of *Drosophila* innate immunity is a cell-mediated defense mechanism. This defense mechanism involves the action of circulating immune cells called hemocytes. Hemocytes recognize and eliminate invading pathogens and parasites within the organism through several mechanisms (Meister and Lagueux 2003; Gold and Brückner 2015). One such mechanism is phagocytosis, where individual hemocytes engulf and digest microbes (Elrod-Erickson *et al.* 2000). Additionally, multiple hemocytes can aggregate together to trap a large number of bacteria in a process known as nodulation (Satyavathi *et al.* 2014). In the case of larger targets like parasites, hemocytes can bind and form a protective capsule around them, a process known as encapsulation (Russo *et al.* 1996). Another key process in the cellular response is melanization, which plays a central role in defense against a broad range of pathogens.

1.2.3.1. *Drosophila* blood cells (hemocytes)

The blood cell population of *Drosophila* can be categorized into three distinct classes: plasmatocytes (I), crystal cells (II), and lamellocytes (III). Plasmatocytes constitute the majority, accounting for 90-95% of the total hemocyte population across all developmental stages (Lanot *et al.* 2001). Functionally analogous to mammalian macrophages, their primary role is to detect and phagocyte pathogens and self dead cells. Crystal cells make up the remaining 5-10% of the blood cell population. These circulating cells are non-phagocytic, but are responsible for biosynthesis and deposition of melanin (Binggeli *et al.* 2014). Melanin is produced by prophenoloxidase (PPO) enzymes. The *Drosophila* genome encodes three *PPOs*:

PPO1, PPO2, and *PPO3*. PPO1 and PPO2 are stored in crystal cells in an inactive crystalline state (Dudzic *et al.* 2019). Upon cellular release, they are activated through a proteolytic cascade mediated by serine proteases. Melanization is a crucial mechanism in *Drosophila* as it is involved in several processes, such as effective wound healing, microorganism sequestration at the site of injury, and parasite encapsulation (Vlisidou and Wood 2015). It also contributes to pathogen elimination by producing toxic intermediates like peroxide and nitric oxide (Foley and O'Farrell 2003; Carton *et al.* 2008; Nappi *et al.* 2009). The third class of blood cells, lamellocytes, are large cells exclusive to the larval stage that are usually absent when larvae are healthy. However, a large number of lamellocytes are induced upon wasp parasitization in order to encapsulate and eliminate wasp eggs (Carton *et al.* 2008).

1.2.3.2. Phagocytosis

Phagocytosis is a conserved cellular process by which a cell engulfs large particles (> 0.5 um). This process leads to the formation of an intracellular plasma membrane derived vesicle, the phagosome (Melcarne *et al.* 2019b). The first description of a phagocytic event was reported more than 150 years ago by the zoologist Ernst Haeckel, when he discovered that blood cells of a marine invertebrate were able to ingest ink particles. This demonstration was a landmark in cellular immunity. Cells capable of performing phagocytosis are referred to as phagocytes and are essential components of the immune system. They are able to engulf and digest invading pathogens present in circulation. Interestingly, they also are responsible for the digestion of self-particles such as apoptotic or necrotic cells, making them key regulators of tissue homeostasis. In *Drosophila*, professional phagocytes are known as "plasmatocytes", and represent the majority of circulating blood cells. Plasmatocytes are characterized by the presence of phagocytic receptors exposed on the extracellular surface of the cell membrane. These receptors recognize and bind to specific motifs on the surface of pathogens and dead cells, such as lipopolysaccharides (LPS) on bacteria, or phosphatidylserines (PS) on apoptotic cells. Upon ligand binding, these phagocytic receptors engage phagocytosis by activating downstream signaling pathways. Over the past decades, a plethora of phagocytic receptors have been identified, the most described ones being the *Nimrod* family (Kocks *et al.* 2005; Chung and Kocks 2011; Melcarne *et al.* 2019a; Ramond *et al.* 2020; Petrignani *et al.* 2021).

1.2.3.3. Encapsulation

A significant proportion of insect species serve as hosts to parasitoids, which are organisms that live at the expense of their host. *Drosophila melanogaster* larvae are frequently targeted by parasitoid wasps, which lay eggs inside their body cavity and allows the wasp to develop while causing the death of the fly. Due to the large size of these foreign eggs, this infection cannot be eliminated by phagocytosis. Therefore, *Drosophila* larvae rely on “encapsulation” to fight parasitoids. When the adult female wasp injects eggs into the body cavity of *Drosophila* larvae, these eggs are recognized as foreign entities. As a response, plasmatocytes are recruited and attach to the surface of the eggs. A yet unidentified signal then triggers a subset of plasmatocytes to differentiate into lamellocytes, which are large, flat, adhesive cells. Together, they form a capsule around the parasitoid wasp egg, acting as a structural barrier between the egg and the hemolymph (insect blood) (Carton *et al.* 2008). This capsule formation is accompanied by the production of melanin and free radicals by phenoloxidases, which aid in killing the wasp egg (Binggeli *et al.* 2014). The capsule limits nutrient access from the hemolymph to the wasp and protects the host from the toxic compounds produced during this process (Nappi *et al.* 2009).

1.2.3.4. Melanization

The melanization reaction can be attributed to both the cellular and humoral immune responses. Indeed, crystal cells, a class of hemocytes, are the main actors in this process as they produce specific enzymes, the PPOs, responsible for the melanization reaction. However, these enzymes are released into circulation by rupture of the crystal cells upon infection or injury, highlighting their involvement in the humoral immune response. The melanization reaction is characterized by the rapid production of melanin through the action of phenoloxidases (POs), which catalyze the oxidation of phenols to form quinones. These quinones then polymerize to produce melanin. This melanogenesis process leads also to the production of cytotoxic intermediates such as reactive oxygen species. Therefore, it needs to be carefully regulated to avoid extensive tissue damage. To prevent this, various regulatory mechanisms have evolved to control the activation of melanization reactions. First, POs are initially produced in an inactive form called prophenoloxidases, which required proteolytic cleavage by Serine Proteases (SPs) to become active (Ross *et al.* 2003; Veillard *et al.* 2016). Additionally, specific proteins known as "Serpins" can inhibit these SPs, providing an

additional means of negatively regulating PO activation (Silverman *et al.* 2001). The deposition of melanin is involved in various processes of the innate immune response in *Drosophila*, including wound healing, encapsulation of parasitoids and immune defense against pathogens.

1.3. The three stages of the immune response

1.3.1. Recognition

The *Drosophila* immune response is always initiated by the recognition of molecular patterns, typically specific to microbes and recognized as infectious "non-self" elements by the organism. This recognition is mediated by receptors, which are able to identify these patterns in specific ways. Fungal β-glucans are recognized by the Gram-negative binding protein 3 (GNBP3) (Gottar *et al.* 2006). Lysine-type peptidoglycans, usually found in the cell walls of Gram-positive bacteria, are recognized by the peptidoglycan recognition protein SA (PGRP-SA) and GNBP1 (Gottar et al. 2002; Gobert et al. 2003; Pili-Floury et al. 2004). DAP-type peptidoglycans, present in Gram-negative bacteria but also in some Gram-positive bacteria (*Bacillus* species), are recognized by several PGRP receptors: the extracellular receptor PGRP-SD, transmembrane receptor PGRP-LC and the intracellular receptor PGRP-LE (Gottar et al. 2002). Viral nucleic acids are recognized by the intracellular protein Dicer-2 or the cytosolic sensor cGAS (Sabin et al. 2010; Takeuchi and Akira 2010; Holleufer et al. 2021). Another class of molecular patterns named Damaged-Associated Molecular Patterns (DAMPs) can also be recognized by the immune system. DAMPs, also known as "danger signals" or "alarmins", are molecules released from damaged or dying cells after trauma or infection. These can also trigger immune activation when recognized by specific receptor. One example is alpha-actinin, which is detected by an unidentified receptor and induces a Src-family kinase dependent cascade, leading to JAK/STAT activation (Srinivasan *et al.* 2016; Gordon *et al.* 2018). Finally, pathogen effectors such as fungal proteases can also cleave the *Drosophila* serine protease Persephone and directly activate immune cascades, in a process reminiscent of Effector-Triggered immunity found in plants (Ligoxygakis *et al.* 2002)

1.3.2. Signaling

1.3.2.1. The Toll Pathway

The Toll pathway is one of the two central NF-κB signaling pathways regulating *Drosophila* innate immunity **(Fig.1.2.)**. This pathway, which is also required for dorsoventral embryonic polarity, was identified for its crucial role in mounting an effective immune response specifically against fungal infection (Lemaitre et al. 1996). Many studies were conducted in the following years to understand the broad-spectrum impact and complexity of the Toll pathway. The activation of the Toll pathway begins outside of the cell. Specific microbial molecular patterns (PAMPs), such as bacterial Lysine-type peptidoglycans and fungal β-glucans, activate the PRRs PGRP-SA and GNBP3 (Pili-Floury et al. 2004; Mishima et al. 2009). This leads to the activation of Modular Serine Protease (ModSP) and the serine protease Grass, which in turn activates the serine proteases Hayan and Persephone (Gottar *et al.* 2006; Buchon *et al.* 2009). Of note, Hayan and Persephone can also directly be activated by microbial serine proteases (Dudzic et al. 2019). Hayan and Persephone cleave Spätzle-Processing Enzyme (SPE) which executes the last step of the extracellular signaling cascade by cleaving the Toll ligand Spätzle, which can then bind and activate the Toll receptor (Morisato and Anderson 1994; Jang et al. 2006). The signal is then transmitted intracellularly. The Toll receptor sequentially recruits and activates Myd88, Tube and Pelle, which allow the activation of the two NF-κB transcription factors Dif and Dorsal by destroying their negative regulator, Cactus (Hecht and Anderson 1993; Ip et al. 1993; Bergmann et al. 1996; Tauszig-Delamasure et al. 2002). This last step allows transcriptional activation of immune induced effectors. One readout commonly used for the activation of the Toll pathway is *Drosomycin*, a potent antifungal peptide strongly induced after infection.

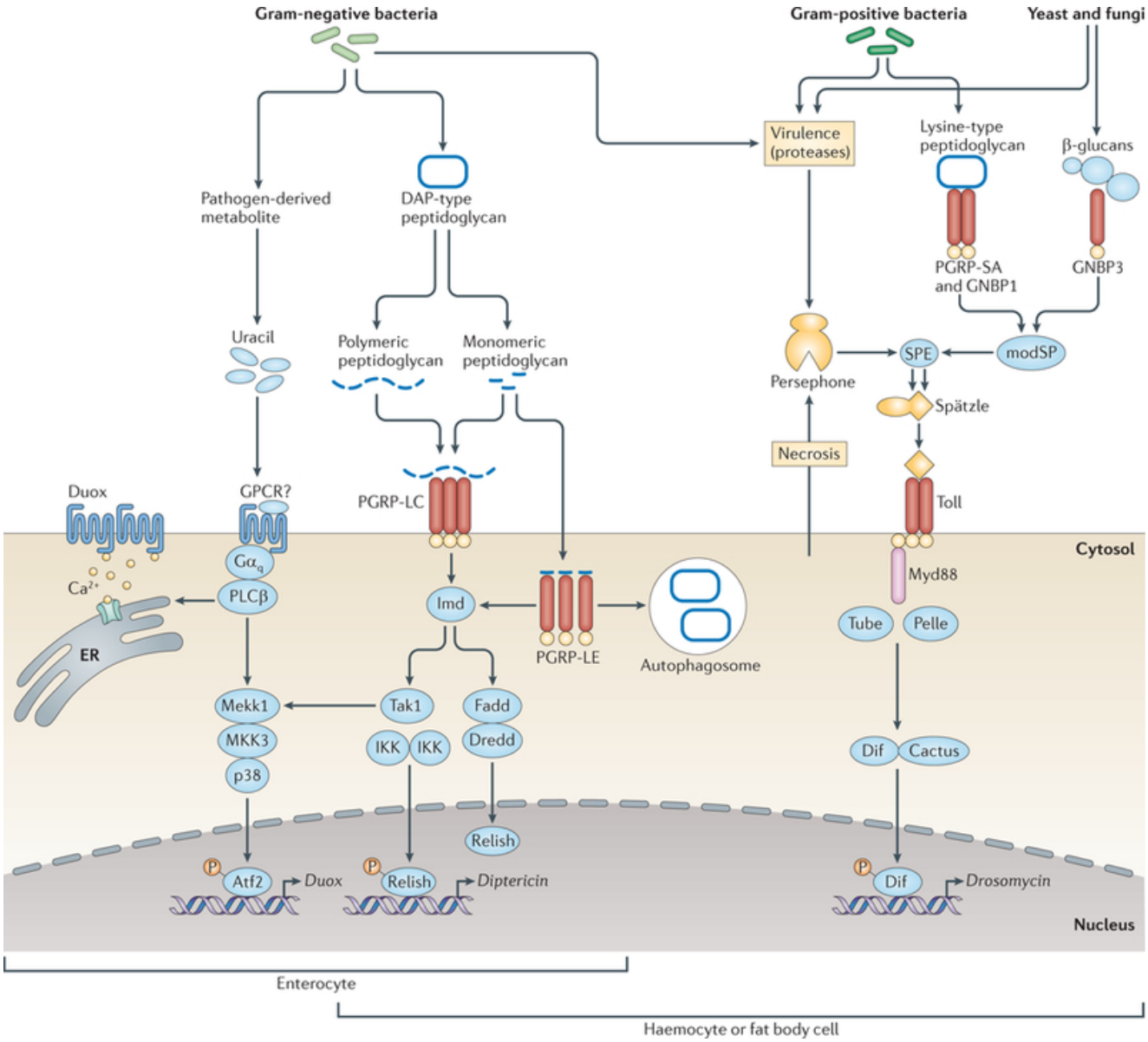

Figure 1.2.: The Imd and Toll pathways in Drosophila melanogaster.
Two major pathways are activated upon the recognition of microbial cell wall components (peptidogylcans) by peptidoglycan recognition proteins (PGRPs) or by the proteases of pathogens (Toll). This recognition triggers downstream signaling cascades leading to the transcription of antimicrobial peptides, which are secreted into the circulation (hemolymph) to eliminate pathogens (from (Buchon *et al.* 2014)).

1.3.2.2. The IMD pathway

The Imd pathway is initiated at the cell membrane, with the recognition of bacterial DAP-type peptidoglycan by transmembrane receptor PGRP-LC **(Fig.1.2.)** (Gottar et al. 2002). The signal is then transmitted intracellularly: the intracellular domain of PGRP-LC recruits the cytosolic protein Imd (Georgel et al. 2001). Imd is able to initiate a signaling cascade leading to the

cleavage and activation of the NF-κB transcription factor Relish via two signaling branches. On one side, Imd activates the Tab2/Tak1 complex, which activates the IKK complex, leading to Relish phosphorylation (Hedengren et al. 1999). On the other side, Imd recruits the adaptor protein Fas-associated death domain (FADD), which activates the caspase Death related ced-3/Nedd2-like (Dredd), which cleaves Relish (Leulier et al. 2000; Naitza et al. 2002). After cleavage and phosphorylation, Relish is able to translocate into the nucleus and activate transcription of immune-induced genes. A common readout for Imd pathway activation is the transcriptional induction of the antimicrobial peptide *Diptericin A*.

1.3.2.3. The JAK/STAT pathway

The Janus kinase/signal transducer and activator of transcription (JAK/STAT) pathway is highly conserved in evolution. In *Drosophila*, the pathway is initiated by three cytokine-like ligands named unpaired (upd), upd2 and upd3 (Myllymäki and Rämet 2014). All three upds bind to a unique receptor, Domeless (Dome), which is associated with hopscotch (hop), the single *Drosophila* JAK. The binding of upds to Dome induces receptor dimerization and activation of Hop proteins, which phosphorylate each other as well as specific tyrosine kinase residues on the cytoplasmic tail of Dome. This phosphorylation cascade allows recruitment of STAT92E proteins via their Src homology 2 (SH2) domains. At the same time, Hop can phosphorylate tyrosine residues present on STATs, inducing their dimerization and translocation into the nucleus, where they induce the transcription of target genes.

Biologically, the JAK/STAT pathway is involved in various contexts. It has been shown to play a key role in several developmental processes, such as embryogenesis and larval imaginal disc development (Bach *et al.* 2003; Lopes and Araujo 2004). The JAK/STAT pathway is also involved in the cellular and humoral immune responses. First, the main function of the cellular immune response is to ensure proper phagocytosis of pathogens and apoptotic host cells. Complex regulation maintains a homeostatic balance between hemocyte proliferation and differentiation, which requires careful control of JAK/STAT signalling levels. Regarding the humoral immune response, after an immune challenge, the cells of the fat body secrete a plethora of immune-related genes, some of which are regulated by the JAK/STAT pathway. For example, a very well-known family of stress-induced genes called the "*Turandots*" (Tot), whose expression is regulated by JAK/STAT, have been shown to be massively secreted from the fat body into the hemolymph after microbial challenge, as well as after abiotic stress

(Ekengren and Hultmark 2001). Finally, the JAK/STAT pathway has been found to contribute to the antiviral response of *Drosophila*, in combination with the Toll and Imd pathways (Dostert *et al.* 2005).

1.3.2.4. The JNK pathway

The c-Jun N-terminal Kinase (JNK) signaling pathway is an evolutionarily conserved pathway that belongs to the *mitogen-activated protein kinase* (*MAPK*) family. The JNK pathway can be initiated extracellularly by the Tumor Necrosis Factor (TNF) ligand Eiger (Egr), which binds two different TNF receptors, Grindelwald (Grnd) and Wengen (Wgn). The binding of Eiger to Grindelwald or Wengen activates Tak1, which activates hemipterous (hep), which activates the sole *Drosophila* JNK protein basket (bsk), leading to the phosphorylation of d-Fos and d-Jun (AP-1) transcription factors. This activation occurs through the phosphorylation of Serine/Threonine and Tyrosine residues (Weston and Davis 2002). Importantly, the JNK pathway also branches out from the Imd pathway at the level of Tak1, which acts in both the Imd and JNK cascades. AP-1 promotes the expression of matrix metalloproteinases MMP1/2, and the family of upd cytokines. Puckered (Puc), a JNK phosphatase, is another target gene of AP-1 that creates a negative feedback loop to control the activity of the signaling cascade in order to limit JNK activity. This complex pathway is involved in various biological processes and is induced by both endogenous and environmental stimuli (Davis 2000). In *Drosophila*, JNK has been shown to be involved in development, cell proliferation and differentiation, ROS production, wound repair, stress response, apoptosis, DNA damage and immunity (Yoshida *et al.* 2005; Shen and Liu 2006; Delaney *et al.* 2006; Arthur and Ley 2013). Today, the exact immunological function of the JNK pathway remains complex and elusive, as different studies point out heterogenous implications and roles for this signaling cascade in *Drosophila* innate immunity. For example, JNK signaling has been shown to antagonise the host immune response. Indeed, the *Drosophila* NF-κB protein Relish promotes proteasomal degradation of Tak1, which is essential for JNK activation. Thus, Tak1 degradation by Relish inhibits JNK signaling, controlling immune-induced apoptosis (Park *et al.* 2004). On the other hand, it has been shown in vitro that the JNK pathway is a key regulator of the antimicrobial peptide response, conferring an immunostimulatory role for this signaling pathway (Kallio *et al.* 2005). Other studies have pointed out the upregulation of JNK pathway target genes after infection

with entomopathogenic nematodes, suggesting another role in promoting *Drosophila* immunity (Castillo *et al.* 2013).

1.3.2.5. The cGAS/STING pathway

The ability of an organism to detect foreign DNA is an evolutionarily conserved mechanism that represents a key process of innate immunity (Morehouse *et al.* 2020). In mammals, this task is mainly operated by the cyclic GMP-AMP synthase (cGAS)-stimulator of interferon genes (*STING*) pathway. The cGAS-STING pathway has been at the center of the research in mammalian immunology for the past decade, and today is extensively characterized. This signaling cascade is initiated by the binding of the cytosolic cGAS to double stranded DNA (dsDNA), which leads to the production of 2'3' cyclic GMP-AMP (cGAMP), which then activates the endoplasmic reticulum (ER) resident second messenger STING (Ishikawa and Barber 2008; Sun *et al.* 2013). STING triggers the activation of the transcription factors IRF3 and TBK1, which promotes a strong type I interferon response, as well the induction of several inflammatory mediators (Decout *et al.* 2021). The remarkable conservation of this immune pathway from bacteria to mammals has raised interest in evaluating the relevance of the cGas-STING pathway in insects, more specifically in *Drosophila* **(Fig.1.3.)**. The *Drosophila* ortholog of human *STING* (*dmSTING*) has a conserved structural domain necessary to bind cyclic dinucleotides (CDNs), but proper binding of dmSTING to CDNs could not be observed in vitro (Kranzusch *et al.* 2015). A subsequent study showed how dmSTING can be transcriptionally induced by ZIKA virus infection through the IMD pathway (Liu *et al.* 2018). This study also defined for the first time an antiviral role for dmSTING. The same year, another study demonstrated an antimicrobial function for dmSTING against *Listeria monocytogenes* (Martin *et al.* 2018). They suggested a role in which dmSTING acts through the IMD pathway upstream of Relish, and stimulates the induction of antimicrobial peptides like *Attacin A* and *Cecropin A2*. Importantly, the same study used a different experimental approach than Kranszusch et al. (Kranzusch *et al.* 2015) to test the CDN binding activity of dmSTING *in vitro*, and were able to show that dmSTING directly binds cGAMP, c-di-AMP and c-di-GMP. Finally, a very recent and pioneering study identified cGAS-like receptors (cGLRs) in *Drosophila* using a genetic approach, and demonstrated that both cGLR1 and cGLR2 respond to viral infection by sensing foreign RNA (Holleufer *et al.* 2021; Slavik *et al.* 2021). Altogether, this recent work

on the cGAS-STING pathway in *Drosophila* uncovers the importance of a novel component of innate immune pathways in insects that must be considered going forward.

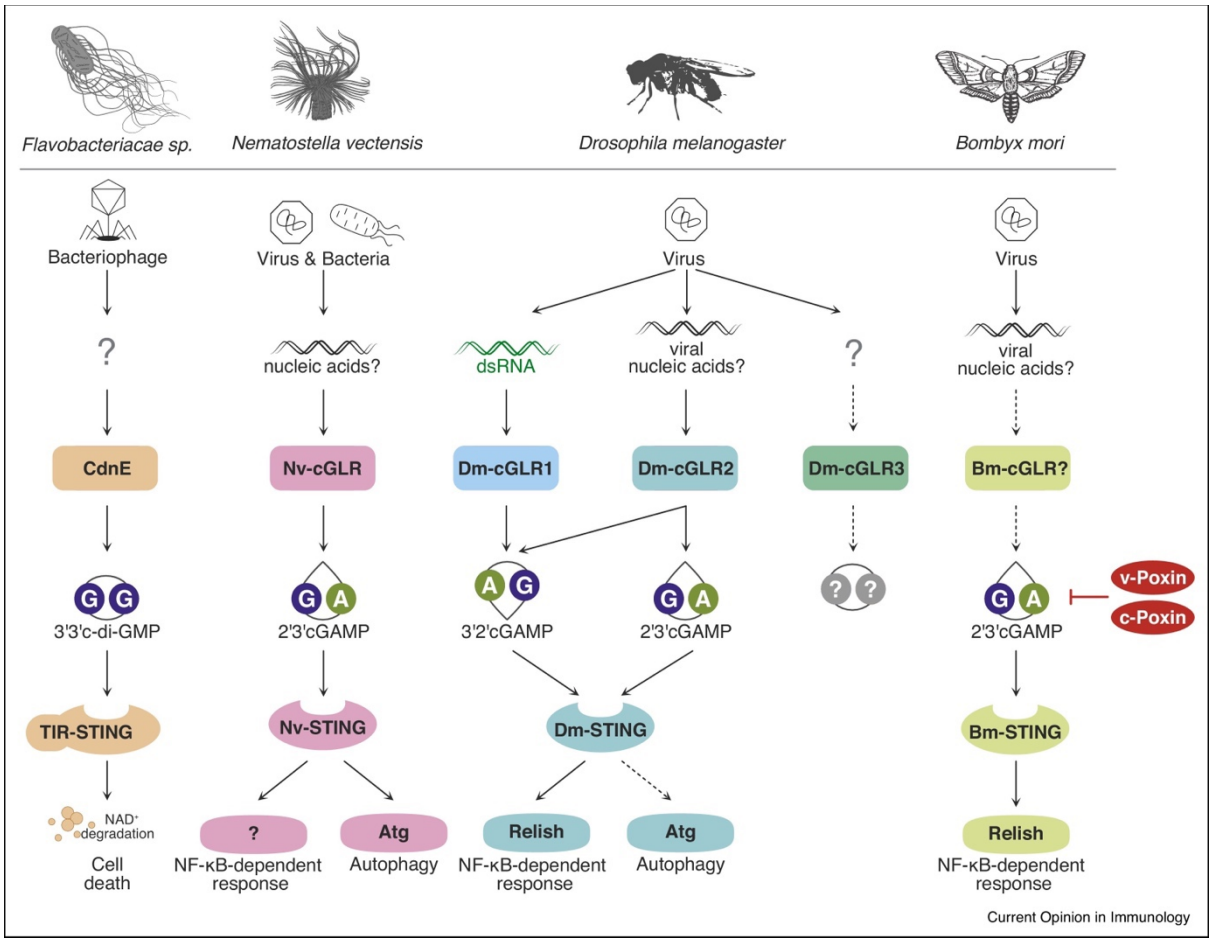

Figure 1.3. The cGAS-STING pathway in bacteria and invertebrates.

Schematic representation of the conserved and divergent elements of the cGAS-STING pathway in the bacteria *Flavobacteriacae sp*., the sea anemone *N. vectensis*, in the dipteran *D. melanogaster* and in the lepidopteran *B. mori* (from (Cai *et al.* 2022)).

1.3.3. Immune effectors

1.3.3.1. Antimicrobial peptides

Antimicrobial peptides (AMPs) are short, cationic or amphipathic peptides. They contribute to innate immune defense by directly killing invading microorganisms through various mechanisms of action (Steiner *et al.* 1981; Imler and Bulet 2005). AMPs lack enzymatic activity, but achieve their microbicidal effects by reaching concentrations into the micromolar range (Imler and Bulet 2005; Seo *et al.* 2012). The first inducible AMP to be isolated, Cecropin,

was harvested from the hemolymph of an infected moth called *Hyalophora cecropia* (Steiner *et al.* 1981). Cecropin was subsequently shown to display potent antibacterial activity *in vitro*, revealing that insects can resist infection by virulent pathogens despite lacking an adaptative immune system. This discovery was a crucial milestone in the field, particularly at a time when immunologists were characterizing the highly specific antibody immune response in mammals. The discovery of Cecropin gave rise to the identification of an array of antimicrobial peptides in insects, but also in other invertebrate and vertebrate animal models. However, as *Drosophila* relies only on innate immune mechanisms to fight infection, it became a powerful model for the study of antimicrobial peptides.

In *Drosophila*, 14 "classical" AMPs have been identified, classified in 7 different families: Cecropins, Attacins, Defensins, Diptericins, Drosomycin, Metchnikowin and Drosocin. In the last decade, novel classes of host defense peptides, such as the Bomanins, Daishos, and Baramycins have been added to the list of *Drosophila* AMPs (Clemmons *et al.* 2015; Cohen *et al.* 2020; Hanson *et al.* 2021). Upon stimuli, AMPs are massively produced by the fat body (mammalian liver analog) through the activation of Toll and Imd pathways, and secreted into the hemolymph. As explained in Chapter 2.1.1., some epithelial surfaces, such as tracheae or the gut, are also able to produce AMPs locally (Lemaitre and Hoffmann 2007). The mechanism of action of most AMPs is not fully understood; however, their antimicrobial activity is believed to hinge upon their cationic and amphipathic characteristics. Indeed, the negatively charged nature of bacterial and fungal membranes renders them susceptible to AMPs through electrostatic interactions. There are different models proposed for the exact molecular mechanism of action of AMPs **(Fig.1.4.)**. Some are thought to have a pore forming activity (Barrel stave model, toroidal pore model), while others may disrupt membranes (carpet model, detergent like model). It is also known that some AMPs can exert toxicity inside the target cell, where they can attack nucleic acids or intracellular organelles (Benfield and Henriques 2020). As eukaryotic membranes are more positively charged, notably due to the presence of cholesterol, they are thought to be protected against AMP killing. However, in certain contexts, eukaryotic cells become more negatively charged due to the transient exposition of negatively charged phospholipids at the outer membrane leaflet, making them targets for AMPs. For example, phosphatidylserine (PS), a phospholipid that is normally sequestered in the inner leaflet of the plasma membrane, is translocated to the outer leaflet when a cell is undergoing apoptosis (Hanson and Lemaitre 2020). This exposure is known to

act as an “eat me” signal for phagocytes and could, in certain contexts, render the cell susceptible to AMP killing (Parvy *et al.* 2019). These recent findings have shed light on the importance of AMPs beyond their function as immune effectors, expanding their applications into novel research domains such as immuno-oncology, pharmacology, and agrobiology.

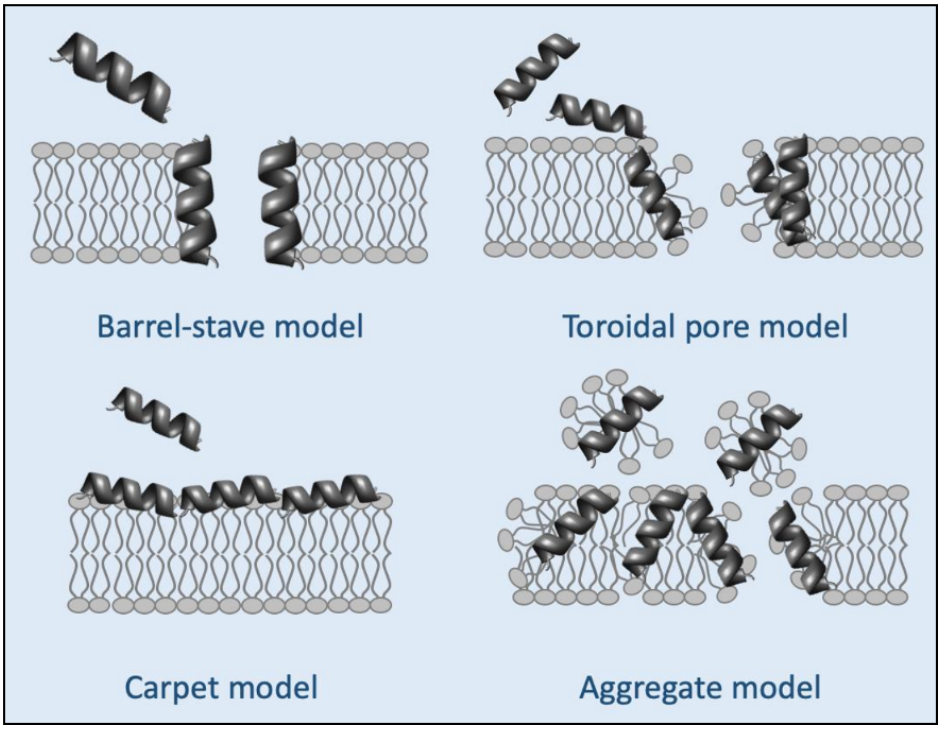

Figure 1.4. Modes of action of antimicrobial peptides with cellular membranes.
In the barrel-stave models, AMPs penetrate into the phosopholipid bilayer to form a ring like a “barrel” pore, with “staves” contained inside the barrel. The toroidal pore model has a similar mechanism to the barrel-stave model, except that AMPs insert into the membrane and bind with lipids to form toroidal pore complexes. This pore forming model is more transient than the barrel-stave model. In the carpet model, AMPs are able to destabilize cellular membranes by accumulating in a parallel direction on the cell membrane. This induces the formation of micelles and destruction of the membrane. In the aggregate model, AMPs bind to the membrane, leading to the formation of peptide-lipid complex micelles. This will form channels allowing the intracellular content to leak out, leading to cell death (adapted from (Raheem and Straus 2019)).

1.3.3.2. The Turandots

The *Turandot* (Tot) gene family is composed of eight genes (*TotA, B, C, Z, M, X, E* and *F*) coding for humoral factors, secreted by the fat body into the hemolymph. The Tot proteins are characterized by three well conserved glycine-rich (1), charged (2) and hydrophobic (3) regions. They were identified in the early 2000s and shown to be transcriptionally inducible

upon different stresses, such as bacterial infection, heat shock, cold exposure, mechanical pressure, oxidative stress or UV exposure (Ekengren and Hultmark 2001). Their induction kinetics after microbial challenge differs from classical antimicrobial peptides: while *Cecropin A1* (CecA1) is immediately induced (6h) after bacterial infection, *TotA* reaches its expression peak 16h after challenge. This late induction suggests a role for Tots in disease tolerance rather than an antimicrobial function.

The Turandots show a complex regulation pattern. First, they are regulated by the JAK/STAT pathway in the fat body after injury (Agaisse and Perrimon 2004). Additionally, Turandot activation also requires the Imd pathway, as *TotA* induction is abolished in flies carrying mutations for the NF-κB transcription factor Relish. Finally, the MAPKKK Mekk1 also plays a role in Turandot regulation, as expression of *TotA* and *TotM* is significantly reduced in *Mekk1* mutant flies. Since their discovery, the Turandots have been used as a readout for the activation of the JAK/STAT pathway, but their molecular function remains unknown. A part of this thesis focuses on the molecular characterization of the Turandots (Chapter 3).

1.3.3.3. Other immune induced proteins

The advent of microarray studies in the late 1990s has clarified the extent of gene expression changes following stimuli. In the context of *Drosophila* immunity, microarray studies have revealed an unexpected number of uncharacterized genes that are differentially expressed after microbial challenge (De Gregorio *et al.* 2002). Indeed, more than 400 genes have been identified as "*Drosophila* immune-regulated genes" (DIRGs) and associated with functions related to the innate immune response. Their regulation is primarily governed by the Toll and Imd pathways, although they can also receive inputs from other immune signaling pathways discussed in Chapter 3.2. While many of these genes encode proteins with known functions, such as antimicrobial peptides for directly combating microbes, transferrins for sequestering iron, catalases for detoxifying ROS, and serine proteases for activating melanization, a substantial portion of the identified genes encode large proteins with functions that remain unidentified. This discovery highlights the existence of promising candidates that could play key roles in *Drosophila* immune response. As an example, two deoxyribonuclease enzymes, called Dnase II and SID, have been shown to be upregulated after microbial challenge,

suggesting a role in *Drosophila* immune defense (Seong *et al.* 2006, 2014). In Chapter 4, we characterize the function of the immune-induced Dnase II in *Drosophila* immunity.

1.4. Objectives of the present PhD thesis

The objective of this PhD thesis is to characterize the molecular functions of three different classes of *Drosophila* immune effectors.

The first part of this thesis focuses on the functional characterization of a family of antimicrobial peptides named Cecropins (Chapter 2). Previous research by our group generated a mutant fly line lacking ten Drosophila AMP genes, including: *Defensin, Drosocin, Diptericins* (*A* and *B*), *Attacins* (*A,B,C* and *D*), *Metchnikowin* and *Drosomycin* (Hanson *et al.* 2019). This study revealed evidence for synergy, additivity and specificity in the action of AMPs against pathogens, but did not address the function of the Cecropin antimicrobial family. Therefore, we generated a fly line lacking the four *Cecropin* genes, named $\Delta Cec^{A\text{-}C}$. Using the $\Delta Cec^{A\text{-}C}$ deficiency alone or in combination with other AMP mutations, we showed that cecropins contribute to defense against certain Gram-negative bacteria and fungi. Our work provides the first genetic demonstration of a role for Cecropins *in vivo*. The results from this part of my thesis resulted in a publication in the journal *Genetics* (Carboni *et al.* 2022).

The second part of this thesis aims at characterizing the molecular function of a family of stress-induced peptides named the Turandots (Chapter 3). The Turandots were identified in the early 2000s and have since then been widely used as a readout of the stress response. However, their molecular function and role in *Drosophila* innate immunity has never been uncoverd. To address this, we generated a mutant fly line lacking 6 *Turandot* genes (A,B,C,Z,M and X) and showed that this deletion increases the fly susceptibility to environmental stresses due to tracheal apoptosis. The high exposure of phosphatidylserine, a negatively charged phospholipid, on the surface of tracheal cells sensitizes them the AMP killing. This study provides the first demonstration of a role for Turandots in immune resilience by mitigating AMP toxicity to host tissues. The results from this second part of my thesis have been submitted as a manuscript for publication.

The third part of this PhD thesis aims to functionally characterize the role of *Drosophila* immune-induced Dnases (Chapter 4). *Dnase II* is a gene strongly expressed in the larval fat body and transcriptionally induced after microbial infection, suggesting a role in *Drosophila*

innate immunity. To investigate this, we generated a null mutant line for *Dnase II* gene. Our preliminary results suggest a role for Dnase II in disease tolerance, as *Dnase II* mutant flies are susceptible to systemic bacterial infection and show constitutive JNK activation. Additionally, we observed the accumulation of apoptotic bodies in hemocytes of *DNAse II* deficient larvae after injury. This suggests an inability to digest phagocytosed apoptotic bodies, leading to enhanced activation of the Imd pathway. This enhanced immune response can be rescued by *STING* knock-out, suggesting the detection of DNA by a yet-unidentified cytosolic DNA sensor. These preliminary results provide the first functional characterization of *Dnase II* enzyme in *Drosophila melanogaster* immunity using a complete knock-out approach. The results from this third part of the PhD thesis are presented here as an unpublished manuscript draft.

Chapter 2: Cecropins contribute to *Drosophila* host defense against a subset of fungal and Gram-negative bacterial infection

Note: This Chapter is based on the published article "Cecropins contribute to *Drosophila* host defense against a subset of fungal and Gram-negative bacterial infection", 2021, Genetics.

Authors: Alexia Carboni, Mark Hanson, Scott Lindsay, Steven Wasserman, and Bruno Lemaitre

Contribution of Alexia Carboni: Conducted the study and wrote the manuscript.

Cecropins contribute to *Drosophila* host defense against a subset of fungal and Gram-negative bacterial infection

Alexia L. Carboni[*], Mark A. Hanson[*], Scott A. Lindsay[†], Steven A. Wasserman[†], and Bruno Lemaitre[*]

[*] Global Health Institute, School of Life Science, École Polytechnique Fédérale de Lausanne (EPFL), 1015 Lausanne, Switzerland. [†] Division of Biological Sciences, University of California San Diego (UCSD), La Jolla, 92093 California, United States of America.

Keywords:

Drosophila melanogaster, innate immunity, antimicrobial peptides, resistance, CRISPR/Cas9, immune effectors, humoral immunity, Cecropin

Corresponding author(s):

Alexia Laurie Carboni (alexia.carboni@epfl.ch, +4121 693 18 33)

Bruno Lemaitre (bruno.lemaitre@epfl.ch, +4121 693 18 31)

ABSTRACT

Cecropins are small helical secreted peptides with antimicrobial activity that are widely distributed among insects. Genes encoding cecropins are strongly induced upon infection, pointing to their role in host-defense. In *Drosophila*, four cecropin genes clustered in the genome (*CecA1, CecA2, CecB* and *CecC*) are expressed upon infection downstream of the Toll and Imd pathways. In this study, we generated a short deletion $\Delta Cec^{A\text{-}C}$ removing the whole cecropin locus. Using the $\Delta Cec^{A\text{-}C}$ deficiency alone or in combination with other antimicrobial peptide (AMP) mutations, we addressed the function of cecropins in the systemic immune response. $\Delta Cec^{A\text{-}C}$ flies were viable and resisted challenge with various microbes as wild-type. However, removing $\Delta Cec^{A\text{-}C}$ in flies already lacking ten other AMP genes revealed a role for cecropins in defense against Gram-negative bacteria and fungi. Measurements of pathogen loads confirm that cecropins contribute to the control of certain Gram-negative bacteria, notably *Enterobacter cloacae* and *Providencia heimbachae*. Collectively, our work provides the first genetic demonstration of a role for cecropins in insect host defense, and confirms their *in vivo* activity primarily against Gram-negative bacteria and fungi. Generation of a fly line (*ΔAMP14*) that lacks fourteen immune inducible AMPs provides a powerful tool to address the function of these immune effectors in host-pathogen interactions and beyond.

INTRODUCTION

In the late nineteen seventies when immunologists were characterizing the antibody immune response of mammals, pioneering studies revealed that insects could resist infection by fearsome human pathogens despite lacking an adaptive immune system. Eventually a landmark discovery by Hans Boman and colleagues showed that insects

produced antimicrobial peptides (AMPs) following infection (Steiner *et al.* 1981), invigorating interest in innate immunity (Ganz *et al.* 1985; Lemaitre 2004). These AMPs differed from other previously identified immune effectors in their small size, cationic charge, and amphipathic structure, allowing a direct disruption of the negatively charged membrane of microbes. In contrast to another class of well-known immune effectors, the lysozymes, AMPs lack enzymatic activity and require concentrations into the micromolar range to achieve their microbicidal effects (Imler and Bulet 2005; Seo *et al.* 2012; Hanson and Lemaitre 2020). Research has now shown that AMPs are common across the tree of life, with similar molecules contributing to host defense in both plants and animals (Broekaert *et al.* 1995). While they contribute to local defense in barrier epithelia of vertebrates, insect AMPs are most famous for being secreted upon systemic infection from the fat body into the hemolymph, where they reach potent concentrations (Bulet *et al.* 1999). The characterization of a plethora of AMPs with diverse modes of action has enriched our understanding of these immune effectors. However, the functional study of AMPs was limited until recently due to technical challenges in mutating the small AMP genes using traditional genetic approaches. This challenge has now been overcome with the advent of CRISPR/Cas9 technology.

Cecropins were the first inducible AMPs to be isolated, found in the hemolymph of infected pupae of the moth *Hyalophora cecropia* (Lepidoptera) (Hultmark *et al.* 1980; Steiner *et al.* 1981). The helix-form of cecropins is thought to promote their interaction with negatively charged bacterial membranes, contributing to pore formation and membrane destabilization, and resulting in the lysis of bacteria (Steiner *et al.* 1988). *In vitro* studies have shown that cecropins have high efficacy against a large panel of Gram-negative bacteria at concentrations below the levels induced in insects upon infection

(25-50μM) (Samakovlis *et al.* 1990), as well as against some filamentous fungi (Steiner *et al.* 1981; DeLucca *et al.* 1997; Ekengren and Hultmark 1999; Ouyang *et al.* 2015). Heterologous expression of *Cecropin* in transgenic rice has also been shown to confer resistance to the rice blast fungus *Magnaporthe oryzae* (Coca *et al.* 2004), and studies have reported an activity of cecropins against tumor cells, bacterial biofilms, and viruses (Chiou *et al.* 2002; Suttmann *et al.* 2008; Deslouches and Di 2017; Kalsy *et al.* 2020).

AMP regulation and function has been extensively studied in the model insect *Drosophila melanogaster*. The *Drosophila* genome encodes four cecropin genes (*CecA1* and *A2, CecB* and *CecC*) and two pseudogenes (*Cec-Ψ1* and *Cec-Ψ2*) that are clustered at position 99E2 at the tip of the right arm of the third chromosome (Kylsten *et al.* 1990; Samakovlis *et al.* 1990; Sackton *et al.* 2007). The cecropin locus is adjacent to another gene named *Andropin,* which encodes a related antibacterial peptide expressed in the ejaculatory duct (Samakovlis *et al.* 1991). CecA1 and CecA2 are identical at the protein level, differing only by a few silent mutations at the nucleotide level, suggesting that they emerged from a recent duplication. The four *Drosophila* cecropin genes are strongly induced in the fat body and hemocytes upon systemic infection. Cecropin genes are regulated by the Imd pathway, but also receive a considerable input from the Toll pathway upon systemic infection (De Gregorio *et al.* 2002). Functional studies analyzing the role of cecropins *in vivo* are scarce. Overexpression of *CecA* in an otherwise *Imd, Toll* immune-deficient background failed to detect a clear protective effect of *CecA* against a battery of pathogens (Tzou *et al.* 2002). Other studies using overexpression approaches have pointed to a role of *CecA* in the regulation of the gut microbiota (Ryu *et al.* 2008). Transgenic mosquitoes overexpressing both Cecropin and Defensin under the control of the vitellogenin promoter displayed an increased resistance to *Pseudomonas aeruginosa* infection,

indicating that these AMPs could act cooperatively against this pathogenic bacterium (Kokoza *et al.* 2010).

We have previously generated fly mutants deleting 10 *Drosophila* AMP genes including: *Defensin*, two *Diptericins* (*DptA* and *B*), *Drosocin*, four *Attacins* (*AttA, B, C,* and *D*), *Metchnikowin*, and *Drosomycin* (Hanson *et al.* 2019a). This study revealed that AMPs play an important role in defense against Gram-negative bacteria and also somewhat in defense against fungi. In contrast, another family of host defense peptides with no overt antimicrobial activity *in vitro*, the bomanins, plays a major role in the elimination of Gram-positive bacteria and fungi (Clemmons *et al.* 2015; Lindsay *et al.* 2018). Importantly, Hanson et al. (Hanson *et al.* 2019a) revealed evidence for synergy and additivity, but also remarkable specificity in the action of AMPs against certain pathogens. However, this study did not address the function of the four cecropins due to a failure to generate a proper cecropin locus deletion. In the present study, we have generated fly lines carrying a small deletion that removes the four immune cecropin genes, and by using flies carrying this deletion alone or in combination with other AMP mutations, we address the role of cecropins in the systemic immune response for the first time.

MATERIALS AND METHODS

Fly stocks and genetics

The w^{1118} DrosDel isogenic (iso w^{1118}) wild type was used as the genetic background for mutant isogenization, as described by Ferreira and colleagues (Ferreira *et al.* 2014). The $\Delta Cec^{A\text{-}C}$ mutation was generated using CRISPR with two gRNAs and a homology directed repair vector by cloning 5' and 3' region-homologous arms into the pHD-DsRed vector, and consequently $\Delta Cec^{A\text{-}C}$ flies express DsRed in their eyes, ocelli and abdomen. The

ΔCec^{A-C} mutation was generated by Cas9 mediated injection into the iso *Mtk*^{R1}*; Drs*^{R1} background. Following this, two rounds of backcrossing were performed to replace the 1st and 2nd chromosome with the *iso DrosDel* 1st and 2nd chromosome, and to recombine the *ΔCec*$^{A-C}$ mutation away from other mutations. The resulting stock is here called iso *ΔCec*$^{A-C}$. Afterwards, the *ΔCec*$^{A-C}$ mutation was recombined independently with *Drs*^{R1} and *AttD*^{SK1} on chromosome 3, and introgressed alongside the other AMP mutations on chromosome 2 to generate *ΔAMP14* flies lacking the 14 classical AMP genes from the *Defensin, Drosocin, Attacin, Diptericin, Metchnikowin, Drosomycin*, and *Cecropin* gene families. The iso *ΔAMP10,* iso *Bom*$^{\Delta 55C}$ and iso *Relish*^{E20} flies are the same as used in Hanson et al. (Hanson *et al.* 2019a); however we removed the aberrant cecropin locus (*Cec*^{SK6}) detected in the *ΔAMP10* line to avoid any potential effects this locus could have on Cecropin-mediated resistance to infection (see Hanson et al. correction notice (Hanson *et al.* 2019b)).

Microbial culture conditions

Bacteria were grown overnight on a shaking plate at 200 RPM in their respective growth media and at their optimal temperature conditions. They were then pelleted by centrifugation (4000 RPM) at 4°C. The bacterial pellets were diluted to the desired optical density at 600nm (OD_{600}).

Pectobacterium carotovorum carotovorum 15 (*Ecc15*) and *Micrococcus luteus* were grown in LB media at 29°C. *Escherichia coli* strain 1106, *Providencia burhodogranariea*, *Providencia rettgeri* and *Providencia heimbachae* were grown in LB media at 37°C. *Enterococcus faecalis*, *Listeria monocytogenes* and *Enterobacter cloacae* were cultured in BHI media at 37°C. *Streptococcus pneumoniae* was grown as described by Krejčová and colleagues (Krejčová *et al.* 2019). *Candida albicans* strain ATCC 2001 was cultured in YPG

media at 37°C. *Aspergillus fumigatus* was grown at 37°C on Malt Agar; spores were collected in sterile PBS, pelleted by centrifugation and resuspended at the desired OD. *Beauveria bassiana* strain R444 and *Metharizium rileyi* strain PHP1705 commercial spores were produced by Andermatt Biocontrol, product: BB-PROTEC and Nomu-PROTEC respectively.

Infection experiments and survival

Systemic infections with *P. carotovorum carotovorum 15* (*Ecc15*) (Basset *et al.* 2000), *M. luteus*, *E. coli* strain 1106, *P. burhodogranariea*, *P. rettgeri, P. heimbachae* (Galac and Lazzaro 2011), *E. faecalis*, *L. monocytogenes*, *E. cloacae* and *C. albicans* were performed as follows: 3-5 day old adult females were pricked in the thorax with a 100μm thick needle dipped into a concentrated pellet of bacteria at a desired OD_{600}. Infected flies were then maintained at 25 or 29°C for survivals. Systemic infection with *S. pneumoniae* (Krejčová *et al.* 2019) or *M. rileyi* was performed by injecting 50nL of a concentrated pellet of bacteria or suspension of fungal spores using a nanoinjector and glass capillary needles.

Natural infections with *B. bassiana* were performed by shaking anesthetized flies in a vial with 200mg of spores. Flies were flipped into fresh vials one day after fungal inoculation. Three independent experiments for survivals to infection were performed with 20 flies per vial(s) on standard fly medium without yeast. Survival was scored daily.

Bacterial load of flies

Flies were infected (systemic infection) with bacteria at the desired OD_{600}. At the indicated time post-infection, flies were anaesthetized using CO_2, surface sterilized by washing briefly in 70% EtOH, and blotted. Pools of 5 flies were transferred in 200μL of

sterile PBS and macerated using a pestle. The homogenates were centrifuged at 8,000 RPM for 3 minutes. The supernatants were serially diluted and 7μL droplets were inoculated on LB agar overnight at 29°C. Colony-forming units (CFUs) were manually counted the following day.

Gene expression levels by qRT-PCR

Flies that either were unchallenged or were infected systemically by pricking in the thorax with a needle dipped in a pellet of *Ecc15* or *M. luteus* (OD_{600}=200) were frozen at -20°C 6h or 12h post-infection, respectively. Three independent experiments (independent day, flies, bacterial pellet) were performed for each infection with two or three technical repeats according to the number of flies available. Gene expression measurements were then performed by RT-qPCR as previously described (Hanson *et al.* 2019a). Briefly, 5 whole flies were homogenized and their RNA was extracted using TRIzol reagent and resuspended in RNase-free water. Reverse transcription was carried out using PrimeScript RT (TAKARA) with random hexamers and oligo dTs. Quantitative PCRs were performed on a LightCycler 480 (Roche) using PowerUp SYBR Green Master Mix.

Cecropin A injection

Commercially available Cecropin from *Hyalophora cecropia* (Sigma-Aldrich) was diluted in PBS (1.37 M NaCl, 0.027 M KCl, 0.08 M Sodium phosphate dibasic, 0.02 M Potassion phosphate monobasic, adjusted at pH7.4 and filtered 0.2 μm) to a concentration of 50μM. Fifty nL of Cecropin was injected into the thorax using a nanoinjector and glass capillary. Flies were left to recover for 2 hours and then pricked with the desired pathogen.

MALDI-TOF

Raw hemolymph samples were collected from either unchallenged flies, or flies pricked with a 1:1 cocktail of *E. coli* and *M. luteus* (OD=200) in 0.1% TFA, as described previously (Hanson *et al.* 2019a). Samples were then added to an acetonitrile universal matrix. Representative spectra are shown. Immune induced peaks were identified based on previous studies (Uttenweiler-Joseph *et al.* 1998; Levy *et al.* 2004) to confirm the absence of AMP-associated peaks, and presence of immune-induced peptides not affected by the included AMP mutations. Spectra were visualized using mMass and figures were additionally prepared using Inkscape v0.92.

Statistical analysis

Survival analyses were performed using a Cox proportional hazards (CoxPH) multiple comparison model, with Benjamini-Hochberg corrections for p-values, in R 3.6.3. Survival curves included three independent experiments with at least one cohort of 20 flies per treatment. Statistics were represented using a Compact Letter Display (CLD) graphical technique: groups were assigned the same letter if they were not significantly different ($p>.05$). Quantitative PCR data included three independent experiments with at least two technical repeats and were compared by one-way ANOVA with Holm-*Šídák* multiple test correction in Prism R7. Bacterial load values were transformed as $\log_{10}(\text{value}+1)$ to allow graphical representation of the absence (0) of CFUs. Bacterial load data were compared by one-way ANOVA with Holm-*Šídák* multiple test correction in Prism 7. Statistics were represented using a CLD graphical technique.

RESULTS

Generation and characterization of cecropin mutants

We generated a fly line lacking the four cecropin genes, *CecA1, CecA2, CecB*, and *CecC,* which are clustered at 99E and are inducible during the systemic response. For this, we used the CRISPR/Cas9 editing method to generate a 6kb deletion (referred as *ΔCec*$^{A-C}$*)* that removes the four inducible cecropins but leaves the related *Andropin* gene intact (Fig. 2.1A). The *ΔCec*$^{A-C}$ mutation was generated by Cas9 mediated injection in the *w, DrosDel* (referred to as *w*^{1118}) background. The background of the *ΔCec*$^{A-C}$ mutation was then cleaned by 2 successive crosses to the *w*^{1118} *iso* background to remove potential off-target alterations. To confirm the absence of cecropin genes in *ΔCec*$^{A-C}$ flies, we performed qRT-PCR for the four Cecropin genes as well as the pseudogene *Cec-Ψ2*. Expression of *CecA* (cumulative expression of *CecA1* and *CecA*2), *CecB*, *CecC* and *Cec-Ψ2* was readily observed in the wild type, but not detected in *ΔCec*$^{A-C}$ flies; the expression of the nearby *Andropin* gene was not affected (Fig. 2.1B-C, FigS2.1A-C).

We previously generated a fly line in the *w*^{1118} *iso* background here referred to as "*ΔAMP10*", harbouring six mutations that remove ten antimicrobial peptide genes: *Defensin*, *Metchnikowin*, the four Attacins (*A/B/C/D*), *Drosomycin*, two *Diptericins* (*A/B*), and *Drosocin* (Hanson et al., 2019). We recombined the iso *ΔCec*$^{A-C}$ mutation with the iso *ΔAMP10* mutations to generate an iso fly line lacking all 14 'classical' antimicrobial peptides (referred to as "*ΔAMP14"*). MALDI-TOF and RT-qPCR analysis confirm the absence of these 14 antimicrobial peptides in *ΔAMP10* and *ΔAMP14* flies (Fig. 2.1B-C and Fig. S2.2). The *ΔCec*$^{A-C}$, *ΔAMP10* and *ΔAMP14* flies were viable and showed no morphological defects. We also confirmed that the two central NF-κB signaling pathways, Toll and Imd, were functional, as quantified by measuring expression of genes

characteristic of each of these pathways (Fig. 2.1D-F). Furthermore, MALDI-TOF proteomic analysis of hemolymph from infected flies 24 hours post infection (hpi) reveals a wild type-like induction of peaks associated with other NF-κB effectors (e.g., Bomanins, Daishos, and Baramicin A) (Fig. S2.2). Collectively, our study indicates that we have generated a fly line lacking all the *Drosophila* 'classical' AMPs, and that deleting these AMPs does not impact the production of other NF-κB effectors.

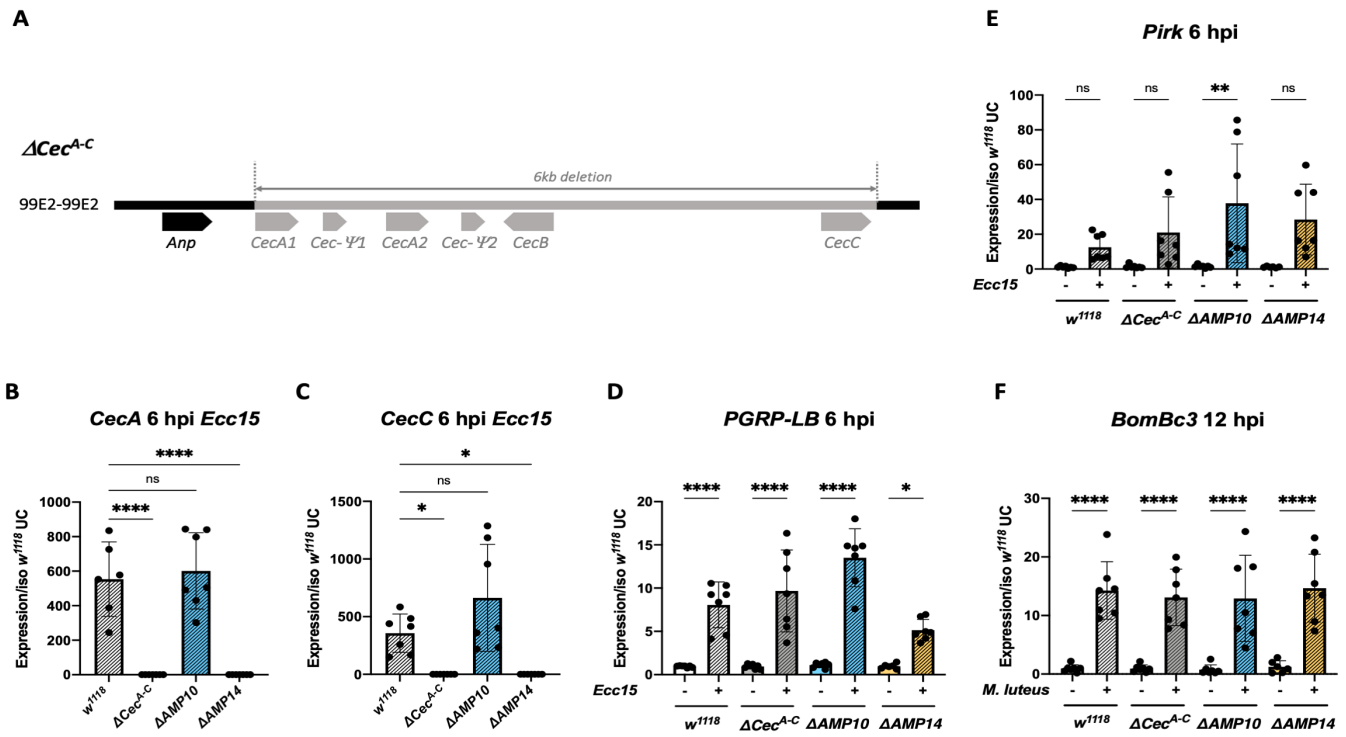

Figure 2.1. Description and validation of ΔCecA-C, ΔAMP10 and ΔAMP14 mutants.
(**A**) Schema of the cecropin locus chromosomal deletion removing *CecA1* and *A2, CecB* and *CecC,* plus 2 pseudo genes, *Cec-Ψ1* and *Cec- Ψ2* clustered at position 99E2 (Chromosome III) (**B,C**) qRT-PCR of *CecA* (B) and *CecC* (C) expression in w^{1118}, ΔCec^{A-C}, *ΔAMP10* and *ΔAMP14* flies 6 hours post *Ecc15* infection. (**D-F**) The Imd (D,E) and Toll (F) pathways are functional in ΔCec^{A-C}, *ΔAMP10* and *ΔAMP14* flies after challenge as revealed by expression of target genes upon septic injury with *Ecc15* or *M. luteus. PGRP-LB* and *Pirk* were used as readouts for the Imd pathway and *Bomanin (BomBc3)* for the Toll pathway. Expression was normalized with w^{1118} UC set as a value of 1.

Cecropins contribute to survival against certain Gram-negative bacterial infections

We used wild-type, ΔCec^{A-C}, *ΔAMP10* and *ΔAMP14* flies to explore the role that cecropins play in defense against pathogens during systemic infection. By performing survival

analyses with wild-type and *ΔCec*$^{A-C}$ flies, we assessed if the absence of the four cecropins is sufficient to cause an immune deficiency. Likewise, any difference in survival rates between *ΔAMP10* and *ΔAMP14* flies would suggest a contribution of cecropins that is only apparent in the absence of other AMPs. We first focused our attention on Gram-negative bacterial infections, as cecropins were initially identified for their activity against this class of bacteria. We challenged wild-type, *ΔCec*$^{A-C}$, *ΔAMP10* and *ΔAMP14* flies with six different Gram-negative bacterial species, using inoculation doses (given as OD_{600}) selected such that Imd deficient, iso *Rel*^{E20} mutant control flies were killed. Our survival experiments did not reveal an overt contribution of cecropins to resistance against the Gram-negative bacteria *Providencia rettgeri, Pectobacterium carotovorum carotovorum (Ecc15)*, *Escherichia coli* or *Providencia burhodogranariea* (Fig 2.2A-D). In all cases, *ΔCec*$^{A-C}$ flies survived as well as wild-type flies, while *ΔAMP10* flies were as susceptible as *ΔAMP14*. One exception was found for *P. burhodogranariea* infection: death of *ΔAMP10* flies was delayed by one day compared to *ΔAMP14* flies, suggesting a contribution of cecropins in combatting this bacterium early in infection.

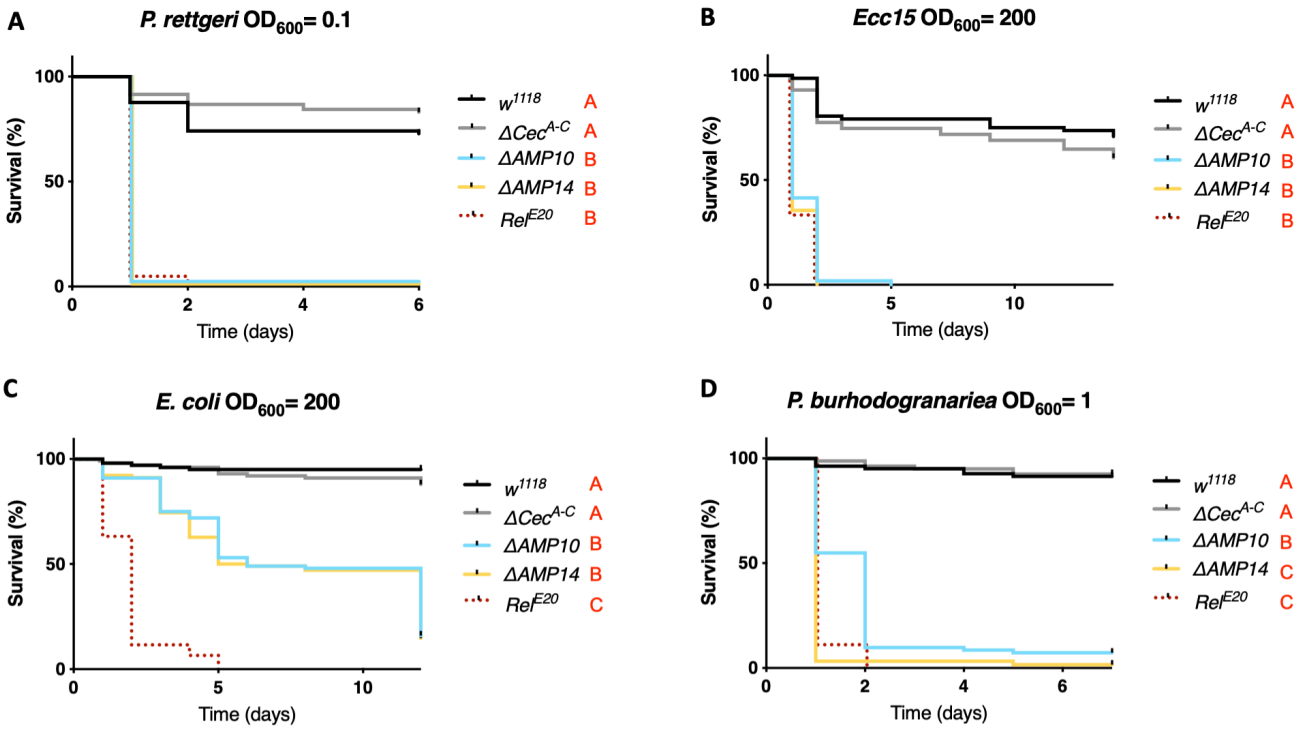

Figure 2.2. Cecropins do not determine resistance to a broad spectrum of Gram negative bacteria

w^{1118} were used as wild-type flies and Rel^{E20} as susceptible flies lacking the Imd pathway for all survival experiments to Gram negative bacterial infection. Female w^{1118}, ΔCec^{A-C}, *ΔAMP10, ΔAMP14,* and Rel^{E20} flies were pricked in the thorax with an inoculum of (**A**) *P. rettgeri,* (**B**) *Ecc15,* (**C**) *E. coli* or (**D**) *P. burhodogranariea.* Cecropins were not critically involved in combating infection with any bacteria presented here as ΔCec^{A-C} survived as well as w^{1118} flies, while *ΔAMP10* and *ΔAMP14* mutant flies died as fast as Rel^{E20} mutants. Bacterial concentrations are indicated in the figure.

Interestingly, we did identify a prominent role for cecropins against two Gram-negative bacterial strains: *Enterobacter cloacae* and *Providencia heimbachae*. Although ΔCec^{A-C} flies survived *E. cloacae* infection like wild-type flies and many *ΔAMP10* flies survived this infection, *ΔAMP14* flies, instead behaved like Rel^{E20} mutants lacking Imd signaling entirely (Fig. 2.3A). This result suggests that the presence of the four cecropin genes confers a protective effect against this bacterium in flies that lack ten other AMP genes. A significant difference in CFUs between *ΔAMP10* and *ΔAMP14* flies at 8h post-infection (hpi) confirmed a role of cecropins in limiting the growth of *E. cloacae* (Fig. 2.3B). We also observed a consistently higher bacterial load in ΔCec^{A-C} flies compared to wild-type controls, though this was not significant ($p = .063$). Moreover, *ΔAMP14* and Rel^{E20} fly CFUs were similar, consistent with survival data showing complete mortality of these genotypes within 24 hours. These results indicate that the knock-out of the 'classical' AMPs in the *ΔAMP14* line fully explains the susceptibility of Imd pathway mutants to *E. cloacae* infection. Next, we attempted to rescue the susceptibility of *ΔAMP10* and *ΔAMP14* flies using commercially available Cecropin. We injected 50 nL of 50μM *Hyalophora cecropia* Cecropin (Sigma-Aldrich) or PBS (control) two hours before challenging flies with *E. cloacae*. Interestingly, when we injected Cecropin two hours prior to *E. cloacae* infection, *ΔAMP10* flies survived significantly better than *ΔAMP10* flies previously injected with only PBS (Fig. 2.3C). This result suggests that priming the fly defense by increasing circulating levels of Cecropin is sufficient to combat *E. cloacae* infection, even

in flies lacking a broad range of other AMPs. However, we did not succeed in rescuing the susceptibility of *ΔAMP14* flies using the same approach. This suggests the rescue effect we observed using *ΔAMP10* flies relies on the total Cecropin levels, which includes both endogenously produced Cecropin and the supplemental Cecropin we injected. Collectively, our *in vivo* analysis is consistent with previous *in vitro* studies that showed commercial Cecropin from *Hyalophora cecropia* has activity against *E. cloacae* (Hultmark *et al.* 1980).

Similarly, we observed a contribution of cecropins against the Gram-negative bacterium *P. heimbachae* in flies lacking other AMPs (fig. 2.3D-F). While *ΔAMP10* flies were able to survive this infection at levels close to wild type flies at OD_{600}=50, *ΔAMP14* flies again behaved like Rel^{E20} mutants and suffered complete mortality (Fig. 2.3D); the ΔCec^{A-C} mutation alone did not increase susceptibility. Bacterial load measurement performed on flies collected 24 hpi revealed a contribution of cecropins both in the presence and absence of other AMPs (Fig. 2.3E). We again injected commercial *H. cecropia* Cecropin in an attempt to rescue the susceptibility of *ΔAMP10* and *ΔAMP14* flies to *P. heimbachae* (Fig. 2.3F). Using this bacterial infection model, previous injection of PBS increased the susceptibility of wild-type flies to *P. heimbachae*. Strikingly however, injection of Cecropin prior to infection rescued survival of *ΔAMP10* flies to a level close to previously uninjured wild-type flies.

We have recently shown that the antibacterial peptide Drosocin (Dro) is specially required to resist infection with *E. cloacae.* This raises the possibility that Cecropin and Drosocin synergistically contribute to the host defense against this bacterium. To investigate this question, we generated a double mutant line for the *Drosocin* and *Cecropin* genes *(Dro^{SK4}; ΔCec^{A-C}).* Ultimately this double mutant line died with similar

kinetics to *Drosocin* single mutants against *E. cloacae* **(Figure S2.3**). We also found no susceptibility of *Drosocin* or *Cecropin* single or double mutants to *P. heimbachae* (Data not shown). Thus, we found no prominent synergy between *Drosocin* and the *Cecropins*. This suggests that Cecropins are redundant alongside other AMPs in defense against these bacteria, and do not have a highly specific interaction like *Drosocin* and *E. cloacae*.

In summary, our results reveal that cecropins contribute to *Drosophila* host defense against a subset of Gram-negative bacteria, and that this contribution is more readily apparent when other AMPs are also lacking.

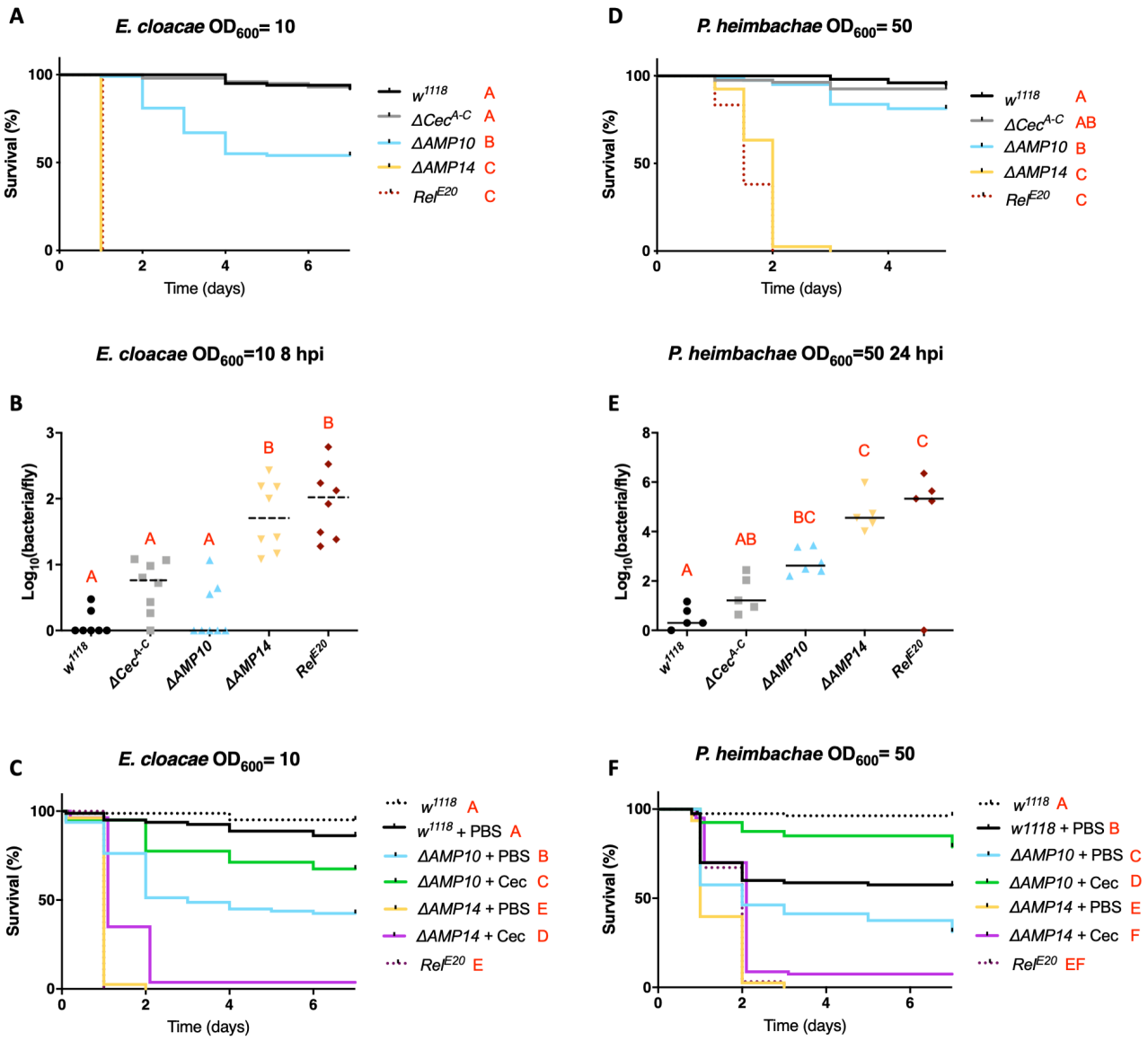

Figure 2.3. Cecropins are essential in the absence of other AMPs to resist E. cloacae and P. heimbachae infection

(**A**) Survival experiments upon infection with *E. cloacae* reveal that AMP deficient flies having cecropins (*ΔAMP10*) are significantly more resistant than those without cecropins (*ΔAMP14*). (**B**) Bacterial loads (CFU counts) of w^{1118}, ΔCec^{A-C}, *ΔAMP10, ΔAMP14,* and Rel^{E20} flies 8 hours post infection reveal a significant role for Cecropins in clearing and controlling *E. cloacae.* (**C**) Commercial Cecropin injection (50 nL at 50 μM) 2 hours prior to *E. cloacae* infection increases the resistance of *ΔAMP10* mutant flies. However, CecA injection did not rescue the susceptibility of *ΔAMP14* flies to *E. cloacae*. (**D-F**) Survival analysis (D), bacterial load measurements 24 hours post infection (E), and Cecropin supplementation experiments (F) in w^{1118}, ΔCec^{A-C}, *ΔAMP10, ΔAMP14,* and Rel^{E20} flies upon infection with *P. heimbachae* (as described for A-C).

Cecropins are not involved in the resistance to Gram-positive bacteria

Previous work with the *ΔAMP10* flies did not reveal a role of *Drosophila* AMPs against Gram-positive bacteria, indicating instead that other immune effectors – notably the bomanins – play a predominant role against this class of microbes (Hanson *et al.* 2019a; Lin *et al.* 2020). Therefore, we were curious if the added loss of cecropins would reveal a cryptic contribution of *Drosophila* AMPs to defense against Gram-positive bacteria. For this, we challenged wild-type, ΔCec^{A-C}, *ΔAMP10* and *ΔAMP14* flies with three Gram-positive bacteria: *E. faecalis*, *S. pneumoniae* and *L. monocytogenes* (Fig. 2.4A-C). *E. faecalis* and *S. pneumoniae* contain Lysine-type peptidoglycan that is known to predominantly activate the Toll pathway while *L. monocytogenes* has DAP-type peptidoglycan, and is known to activate both the Toll and Imd pathways (Leulier *et al.* 2003). In these experiments, we included iso $Bom^{\Delta 55C}$ control flies, which lack ten *Bomanin* genes and are known to be susceptible to Gram-positive bacterial and fungal infections (Clemmons *et al.* 2015). Our survival experiments did not reveal a major role of cecropins individually or alongside other AMPs in combating these Gram-positive bacterial species, but confirmed the importance of bomanins (Fig. 2.4A-C).

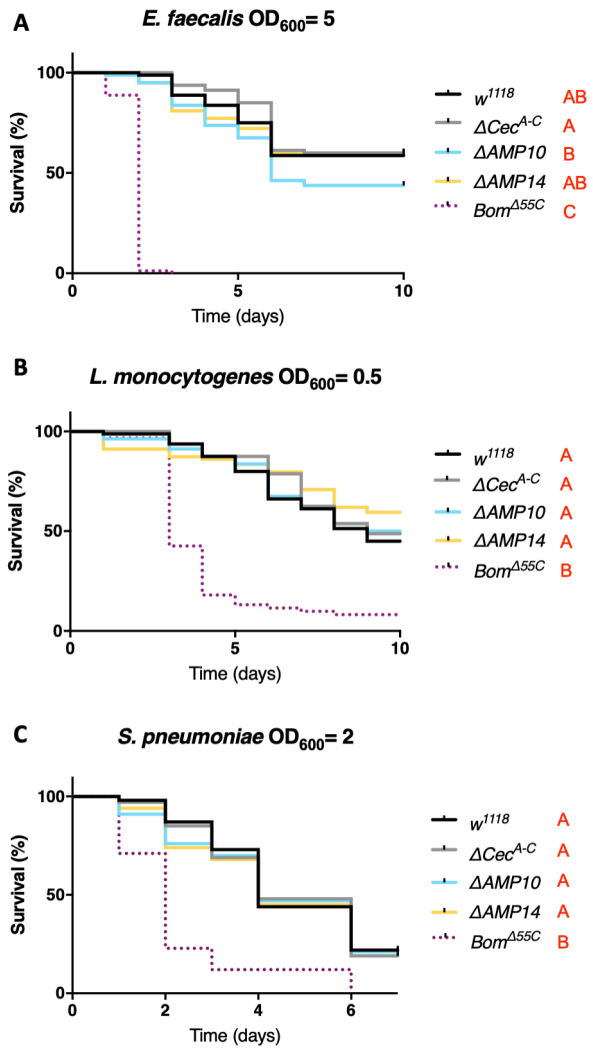

Figure 2.4. Cecropins are not involved in resistance to Gram-positive bacteria
w^{1118} were used as wild-type flies and $Bom^{\Delta 55C}$ as susceptible flies lacking 10 *Bomanin* genes for all survival experiments to Gram positive bacterial infection. w^{1118}, $\Delta Cec^{A\text{-}C}$, *ΔAMP10, ΔAMP14,* and $Bom^{\Delta 55C}$ flies were pricked in the thorax with an inoculum of (**A**) *E. faecalis,* (**B**) *L. monocytogenes*, or (**C**) *S. pneumoniae*. Cecropins were not involved in combating infection of these 3 bacterial species: $\Delta Cec^{A\text{-}C}$, *ΔAMP10,* and *ΔAMP14* flies survived as well as w^{1118} flies. Bacterial concentrations are indicated in the figure.

Cecropins can contribute to antifungal defense

While cecropins were initially identified as antibacterial peptides, further *in vitro* studies have also suggested an antifungal activity (Ekengren and Hultmark 1999; Andrä *et al.* 2001). We therefore investigated the contribution of cecropins to resistance upon septic injury with four fungal species: the entomopathogenic fungi *Metarhizium rileyi* and

Beauveria bassiana, the opportunistic mold *Aspergillus fumigatus,* and the yeast *Candida albicans*. Survival analysis did not reveal a major susceptibility of any AMP mutants against *M. rileyi* (Fig. 2.5A). However, *ΔAMP14* flies were more susceptible to *A. fumigatus* and *C. albicans* septic infection, and suffered greater mortality to *B. bassiana* natural infection, compared to *ΔAMP10* and wild-type flies (Fig. 2.5B-D). This indicates a role for *Cecropins* in resistance to these three fungi, revealed best in the absence of other AMPs. In order to confirm the importance of Cecropins in limiting fungal proliferation, we introduced *B. bassiana* spores directly into the hemolymph by septic injury for more controlled fungal infection kinetics, and measured fungal load at 48h hpi by qPCR. Monitoring pathogen load revealed that in *ΔAMP14* flies, *B. bassiana* loads were higher than levels found in wild type (p=.07) and *ΔAMP10* flies (Fig. 2.5E), albeit not significantly. Taken together, these results show a contribution of cecropins to defense against fungal pathogens such s *B. bassiana*, *A. fumigatus* and *C. albicans*.

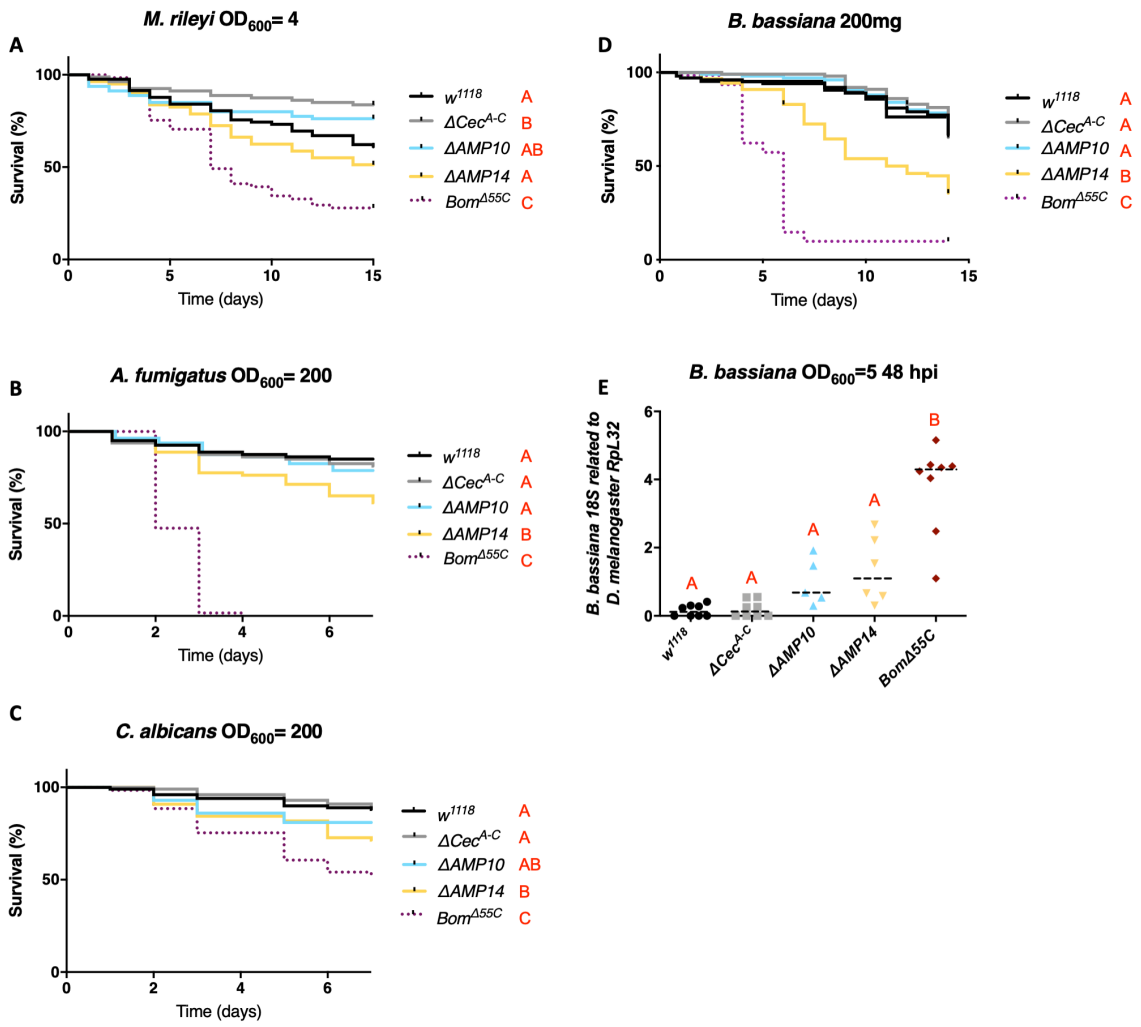

Figure 2.5. Cecropins contribute to antifungal defense against A. fumigatus, C. albicans, and B. bassiana

(**A-C**) *w*^{1118} were used as wild-type flies and *Bom*$^{\Delta 55C}$ as susceptible flies lacking 10 *Bomanin* genes for all survival experiments to fungal infections. Cecropins were not involved in combating infection of (**A**) *M. rileyi* as *w*^{1118}, *ΔCec*$^{A\text{-}C}$, *ΔAMP10,* and *ΔAMP14* flies survived as well as *w*^{1118} flies. Survival upon (**B**) *A. fumigatus* or (**C**) *C. albicans* septic infection, and (**D**) natural infection with *B. bassiana* reveals a significant increase in resistance of *ΔAMP10* flies compared to *ΔAMP14* flies, suggesting an important role for cecropins in fighting these fungi. (**E**) *B. bassiana* load (measured by *B. bassiana* 18S expression related to *D. melanogaster RpL32*) is higher (p = .07) in *ΔAMP14* flies compared to *w*^{1118}, *ΔCec*$^{A\text{-}C}$, and *ΔAMP10* flies 48 hours post septic infection. Fungal concentrations are indicated in the figure.

DISCUSSION

In this study, we generated flies lacking the four-immune inducible cecropin genes to address their function alone or in combination with other *AMP* gene mutations. *ΔCec*$^{A\text{-}C}$ and *ΔAMP14* flies were viable, fertile and did not show any morphological defect. Moreover, they display normal activation of the Imd and Toll pathways, suggesting that the classical *Drosophila* AMPs do not contribute to immune signaling, in contrast to mammalian AMPs (Mookherjee *et al.* 2020).

Our survival analyses reveal a role of cecropins in the defense against certain Gram-negative bacterial species (specifically against Gammaproteobacteria). However, we could not identify a bacterial species or context for which flies mutant for cecropin genes alone succumb faster than wild-type. Studies of other AMPs have revealed that certain AMPs exhibit a high degree of specificity in determining host-pathogen interactions, as illustrated by the requirement of *Diptericin* in defense against *P. rettgeri*, *Drosocin* in defense against *E. cloacae*, and the recently-described *Daisho* and *Baramicin A* genes in defense against *Fusarium oxysporum* and *Beauveria bassiana* fungi, respectively (Unckless *et al.* 2016; Hanson *et al.* 2019a, 2021; Cohen *et al.* 2020). Further studies may reveal bacteria for which the presence of cecropins is essential for survival.

The most striking phenotype in the present study was that loss of cecropins has a marked effect on *E. cloacae* and *P. heimbachae* infection in flies also lacking other AMP genes. As such, we reveal an important but cryptic contribution of cecropins in defense against these bacteria. Generation of flies lacking refined subsets of AMPs might narrow down the specific groups of peptides key to defense against *E. cloacae* and *P. heimbachae*. The enhanced growth of *E. cloacae* in AMP mutants that also lack cecropins is a particularly striking demonstration of their importance. In this infection model, the presence of cecropins dictates whether AMP mutant flies initially suppress bacterial

growth, or phenocopy *Rel*^{E20} flies deficient for Imd signaling. Cecropins are induced with faster kinetics than most other AMPs, with a peak expression as early as 3hpi (Lemaitre *et al.* 1997; De Gregorio *et al.* 2002; Schlamp *et al.* 2021). As cecropins encode simple helical peptides that do not require extensive post-translational modification, it is tempting to speculate that they become functional more rapidly, and play an important role in combatting bacteria specifically at this early phase of infection, likely in cooperation with melanization and phagocytosis, two more immediate host defenses (Haine *et al.* 2008; Dudzic *et al.* 2019).

Our study also reveals that endogenous cecropins can play a role in defense against certain fungi, but not against Gram-positive bacteria tested so far (i.e., Firmicutes). Thus, our *in vivo* study corroborates the antifungal and antibacterial activities of cecropins previously observed with *in vitro* studies (Samakovlis *et al.* 1990; DeLucca *et al.* 1997; Ekengren and Hultmark 1999). While IMD is crucial for the expression of the four cecropins, the cecropin response to infection also relies on Toll signaling (De Gregorio *et al.* 2002; Hedengren-Olcott *et al.* 2004). As such, the contribution of cecropins to defense against fungi could help explain the regulation of the cecropin locus by both the Toll and Imd pathways.

The observations that AMP genes are induced to great extent, reach high peptide concentrations in the hemolymph, and display *in vitro* microbicidal activity are all consistent with a role as immune effectors. Use of both *ΔAMP10* and *ΔAMP14* flies has confirmed the important contribution of AMPs to host defense against certain Gram-negative bacteria and fungi, but not against the Gram-positive bacteria tested so far. It is possible that incorporating more diverse bacteria and fungi could reveal additional roles of AMPs, as the pathogens traditionally used in *Drosophila* immune studies are restricted to only a few major clades. *Drosophila* AMPs also regulate the gut microbiota downstream

of the Imd pathway, a function consistent with their bactericidal activity (Marra *et al.*). However, recent studies have suggested that AMP-like genes may play more subtle roles in other processes like memory formation (Barajas-Azpeleta *et al.* 2018), an erect wing response upon infection (Hanson *et al.* 2021), tumor control (Parvy *et al.* 2019; Araki *et al.* 2019), or regulation of JNK signaling in the salivary gland (Krautz *et al.* 2020). While we confirm a primary importance for cecropins and other AMPs in the systemic immune response, exploring the functions of AMPs in non-canonical roles is an exciting future direction of research.

Our study and others contribute to the rapid progress made towards understanding the roles of *Drosophila* immune effectors. Research on the effector response has stagnated for over a decade, but recent functional characterizations by loss of function of key effectors (*Cecropins, Defensin, Attacins, Diptericins, Drosocin, Drosomycin, Metchnikowin, Bomanins, Daishos,* and *Baramicin*) has greatly advanced our understanding of the roles of these effectors (Lindsay *et al.* 2018; Hanson *et al.* 2019a; Cohen *et al.* 2020; Huang *et al.* 2020). Most importantly, these studies amend the assumptions of the previous "cocktail" model for AMP-pathogen interactions (Yan and Hancock 2001; Lazzaro 2008; Zdybicka-Barabas *et al.* 2012; Rahnamaeian *et al.* 2016), revealing some AMPs to be general effectors against most pathogens, while others act as "silver bullets" specifically required for defense against certain pathogens. The susceptibility of Toll and Imd pathway mutants to specific pathogens can now be directly linked to the susceptibility of mutants for immune effectors regulated by these pathways (Hanson and Lemaitre 2020). As new genetic techniques allow greater characterization of the roles of known immune effectors, many of them remain to be characterized, notably a number of short peptide genes highlighted by transcriptomic studies (Gregorio *et al.* 2001; Troha *et al.* 2018; Tattikota *et al.* 2020; Cattenoz *et al.* 2020; Schlamp *et al.* 2021).

However, we are likely still exploring inside the box when assuming a uniquely immune role for these peptides.

Our study also highlights the power of multiple mutation analysis, as the role of cecropins would not have been uncovered *in vivo* by mutating individual genes. While we have begun exploring the combinatory potential of AMPs in defense against infection, future studies will benefit from probing the interaction of immune effectors like AMPs with other mechanisms of host defense such as phagocytosis or melanization. With the advent of CRISPR/Cas9 technology and many recently described mutants, the interactions of AMPs in defense are just the tip of the iceberg in developing a global framework to understand the *Drosophila* immune response.

SUPPLEMENTAL FIGURES

Figure S1

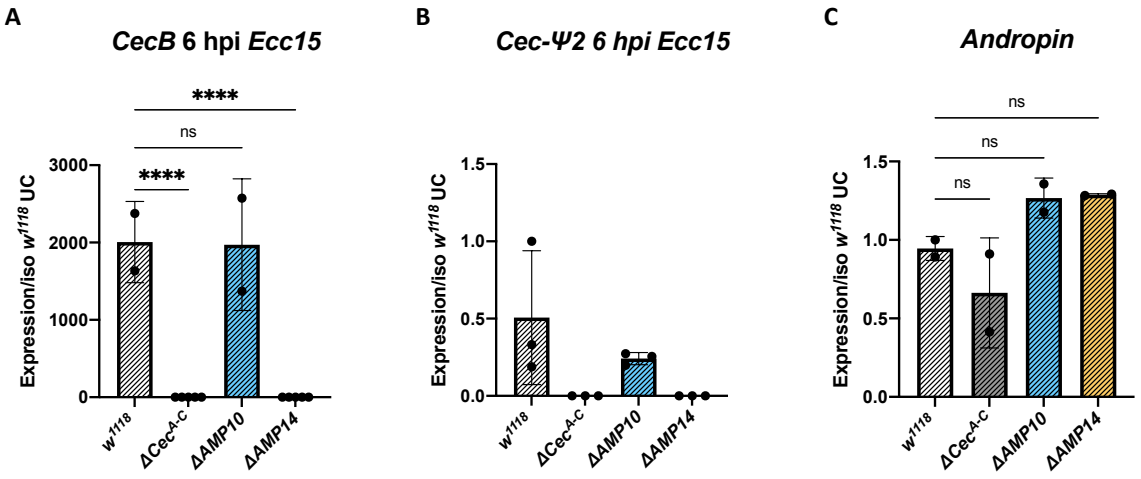

Figure S2.1: Validation of *CecB*, *Cec-Ψ2* and *Andropin* gene expression
(**A.B**) qRT-PCR of *CecB* (A) and *Cec-Ψ2* (B) expression in w^{1118}, ΔCec^{A-C}, *ΔAMP10* and *ΔAMP14* flies 6 hours post *Ecc15* infection. (C) qRT-PCR of *Andropin* expression in w^{1118}, ΔCec^{A-C}, *ΔAMP10,* and *ΔAMP14* male flies (unchallenged conditions).

Figure S2

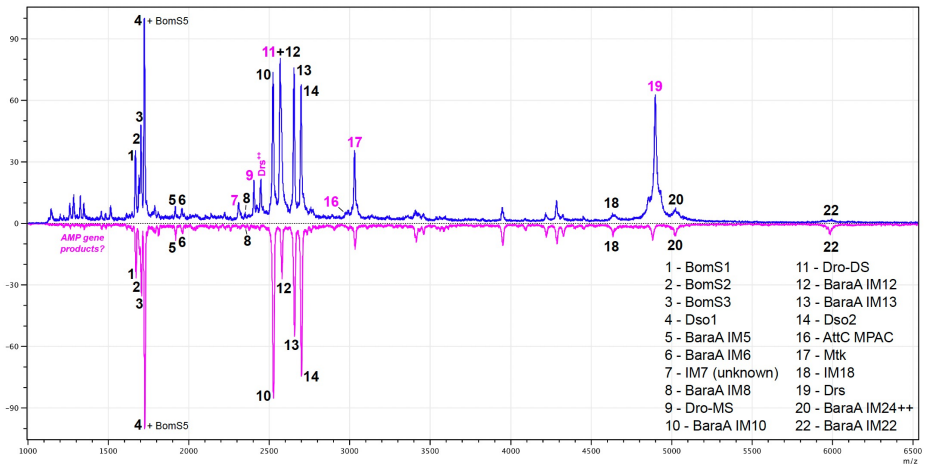

Figure S2.2: *ΔAMP14* flies retain the induction of non-AMP Immune Molecules (IMs) upon systemic infection. Pools of ~40 mixed male and female flies were pricked with a 1:1 mix of OD_{600}=200 *E. coli* and *M. luteus* bacteria, and hemolymph from infected w^{1118} wild-type in blue

(top) and *ΔAMP14* flies in pink (bottom) are shown. Peaks corresponding to AMP products in the wild-type are labelled in pink, including IM7 whose sequence is unknown, but is absent in *ΔAMP14* flies. *Drosophila* IMs are described in (Levy *et al.* 2004), Hanson et al. (2021 (Hanson *et al.* 2021)), and (Uttenweiler-Joseph *et al.* 1998). IM24++ denotes the doubly-charged form of IM24 (~10,031 kDa) that appears at half its mass/charge ratio (~5,015 kDa).

Figure S3

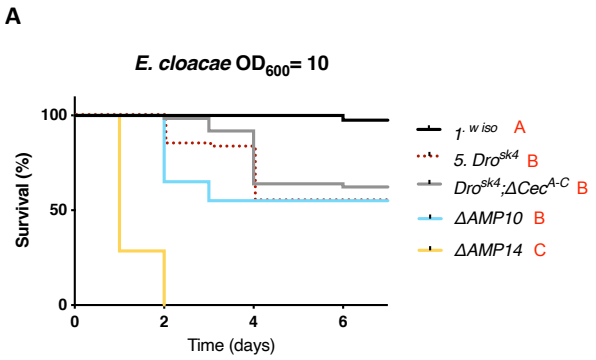

Figure S2.3: *Drosocin^{SK4};ΔCec^{A-C}* double mutants are as susceptible as Drosocin^{SK4} single mutants to *E. cloacae*

(**A**) Survival of single and double mutants following infection suggests that Cecropins do not specifically synergize with Drosocin in defense against *E. cloacae.*

Table 1: Primer list

Species	Gene	F/R	Sequence	Tm	Reference
D. melanogaster	*rpL32*	F	GACGCTTCAAGGGACAGTATC	60°	Bruno Lemaitre
		R	AAACGCGGTTCTGCATGA	60°	
	Pirk	F	CGATGACGAGTGCTCCAC	60°	Kounatidis et al. (2017)
		R	TGCTGCCCAGGTAGATCC	60°	
	PGRP-LB	F	GGACATGCAGGACTTCCA	60°	Iatsenko et al. (2016)
		R	GGTTCTCCAATCTCCGAT	60°	
	BombBc3	F	CTGATCGGCGCTCATCCCAG	60°	Hanson et al. (2016)
		R	GGGATGAGGAGAAGCTGCGG	60°	
	CecA1 and CecA2	F	GAA CTT CTA CAA CAT CTT CGT	60°	Neyen et al. (2014)
		R	TCC CAG TCC CTG GAT T	60°	
	CecB	F	GTCTTTGTGGCACTCATCCTGG	60°	This study
		R	GTATGCTGACCAATGCGTTCGAT	60°	
	Cec-Ψ2	F	TCATCCTGACAATTAACTTGCAACACT	60°	This study
		R	GACGTCAATGACCTCCAATGCTG	60°	
	Andropin	F	CTTGTCGTCCTGGCCCTCAT	60°	This study
		R	AGCATTGTGTATTGCGTTTTCCACT	60°	
	CecC	F	CAACCATTCAAGGACTGGGA	60°	Bruno Lemaitre
		R	CGTTATCCTGGTAGAGTCCTTTG	60°	
B. bassiana	*B. bassiana 18S*	F	18s-1: CGGGTAACGGAGGGTTAGG	60°	Zhang et al. (2009)
		R	18s-2: AGTACACGCGGTGAGGCGG	60°	

DATA AVAILABILITY STATEMENT

Data generated or analyzed during this study are included in the manuscript and supporting files.

ACKNOWLEDGEMENTS

We are thankful to the EPFL Proteomics Core Facility for help with the MALDI-TOF analysis. Brian Lazzaro generously provided *Providencia* species (Galac and Lazzaro 2011) and Adam Bajgar (Krejčová *et al.* 2019) provided *Streptococcus pneumoniae* species used in this study. We thank Hannah Westlake for editing of the manuscript.

FUNDING

This study was funded by the SNF Sinergia grant CRSII5_186397.

CONFLICT OF INTEREST

The authors declare that there is no conflict of interest.

REFERENCES

Andrä J., O. Berninghausen, and M. Leippe, 2001 Cecropins, antibacterial peptides from insects and mammals, are potently fungicidal against Candida albicans. Med Microbiol Immunol 189: 169–173. https://doi.org/10.1007/s430-001-8025-x

Araki M., M. Kurihara, S. Kinoshita, R. Awane, T. Sato, *et al.*, 2019 Anti-tumour effects of antimicrobial peptides, components of the innate immune system, against haematopoietic tumours in Drosophila mxc mutants. Dis Model Mech 12. https://doi.org/10.1242/dmm.037721

Barajas-Azpeleta R., J. Wu, J. Gill, R. Welte, C. Seidel, *et al.*, 2018 Antimicrobial peptides modulate long-term memory. PLoS Genet 14. https://doi.org/10.1371/journal.pgen.1007440

Basset A., R. S. Khush, A. Braun, L. Gardan, F. Boccard, *et al.*, 2000 The phytopathogenic bacteria Erwinia carotovora infects Drosophila and activates an immune response. PNAS 97: 3376–3381. https://doi.org/10.1073/pnas.97.7.3376

Broekaert W. F., G. Terras', A. Cammue, and R. W. Osborn, 1995 Plant Defensins: Nove1 Antimicrobial Peptides as Components of the Host Defense System'. 108: 6.

Bulet P., C. Hetru, J.-L. Dimarcq, and D. Hoffmann, 1999 Antimicrobial peptides in insects; structure and function. Developmental & Comparative Immunology 23: 329–344. https://doi.org/10.1016/S0145-305X(99)00015-4

Cattenoz P. B., R. Sakr, A. Pavlidaki, C. Delaporte, A. Riba, *et al.*, 2020 Temporal specificity and heterogeneity of Drosophila immune cells. EMBO J 39: e104486. https://doi.org/10.15252/embj.2020104486

Chiou P. P., C.-M. Lin, L. Perez, and T. T. Chen, 2002 Effect of Cecropin B and a Synthetic Analogue on Propagation of Fish Viruses In Vitro. Mar. Biotechnol. 4: 294–302. https://doi.org/10.1007/s10126-002-0021-1

Clemmons A. W., S. A. Lindsay, and S. A. Wasserman, 2015 An effector Peptide family required for Drosophila toll-mediated immunity. PLoS Pathog 11: e1004876. https://doi.org/10.1371/journal.ppat.1004876

Coca M., C. Bortolotti, M. Rufat, G. Peñas, R. Eritja, *et al.*, 2004 Transgenic Rice Plants Expressing the Antifungal AFP Protein from Aspergillus Giganteus Show Enhanced Resistance to the Rice Blast Fungus Magnaporthe Grisea. Plant Mol Biol 54: 245–259. https://doi.org/10.1023/B:PLAN.0000028791.34706.80

Cohen L. B., S. A. Lindsay, Y. Xu, S. J. H. Lin, and S. A. Wasserman, 2020 The Daisho Peptides Mediate Drosophila Defense Against a Subset of Filamentous Fungi. Front. Immunol. 11. https://doi.org/10.3389/fimmu.2020.00009

De Gregorio E., P. T. Spellman, P. Tzou, G. M. Rubin, and B. Lemaitre, 2002 The Toll and Imd pathways are the major regulators of the immune response in Drosophila. The EMBO Journal 21: 2568–2579. https://doi.org/10.1093/emboj/21.11.2568

DeLucca A. J., J. M. Bland, T. J. Jacks, C. Grimm, T. E. Cleveland, *et al.*, 1997 Fungicidal activity of cecropin A. Antimicrobial Agents and Chemotherapy 41: 481–483. https://doi.org/10.1128/AAC.41.2.481

Deslouches B., and Y. P. Di, 2017 Antimicrobial peptides with selective antitumor mechanisms: prospect for anticancer applications. Oncotarget 8: 46635–46651. https://doi.org/10.18632/oncotarget.16743

Dudzic J. P., M. A. Hanson, I. Iatsenko, S. Kondo, and B. Lemaitre, 2019 More Than Black or White: Melanization and Toll Share Regulatory Serine Proteases in Drosophila. Cell Rep 27: 1050-1061.e3. https://doi.org/10.1016/j.celrep.2019.03.101

Ekengren S., and D. Hultmark, 1999 Drosophila cecropin as an antifungal agent. Insect Biochemistry and Molecular Biology 29: 965–972. https://doi.org/10.1016/S0965-1748(99)00071-5

Ferreira Á. G., H. Naylor, S. S. Esteves, I. S. Pais, N. E. Martins, *et al.*, 2014 The Toll-Dorsal Pathway Is Required for Resistance to Viral Oral Infection in Drosophila. PLOS Pathogens 10: e1004507. https://doi.org/10.1371/journal.ppat.1004507

Galac M. R., and B. P. Lazzaro, 2011 Comparative pathology of bacteria in the genus Providencia to a natural host, Drosophila melanogaster. Microbes and Infection 13: 673–683. https://doi.org/10.1016/j.micinf.2011.02.005

Ganz T., M. E. Selsted, D. Szklarek, S. S. Harwig, K. Daher, *et al.*, 1985 Defensins. Natural peptide antibiotics of human neutrophils. J Clin Invest 76: 1427–1435. https://doi.org/10.1172/JCI112120

Gregorio E. D., P. T. Spellman, G. M. Rubin, and B. Lemaitre, 2001 Genome-wide analysis of the Drosophila immune response by using oligonucleotide microarrays. PNAS 98: 12590–12595. https://doi.org/10.1073/pnas.221458698

Haine E. R., Y. Moret, M. T. Siva-Jothy, and J. Rolff, 2008 Antimicrobial Defense and Persistent Infection in Insects. Science 322: 1257–1259. https://doi.org/10.1126/science.1165265

Hanson M. A., A. Dostálová, C. Ceroni, M. Poidevin, S. Kondo, *et al.*, 2019a Synergy and remarkable specificity of antimicrobial peptides in vivo using a systematic knockout approach. eLife 8. https://doi.org/10.7554/eLife.44341

Hanson M. A., A. Dostálová, C. Ceroni, M. Poidevin, S. Kondo, *et al.*, 2019b Correction: Synergy and remarkable specificity of antimicrobial peptides in vivo using a systematic knockout approach. eLife 8: e48778. https://doi.org/10.7554/eLife.48778

Hanson M. A., and B. Lemaitre, 2020 New insights on Drosophila antimicrobial peptide function in host defense and beyond. Current Opinion in Immunology 62: 22–30. https://doi.org/10.1016/j.coi.2019.11.008

Hanson M. A., L. B. Cohen, A. Marra, I. Iatsenko, S. A. Wasserman, *et al.*, 2021 The Drosophila Baramicin polypeptide gene protects against fungal infection. PLOS Pathogens 17: e1009846. https://doi.org/10.1371/journal.ppat.1009846

Hedengren-Olcott M., M. C. Olcott, D. T. Mooney, S. Ekengren, B. L. Geller, *et al.*, 2004 Differential Activation of the NF-κB-like Factors Relish and Dif in Drosophila melanogaster by Fungi and Gram-positive Bacteria. Journal of Biological Chemistry 279: 21121–21127. https://doi.org/10.1074/jbc.M313856200

Huang J., Y. Lou, J. Liu, P. Bulet, R. Jiao, *et al.*, 2020 The BaramicinA gene is required at several steps of the host defense against Enterococcus faecalis and Metarhizium robertsii in a

septic wound infection model in Drosophila melanogaster. bioRxiv 2020.11.23.394809. https://doi.org/10.1101/2020.11.23.394809

Hultmark D., H. Steiner, T. Rasmuson, and H. G. Boman, 1980 Insect Immunity. Purification and Properties of Three Inducible Bactericidal Proteins from Hemolymph of Immunized Pupae of Hyalophora cecropia. European Journal of Biochemistry 106: 7–16. https://doi.org/10.1111/j.1432-1033.1980.tb05991.x

Imler J.-L., and P. Bulet, 2005 Antimicrobial Peptides in Drosophila: Structures,Activities and Gene Regulation. Mechanisms of Epithelial Defense 86: 1–21. https://doi.org/10.1159/000086648

Kalsy M., M. Tonk, M. Hardt, U. Dobrindt, A. Zdybicka-Barabas, *et al.*, 2020 The insect antimicrobial peptide cecropin A disrupts uropathogenic Escherichia coli biofilms. npj Biofilms and Microbiomes 6: 1–8. https://doi.org/10.1038/s41522-020-0116-3

Kokoza V., A. Ahmed, S. Woon Shin, N. Okafor, Z. Zou, *et al.*, 2010 Blocking of Plasmodium transmission by cooperative action of Cecropin A and Defensin A in transgenic Aedes aegypti mosquitoes. Proc Natl Acad Sci U S A 107: 8111–8116. https://doi.org/10.1073/pnas.1003056107

Krautz R., D. Khalili, and U. Theopold, 2020 Tissue-autonomous immune response regulates stress signaling during hypertrophy. Elife 9. https://doi.org/10.7554/eLife.64919

Krejčová G., A. Danielová, P. Nedbalová, M. Kazek, L. Strych, *et al.*, 2019 Drosophila macrophages switch to aerobic glycolysis to mount effective antibacterial defense. eLife 8. https://doi.org/10.7554/eLife.50414

Kylsten P., C. Samakovlis, and D. Hultmark, 1990 The cecropin locus in Drosophila; a compact gene cluster involved in the response to infection. The EMBO Journal 9: 217–224. https://doi.org/10.1002/j.1460-2075.1990.tb08098.x

Lazzaro B. P., 2008 Natural selection on the Drosophila antimicrobial immune system. Curr Opin Microbiol 11: 284–289. https://doi.org/10.1016/j.mib.2008.05.001

Lemaitre B., J.-M. Reichhart, and J. A. Hoffmann, 1997 Drosophila host defense: Differential induction of antimicrobial peptide genes after infection by various classes of microorganisms. PNAS 94: 14614–14619. https://doi.org/10.1073/pnas.94.26.14614

Lemaitre B., 2004 The road to Toll. Nature Reviews Immunology 4: 521–527. https://doi.org/10.1038/nri1390

Leulier F., C. Parquet, S. Pili-Floury, J.-H. Ryu, M. Caroff, *et al.*, 2003 The Drosophila immune system detects bacteria through specific peptidoglycan recognition. Nature Immunology 4: 478–484. https://doi.org/10.1038/ni922

Levy F., P. Bulet, and L. Ehret-Sabatier, 2004 Proteomic Analysis of the Systemic Immune Response of Drosophila*. Molecular & Cellular Proteomics 3: 156–166. https://doi.org/10.1074/mcp.M300114-MCP200

Lin S. J. H., L. B. Cohen, and S. A. Wasserman, 2020 Effector specificity and function in Drosophila innate immunity: Getting AMPed and dropping Boms. PLOS Pathogens 16: e1008480. https://doi.org/10.1371/journal.ppat.1008480

Lindsay S. A., S. J. H. Lin, and S. A. Wasserman, 2018 Short-Form Bomanins Mediate Humoral Immunity in Drosophila. J Innate Immun 10: 306–314. https://doi.org/10.1159/000489831

Marra A., M. A. Hanson, S. Kondo, B. Erkosar, and B. Lemaitre, Drosophila Antimicrobial Peptides and Lysozymes Regulate Gut Microbiota Composition and Abundance. mBio 12: e00824-21. https://doi.org/10.1128/mBio.00824-21

Mookherjee N., M. A. Anderson, H. P. Haagsman, and D. J. Davidson, 2020 Antimicrobial host defence peptides: functions and clinical potential. Nat Rev Drug Discov 19: 311–332. https://doi.org/10.1038/s41573-019-0058-8

Ouyang L., X. Xu, S. Freed, Y. Gao, J. Yu, *et al.*, 2015 Cecropins from Plutella xylostella and Their Interaction with Metarhizium anisopliae. PLOS ONE 10: e0142451. https://doi.org/10.1371/journal.pone.0142451

Parvy J.-P., Y. Yu, A. Dostalova, S. Kondo, A. Kurjan, *et al.*, 2019 The antimicrobial peptide defensin cooperates with tumour necrosis factor to drive tumour cell death in Drosophila. eLife 8. https://doi.org/10.7554/eLife.45061

Rahnamaeian M., M. Cytryńska, A. Zdybicka-Barabas, and A. Vilcinskas, 2016 The functional interaction between abaecin and pore-forming peptides indicates a general mechanism of antibacterial potentiation. Peptides 78: 17–23. https://doi.org/10.1016/j.peptides.2016.01.016

Ryu J.-H., S.-H. Kim, H.-Y. Lee, J. Y. Bai, Y.-D. Nam, *et al.*, 2008 Innate immune homeostasis by the homeobox gene caudal and commensal-gut mutualism in Drosophila. Science 319: 777–782. https://doi.org/10.1126/science.1149357

Sackton T. B., B. P. Lazzaro, T. A. Schlenke, J. D. Evans, D. Hultmark, *et al.*, 2007 Dynamic evolution of the innate immune system in Drosophila. Nat Genet 39: 1461–1468. https://doi.org/10.1038/ng.2007.60

Samakovlis C., D. A. Kimbrell, P. Kylsten, A. Engström, and D. Hultmark, 1990 The immune response in Drosophila: pattern of cecropin expression and biological activity. The EMBO Journal 9: 2969–2976. https://doi.org/10.1002/j.1460-2075.1990.tb07489.x

Samakovlis C., P. Kylsten, D. A. Kimbrell, A. Engström, and D. Hultmark, 1991 The andropin gene and its product, a male-specific antibacterial peptide in Drosophila melanogaster. The EMBO Journal 10: 163–169. https://doi.org/10.1002/j.1460-2075.1991.tb07932.x

Schlamp F., S. Y. N. Delbare, A. M. Early, M. T. Wells, S. Basu, *et al.*, 2021 Dense time-course gene expression profiling of the Drosophila melanogaster innate immune response. BMC Genomics 22: 304. https://doi.org/10.1186/s12864-021-07593-3

Seo M.-D., H.-S. Won, J.-H. Kim, T. Mishig-Ochir, and B.-J. Lee, 2012 Antimicrobial Peptides for Therapeutic Applications: A Review. Molecules 17: 12276–12286. https://doi.org/10.3390/molecules171012276

Steiner H., D. Hultmark, A. Engström, H. Bennich, and H. G. Boman, 1981 Sequence and specificity of two antibacterial proteins involved in insect immunity. Nature 292: 246–248. https://doi.org/10.1038/292246a0

Steiner H., D. Andreu, and R. B. Merrifield, 1988 Binding and action of cecropin and cecropin analogues: Antibacterial peptides from insects. Biochimica et Biophysica Acta (BBA) - Biomembranes 939: 260–266. https://doi.org/10.1016/0005-2736(88)90069-7

Suttmann H., M. Retz, F. Paulsen, J. Harder, U. Zwergel, *et al.*, 2008 Antimicrobial peptides of the Cecropin-family show potent antitumor activity against bladder cancer cells. BMC Urology 8: 5. https://doi.org/10.1186/1471-2490-8-5

Tattikota S. G., B. Cho, Y. Liu, Y. Hu, V. Barrera, *et al.*, 2020 A single-cell survey of Drosophila blood. Elife 9. https://doi.org/10.7554/eLife.54818

Troha K., J. H. Im, J. Revah, B. P. Lazzaro, and N. Buchon, 2018 Comparative transcriptomics reveals CrebA as a novel regulator of infection tolerance in D. melanogaster. PLOS Pathogens 14: e1006847. https://doi.org/10.1371/journal.ppat.1006847

Tzou P., J.-M. Reichhart, and B. Lemaitre, 2002 Constitutive expression of a single antimicrobial peptide can restore wild-type resistance to infection in immunodeficient Drosophila mutants. Proc Natl Acad Sci U S A 99: 2152–2157. https://doi.org/10.1073/pnas.042411999

Unckless R. L., V. M. Howick, and B. P. Lazzaro, 2016 Convergent Balancing Selection on an Antimicrobial Peptide in Drosophila. Current Biology 26: 257–262. https://doi.org/10.1016/j.cub.2015.11.063

Uttenweiler-Joseph S., M. Moniatte, M. Lagueux, A. V. Dorsselaer, J. A. Hoffmann, *et al.*, 1998 Differential display of peptides induced during the immune response of Drosophila: A matrix-assisted laser desorption ionization time-of-flight mass spectrometry study. PNAS 95: 11342–11347. https://doi.org/10.1073/pnas.95.19.11342

Yan H., and R. E. W. Hancock, 2001 Synergistic Interactions between Mammalian Antimicrobial Defense Peptides. Antimicrobial Agents and Chemotherapy 45: 1558–1560. https://doi.org/10.1128/AAC.45.5.1558-1560.2001

Zdybicka-Barabas A., P. Mak, A. Klys, K. Skrzypiec, E. Mendyk, *et al.*, 2012 Synergistic action of Galleria mellonella anionic peptide 2 and lysozyme against Gram-negative bacteria. Biochimica et Biophysica Acta (BBA) - Biomembranes 1818: 2623–2635. https://doi.org/10.1016/j.bbamem.2012.06.008

Chapter 3: A humoral stress response protects Drosophila tissues from antimicrobial peptides

Note: This Chapter is based on the manuscript "A humoral stress response protects *Drosophila* tissues from antimicrobial peptides" submitted for publication.

Authors: Samuel Rommelaere, Alexia Carboni, Juan F. Bada Juarez, Jean-Philippe Boquete, Luciano A. Abriata, Fernando Teixeira Pinto Meireles, Verena Rukes, Crystal Vincent, Shu Kondo, Marc S. Dionne, Matteo Dal Peraro, Chan Cao, and Bruno Lemaitre.

Contribution of Alexia Carboni: Designed and performed experiments (survival assays, qPCRs, Western Blots, *in vitro* assays, immunostainings, metabolite quantifications, statistical analysis), analyzed data, gave inputs to the manuscript.

A humoral stress response protects *Drosophila* tissues from antimicrobial peptides

Samuel Rommelaere[1*], Alexia Carboni[1], Juan F. Bada Juarez[2], Jean-Philippe Boquete[1], Luciano A. Abriata[2], Fernando Teixeira Pinto Meireles[2], Verena Rukes[2], Crystal Vincent[3], Shu Kondo[4], Marc S. Dionne[3], Matteo Dal Peraro[2], Chan Cao[1], and Bruno Lemaitre[1*]

[1]- Global Health Institute, School of Life Science, École Polytechnique Fédérale de Lausanne (EPFL), Lausanne, Switzerland

[2]- Institute of Bioengineering, School of Life Science, École Polytechnique Fédérale de Lausanne (EPFL), Lausanne, Switzerland

[3]- Centre for Bacterial Resistance Biology and Department of Life Sciences, Imperial College London, London SW7 2AZ, United Kingdom

[4]-Department of Biological Science and Technology, Faculty of Advanced Engineering, Tokyo University of Science, Tokyo, Japan

*Corresponding authors:
Samuel Rommelaere: samuel.rommelaere@epfl.ch
Bruno Lemaitre : bruno.lemaitre@epfl.ch

Abstract

The immune response against an invading pathogen is generally associated with collateral tissue damage caused by the immune system itself. Consequently, several resilience mechanisms have evolved to attenuate the negative impacts of immune effectors. Antimicrobial peptides (AMPs) are small, cationic peptides that contribute to innate defenses by targeting negatively charged membranes of microbes[1,2]. While being protective against pathogens, AMPs can be cytotoxic to host cells[1,3]. Little is known of mechanisms that protect host tissues from AMP-induced immunopathology. Here, we reveal that a family of stress-induced proteins, the Turandots[4,5], protect *Drosophila* host tissues from AMPs, increasing resilience to stress. Deletion of several *Turandot* genes increases fly susceptibility to environmental stresses due to trachea apoptosis and poor oxygen supply. Tracheal cell membranes expose high levels of phosphatidylserine, a negatively charged phospholipid, sensitizing them to the action of AMPs. Turandots are secreted from the fat body upon stress and bind to tracheal cells to protect them against AMPs. *In vitro*, Turandot A binds to phosphatidylserine on membranes and inhibits the pore-forming activity of *Drosophila* and human AMPs on eukaryotic cells without affecting their microbicidal activity. Collectively, these data demonstrate that Turandot stress proteins mitigate AMP cytotoxicity to host tissues and therefore improve their efficacy. This provides a first example of a humoral mechanism used by animals limiting host-encoded AMP collateral damages.

Introduction

Multiple mechanisms have evolved in animals to ensure homeostasis upon biotic and abiotic stresses. These include the production of heat-shock proteins, cryoprotectants, antioxidants, the unfolded protein response, and compensatory proliferation to replace dead cells, all of which contribute to resilience in stressful conditions[6–8]. These stress pathways also play an active role in defense against microbes, not only to prevent pathogen-induced damage but also to protect the host from deleterious effects of the immune response itself.

Antimicrobial peptides (AMPs) are small, cationic, usually amphipathic peptides that contribute to innate immune defense in plants and animals[1,2,9]. Most display potent antimicrobial activity *in vitro* by disrupting negatively charged microbial membranes. Host membranes of animals typically have a neutral charge and are therefore not affected by pore-forming AMP activity. However, AMPs can be cytotoxic to host cells in certain contexts when expressed at high levels[10–12]. Hypotheses suggest that AMPs could target cell membranes that become negatively charged due to translocation of the phospholipid phosphatidylserine (PS) to the outer leaflet upon stress[13,14]. To date, little is known of host mechanisms that protect tissues against AMP collateral damage during the immune response.

Antimicrobial peptides are well characterized in the fruit fly *Drosophila melanogaster* where they enable resistance of microbial infections and shape the microbiota[1,15,16]. In this insect, systemic infection triggers massive secretion of multiple AMPs by the fat body, an equivalent of the mammalian liver. AMPs can also be induced by abiotic stressors such as osmotic stress or desiccation[17,18]. In *Drosophila*, the *Turandot* (*Tot*) gene family produces eight small secreted proteins that are highly expressed in AMP-like patterns during stress and immune responses[4,5]. Although expression of *Tot* genes is widely used as a readout of the stress response[19–21], their molecular function is unknown. Here we show that Turandot proteins are humoral factors that protect host tissues, notably the respiratory epithelium, from antimicrobial peptides, contributing to stress resilience and host defense.

Results

Turandot-deficient flies have low resilience to stress

Because of their sequence similarity and overlapping expression patterns, we anticipated functional redundancies among the eight *Turandot* genes. To assess their function, we generated compound mutants inactivating up to 6 out of 8 Turandot genes. We first generated a mutant deleted for a genomic cluster of four genes (*TotA*, *TotB*, *TotC* and *TotZ*) called Tot^{AZ}. In this mutant, we then inactivated *TotM*, *TotX,* or both, creating the Tot^{MAZ}, Tot^{AZX} or Tot^{XMAZ} lines, respectively. Tot-deficient flies were viable and fertile. The expression pattern of *Turandot* genes implied that they might play an important role against a broad range of stresses[4,19,20,22,23]. We therefore subjected *Tot*-deficient flies to biotic and abiotic challenges. Tot^{XMAZ} animals showed a mild, yet not significant, susceptibility to systemic infection with *Drosophila* C virus, *Pectobacterium carotovorum carotovorum* (*Ecc15*) or *Enterococcus faecalis*

(**Extended Data Fig. 1a-c**), as compared to isogenic wild-type flies. Strikingly, *Tot*^{XMAZ} flies were more susceptible than wild-type animals to starvation, heat, and osmotic stresses (**Fig. 3.1A-C**). *Tot*^{AZ} mutants showed a mild and variable susceptibility to these stresses, while both *Tot*^{MAZ} and *Tot*^{AZX} displayed a strong and consistent susceptibility to these challenges. *Tot*^{AZX} and *Tot*^{XMAZ} flies were similarly susceptible to all challenges tested (**Fig. 3.1D**). Thus, we mostly used *Tot*^{AZX} and *Tot*^{XMAZ} flies to address Turandot function in the following genetic characterization (see methods). Overexpression of *TotA* alone in the fat body of *Tot*^{XMAZ} flies partially rescued resistance to osmotic stress (**Fig. 3.1E**), confirming that the susceptibility is caused by *Tot* deficiency. Interestingly, ubiquitous overexpression of *TotA* in the *Tot*^{XMAZ} background failed to rescue the survival phenotype, suggesting that ectopic or excessive expression of *TotA* is detrimental to flies (**Extended Data Fig. 1d,e**). Together, these data demonstrate that *Turandot* genes are required for optimal resilience to a broad set of environmental challenges.

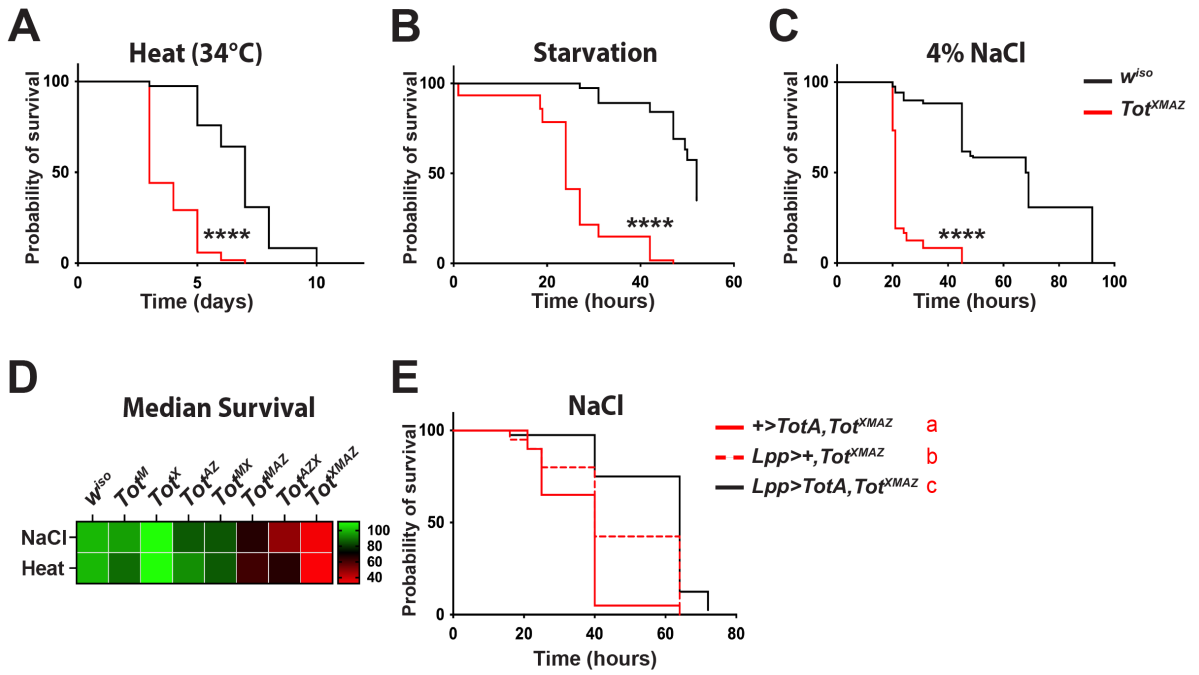

Figure 3.1. Turandot-deficient flies are susceptible to stress

A-C. Survival of wild-type w^{iso} control (black, n=120) and *Tot*^{XMAZ} flies (red, n=120) maintained at 34°C (**A**) or on agar only (**B**) or on food containing 4% NaCl (**C**). **D**. Heatmap representing the median survival of different *Tot*-deficient fly lines to heat and osmotic stresses (normalized to w^{iso}). **E**. Survival upon osmotic stress of +>*TotA;Tot*^{XMAZ} (red, solid line, n=60), *lpp>+;TotA;Tot*^{XMAZ} (red, dashed line, n=80) or *Tot*^{XMAZ} overexpressing *TotA* in the fat body (*lpp>TotA;Tot*^{XMAZ} black, n=80). Results shown are a pool of 3 independent experiments. (****, p<0.00005; CoxPH test, followed by bonferonni correction when applicable. In this case, a compact letter display was used to show the statistics (see methods)).

Secreted TotA binds to trachea

We next analyzed the expression pattern of Tot proteins, focusing on TotA. Western blot with an anti-TotA polyclonal antibody confirmed secretion of this protein into the hemolymph (insect circulatory fluid) (**Fig. 3.2A**). Immunostaining also revealed the presence of TotA in the fat body and, to a lesser extent, on trachea (insect respiratory system) and visceral muscles of unchallenged flies (**Fig. 2B and Extended Data Fig. 2a,b**). TotA was mostly localized at the plasma membrane and in intracellular punctae **(Fig. 3.2B)**. Osmotic stress and bacterial infection increased TotA staining in the fat body and the trachea (**Fig. 3.2C and 3.2D**). Because TotA is weakly expressed in trachea in basal conditions (**Extended Data Fig. 2c**), we hypothesized that this staining could result from tracheal binding of TotA secreted by the fat body. Consistent with this, HA-tagged TotA was observed on trachea when remotely expressed in the fat body **(Fig. 3.2E)**. Similar results were obtained with TotM overexpression, suggesting that fat body-derived Tots bind to trachea (**Extended Data Fig. 2d**). Conversely, knocking down TotA in the fat body reduced TotA staining of the trachea (**Fig. 3.2F**). Finally, we injected recombinant TotA protein into *TotA*-deficient animals and detected it on the plasma membranes of the fat body and trachea (**Fig. 3.2G**). These data show that upon stress TotA is secreted into the hemolymph and binds to fat and tracheal cells.

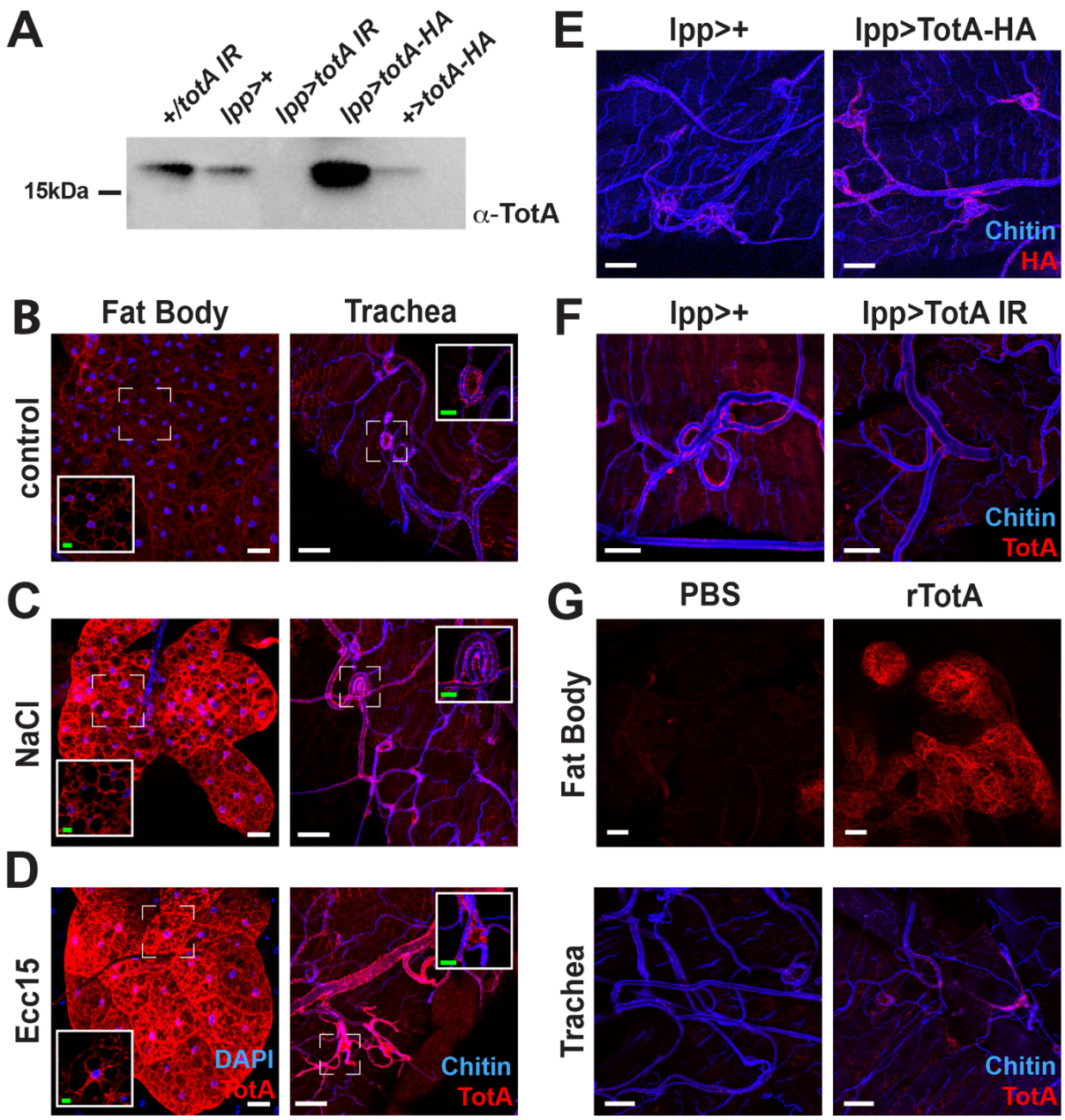

Figure 3.2. Fat body-secreted Turandots bind to trachea

A. Anti-TotA Western blot analysis of hemolymph from animals overexpressing TotA-HA or TotA RNAi in the fat body. **B-D**. Anti-TotA immunostaining of fat bodies (left) or gut trachea (right) of unchallenged flies (**B**) or flies exposed to osmotic stress (NaCl, **C**) or *Ecc15* infection (**D**). Insets show high magnification of the area defined by the white dotted square. Image brightness in these insets was adjusted to highlight the punctated structures **E**. Anti-HA immunostaining of trachea from control (left) or TotA-HA overexpressing (right) flies. **F**. Anti-TotA immunostainings of trachea from wild-type flies (left) or flies overexpressing TotA RNAi in the fat body (right). **G**. Anti-TotA immunostaining of fat bodies (upper panels) and trachea (lower panels) from flies injected with PBS (left) or with recombinant TotA. Blue, chitin; Red, TotA or TotA-HA. Scale bar: white, 20μm, green, 5 μm.

Turandots maintain tissue oxygenation by protecting trachea from apoptosis.

The binding of fat body-produced Tot proteins to trachea was unexpected. Therefore, we further investigated the role of Turandots in the respiratory epithelium upon stress, focusing on the tracheal network around the gut. We found that *Tot*^{XMAZ} mutant flies had fewer terminal tracheal cells (TTC), and reduced tracheal coverage of the midgut compared to wild-type flies, as revealed by autofluorescence[24] (**Fig. 3.3A-C**) or a *dSRF>GFP* tracheal reporter[25] (**Fig. 3.3D**). Overexpressing *TotA* in the fat body of *Tot*^{XMAZ} flies was sufficient to restore TTC numbers comparable to wild-type flies (**Fig. 3.3E)**. As we did not detect any anatomical defect in the trachea of *Tot*^{XMAZ} larvae (**Extended Data Fig. 3**), we speculated that Turandots were required during metamorphosis to ensure proper tracheal morphogenesis, consistent with the high expression of Tots at the pupal stage[26]. Adult tracheal branching is modulated by nutrient cues and infection[24,27,28], which prompted us to test whether stress could affect tracheation. Osmotic stress significantly reduced TTC number and tracheal coverage in wild-type animals to the level observed in unchallenged *Tot*^{XMAZ} flies, showing that the tracheal system is intrinsically vulnerable to environmental stresses (**Fig. 3.3B and 3.3C**). Osmotic stress did not further reduce TTC number in *Tot*^{XMAZ} flies, suggesting that tracheation was reduced in these flies regardless of challenge.

The main function of trachea is tissue oxygenation and CO_2 disposal[29]. As expected, the reduced tracheation observed in *Tot* mutant flies resulted in lower tissue oxygenation, as measured by a transgene expressing a fluorescent oxygen sensor[30] (**Fig. 3.3F**). Furthermore, flow-through respirometry revealed that *Tot*^{XMAZ} flies consumed less O_2 and produced less CO_2 than wild-type (**Fig. 3.3G**). These results suggested that O_2 delivery may limit the ability of *Tot*-deficient flies to cope with stress. To test this hypothesis, we exposed flies to osmotic stress at varying oxygen pressures. Hypoxia increased the susceptibility of both wild-type and *Tot*^{XMAZ} flies to osmotic stress (**Fig. 3.3H**), highlighting the importance of oxygenation to resist this stress. Strikingly, hyperoxia partially rescued *Tot*^{XMAZ} susceptibility to osmotic stress (**Fig. 3.3I**). These data demonstrate that Turandot-mediated support of oxygen delivery by trachea is critical to survive environmental stress.

Because *Tot*-deficient flies had reduced terminal tracheal cells, we hypothesized that these cells may undergo apoptosis. Consistent with this, we observed increased cleaved caspase-3 and TUNEL staining in trachea of *Tot*-deficient animals upon osmotic stress, as compared to wild-type flies (**Fig. 3.3J-L**). Conversely, expression of the apoptosis inhibitor p35[31] in trachea restored wild-type TTC numbers in *Tot*^{AZX} animals (**Fig. 3.3M**) and restored resilience to osmotic stress (**Fig. 3.3N**). These results show that Turandot proteins maintain oxygen supply upon stress by preventing tracheal cell apoptosis.

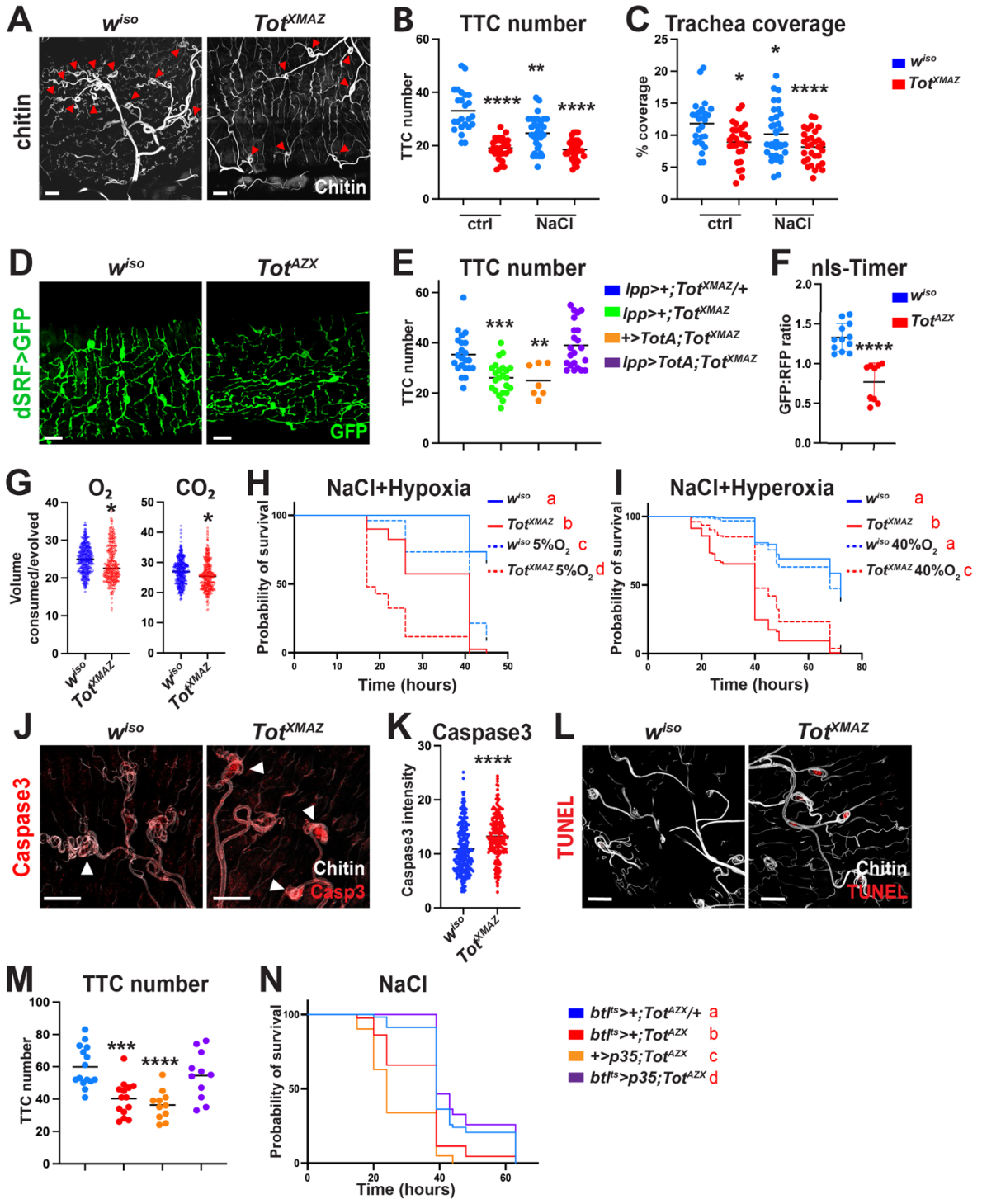

Figure 3.3. Turandots promote resilience to stress by preventing tracheal apoptosis

A. Chitin autofluorescence (grey) of gut trachea of w^{iso} (left) or Tot^{XMAZ} (right) flies. Red arrowheads indicate TTC. **B,C**. Quantification of gut TTC (**B**) and tracheal coverage (**C**) from w^{iso} (blue) and Tot^{XMAZ} (red) flies in unchallenged condition or exposed to osmotic stress. **D**. Anti-GFP immunostaining (green) of gut trachea from *dsrf>GFP* (left) or *dsrf>GFP,*Tot^{AZX} (right) flies. **E**. Expression of TotA by the fat body Gal4 driver (*lpp-Gal4*) restores wild-type TTC counts in Tot^{XMAZ} flies. **F**. Ratiometric analysis of the oxygen *nls-timer* fluorescence in wild-type (blue) or Tot^{AZX} flies (red). **G**. O_2 consumption (left) and CO_2 production (right) of w^{iso} (blue) or Tot^{XMAZ} (red) flies. **H,I**. Survival to osmotic stress of w^{iso} (blue) and Tot^{XMAZ} (red) flies kept in normoxia (solid line), hypoxia (dashed line, **H**) or hyperoxia (dashed line, **I**). **J**. Cleaved caspase-3 (red, arrowheads) staining of

trachea (chitin, white) from w^{iso} (left) or Tot^{XMAZ} flies exposed to osmotic stress. **K**. Quantification of caspase-3 staining intensity in TTC from w^{iso} (blue) or Tot^{XMAZ} (red) flies fed NaCl food. **L**. TUNEL staining (red) staining of trachea (chitin, white) from w^{iso} (left) or Tot^{XMAZ} flies exposed to osmotic stress. **M,N.** Gut TTC quantification (**M**) and survival to osmotic stress (**N**) of Tot^{AZX} flies overexpressing p35 in trachea using the *btl-Gal4* driver. Scale bar: 20μm. Histograms: the horizontal bar indicates the mean, each dot represents an independent animal, except in panel K. Survival plots show a pool of at least 3 independent experiments. Statistics: ordinary one-way ANOVA followed by a Dunnett's multiple comparisons test (B,C,E); Mann-Whitney test (F,K); Welch two sample t-test (G); CoxPH test followed by bonferonni corrections (H,I). ns, not significant; $p \geq 0.05$, * for *P* between 0.01 and 0.05; ** for *P* between 0.001 and 0.01, *** for *P* between 0.0001 and 0.001, **** for $p \leq 0.0001$.

Turandots prevent PS-dependent tracheal cell killing

Since TTC appeared to die from apoptosis in *Tot*-deficient flies, we looked at the presence of phosphatidylserine (PS), an early marker of cell death[13,14]. PS is usually confined to the cytoplasmic leaflet of the membrane but becomes exposed upon apoptosis. PS asymmetry is maintained by flippases of the P4-ATPase family, while scramblases promote PS exposure on the outer layer of the membrane[32,33]. A transgene expressing Annexin-V-GFP revealed increased levels of PS at the surface of tracheal membranes of *Tot*-deficient flies upon osmotic stress, as compared to wild-type flies (**Extended Data Fig. 4a,b**). Unexpectedly, we found that both wild-type and *Tot* mutant trachea spontaneously exposed measurable amounts of PS compared to other tissues, even without external challenge (**Fig. 3.4A and Extended Data Fig. 4c**). Strong Annexin-V staining was restricted to trachea and some muscles (**Extended Data Fig. 4 d,e**). We then explored whether the high PS exposure on tracheal cells could explain their susceptibility to stress. Overexpressing the mouse scramblase *xkr8* in trachea of wild-type flies to increase PS exposure reduced TTC numbers and resilience to osmotic stress (**Fig. 3.4B and 3.4C).** Conversely, lowering levels of PS exposed on trachea by knocking down *scramblase 1* in *Tot*-deficient flies restored normal TTC numbers and reduced susceptibility to stress (**Fig. 3.4D and 3.4E**). Collectively, these results indicate that high constitutive PS exposure on trachea contributes to their vulnerability to stressful conditions.

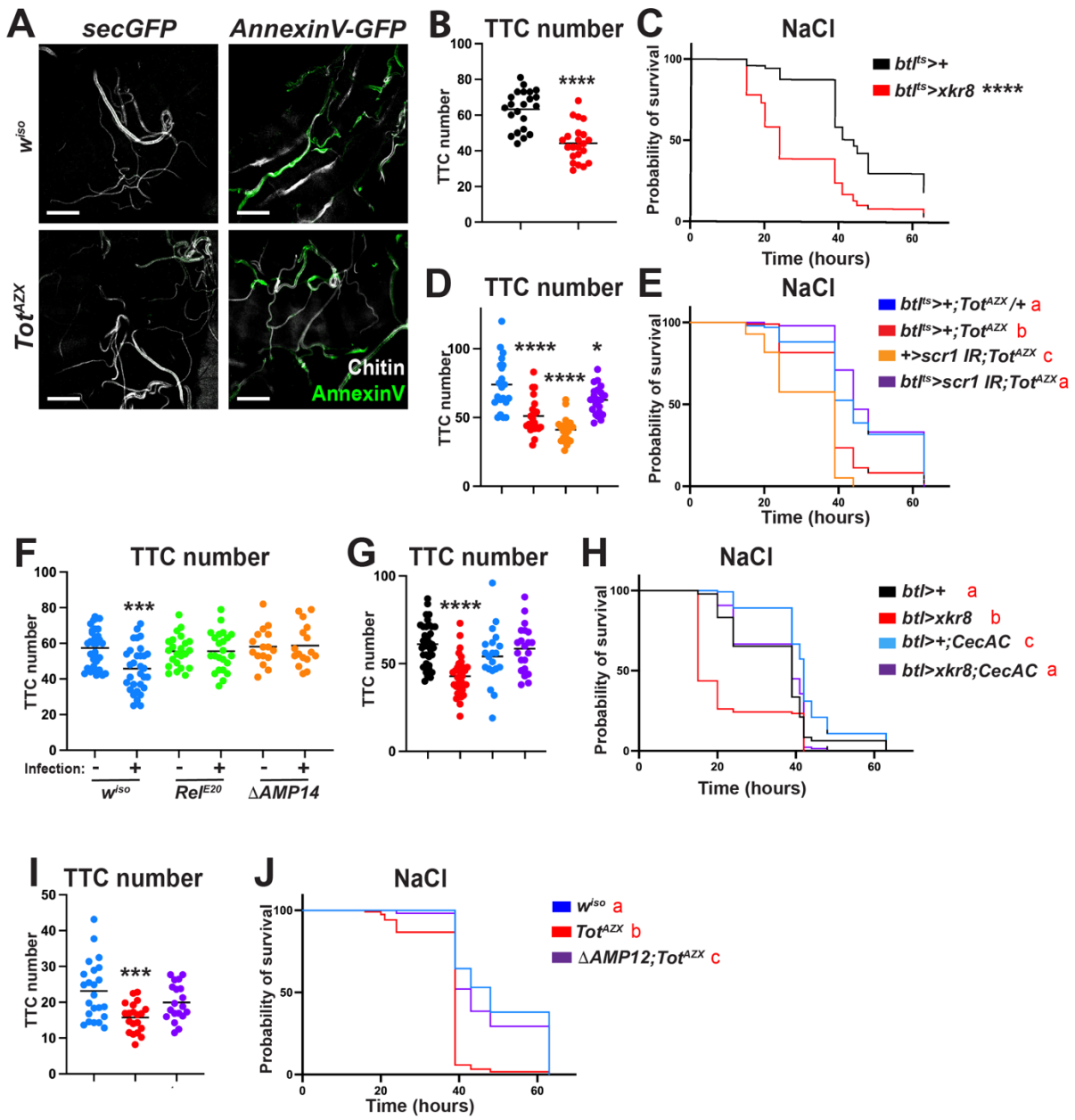

Figure 3.4. Turandots prevent PS-dependent tracheal cell killing by AMPs

A. Immunostaining of trachea from control (upper panels) and *Tot*-deficient flies (lower panels) overexpressing a secreted GFP (secGFP) (left) or Annexin-V-GFP (right) in the fat body. Blue, Chitin; Green, GFP; Scale bar: 20µm. **B,C**. Quantification of TTC numbers (**B**) and survival to osmotic stress (**C**) of wild-type flies overexpressing *xkr8* in trachea with the *btl*^{ts} driver. **D,E**. Quantification of TTC numbers (**D**) and survival to osmotic stress (**E**) of *Tot*^{AZX} flies over-expressing *scramblase 1* RNAi in trachea with the *btl*^{ts} driver. (**F**) Quantification of TTC numbers of *w*^{iso} (blue), *Rel*^{E20} (green) and *ΔAMP14* (orange) flies unchallenged or injured with heat-killed bacteria. **G,H**. A deletion removing four *Cecropin* genes (*CecA*C) rescues TTC numbers (**G**) and survival to osmotic stress of flies overexpressing *xkr8*. **I,J.** Quantification of TTC number (**I**) and survival to osmotic stress (**J**) of *w*^{iso} (blue), *Tot*^{AZX} (red) and *ΔAMP12;Tot*^{AZX} (purple) flies. Scale bar: 20µm. Histograms: the horizontal bar indicates the mean, each dot represents an independent animal. Survival plots show a pool of at least 3 independent experiments. Statistics: ordinary one-way ANOVA followed by a Dunnett's multiple comparisons test (B,F,G,I); Mann-Whitney test (D); CoxPH test followed by bonferonni correction (C,E,H,J). ns, not significant; p ≥ 0.05, * for *P* between 0.01 and 0.05; *** for *P* between 0.0001 and 0.001, **** for p ≤ 0.0001.

TotA prevents PS-dependent apoptosis of trachea by antimicrobial peptides.

As PS is negatively charged, exposure on the outer leaflet is expected to sensitize cells to damage by cationic pore-forming AMPs[1,11,34]. We hypothesized that Tot may promote tracheal survival by preventing AMP-dependent cell death. To test this model, we monitored tracheal morphology in immune-challenged flies expressing high levels of AMPs. Infection with heat-killed bacteria decreased TTC number in wild-type animals, showing that the innate immune response adversely impacts trachea survival. Strikingly, neither Imd pathway deficient flies (*Relish*^{E20})[35], that fail to express most AMPs, nor flies lacking 14 AMP genes *(ΔAMP14*)[36], showed a reduction in TTC number after infection with heat-killed bacteria (**Fig. 3.4F**). These observations strongly suggested that AMPs directly kill tracheal cells during the immune response. We next tested whether tracheal killing by AMPs relied on PS exposure. The reduction of TTC numbers and the vulnerability to stress of flies displaying high PS exposure due to the overexpression of *xkr8* in trachea was rescued in absence of Cecropins, a major class of AMPs[36,37] **(Fig. 3.4G and 3.4H).** These data reveal that AMPs kill tracheal cells in a PS-dependent manner, leading to reduced resilience to osmotic stress. Assuming that Tots protect against AMP cytotoxic activity, we expected that removing AMP genes would be sufficient to reduce the vulnerability of *Tot* flies to stress. To test this notion, we generated a fly line simultaneously lacking six Tots and 12 AMPs and monitored tracheation and stress resilience in these flies. Strikingly, tracheation and resilience to osmotic stress in *ΔAMP12, Tot*^{AZX} flies were similar to those observed in wild-type flies (**Fig. 3.4I and 3.4J**). We conclude that Tot proteins mitigate damage caused by AMPs to tracheal cells exposing PS.

TotA prevents AMP-dependent pore formation

Previous studies have shown that AMPs can be cytotoxic to host cells in certain contexts[1,3].We therefore explored whether Tot proteins could protect host cells from AMP activity *in vitro*, focusing on *TotA*. Electrophysiology recordings on artificial lipid bilayers mimicking eukaryotic membranes confirmed that the antibacterial peptides Cecropin A (CecA) made transient pores in PS-rich membranes[38–40] (**Fig. 3.5A**). Strikingly, addition of TotA abrogated CecA-induced pore formation (**Fig. 3.5B and 3.5C**). This result was confirmed in a liposome leakage assay (**Fig. 3.5D**). While CecA alone induced liposome permeabilization, addition of TotA was sufficient to abolish CecA-induced dye leakage. This protective role of TotA was not restricted to CecA. Indeed, TotA was able to prevent liposome leakage caused by Melittin, a potent pore-forming honey bee toxin with AMP activity[41] (**Fig. 3.5E**).

In addition to its antimicrobial activity, the human AMP LL37 has potent antitumoral properties, being capable of killing HL60 human leukemia cells[42]. We explored the impact of TotA on both LL37 microbicidal and antitumoral activities. TotA did not affect LL37 antibacterial activity on *Escherichia coli* (**Fig. 3.5F**). However, HL60 cells treated with a mixture of LL37 and TotA had higher viability than cells treated with

LL37 only, showing that TotA inhibited LL37 activity specifically against eukaryotic cells (**Fig. 3.5G**). These data indicate that TotA directly inhibits the activity of a broad range of AMPs specifically on host cells.

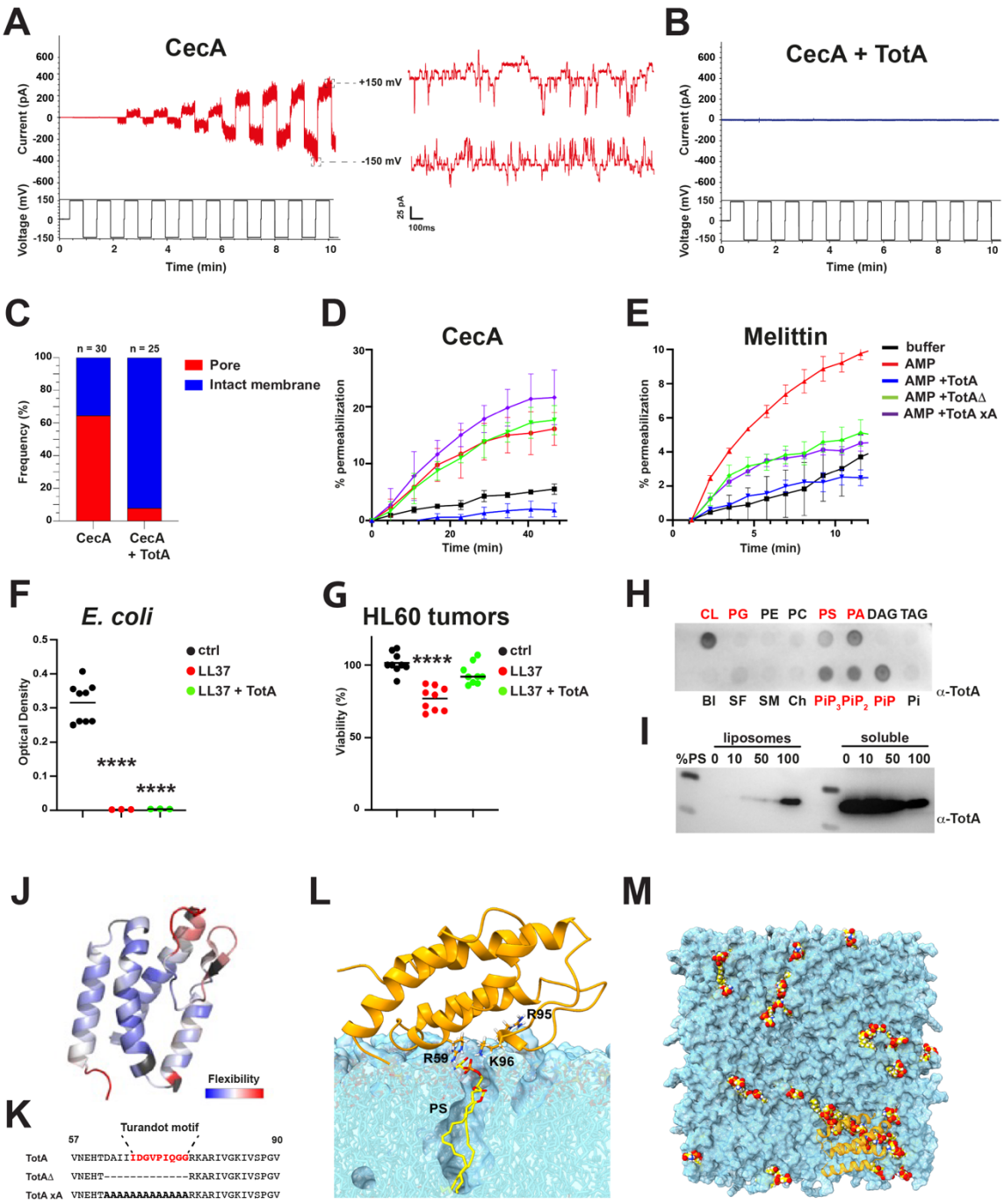

Figure 3.5. TotA prevents pore formation by AMPs

(A-C). Current recordings through lipid bilayer after addition of CecA (**A**) or CecA + TotA (1:2) (**B**). Right panels in **A** show magnified current recordings at positive (upper panel) and negative (lower panel) voltages. (**C**). Quantification of pore formation (red) and intact membranes (blue) after addition of CecA (left) or CecA + TotA (right) to artificial bilayers in 3 independent experiments. (**D-E**) Kinetics of calcein leakage from liposomes incubated with buffer (black), CecA (**D**) or Melittin

(**E**) and buffer (red), or 1μM TotA (blue), TotAΔ (green) or TotAxA (purple). Lines represent averaged values of 3 (cecA) or 2 (melittin) independent experiments with standard deviations. (**F,G**) Viability of *E. coli* (**F**) and HL60 cells (**G**) after incubation with buffer (white), LL37 (orange) or TotA + LL37 (blue). Shown are means (bar) and individual values of 3 independent experiments. (**H**) Representative membrane of a lipid overlay assay incubated with TotA and revealed by anti-TotA antibody. CL, cardiolipin; PG, phosphatidylglycerol ; PE, phosphatidylethanolamine; PC, phosphatidylcholine; PS, phosphatidylserine; PA, phosphatidic acid; DAG, diacylglycerol; TAG, triacylglycerol; PI, phosphatidylinositol; PiP, phosphatidylinositol (4)-phosphate; PiP_2, phosphatidylinositol (4,5)-bisphosphate; PiP_3 phosphatidylinositol (3,4,5)-trisphosphate; Ch, cholesterol; SM, sphingomyelin; SF, 3-sulfogalactosylceramide; Bl, blank. Negatively charged lipids are highlighted in red. (**I**) Anti-TotA Western blot analysis of liposome-containing and soluble fractions after incubation of TotA with liposomes containing increasing amounts of PS. (**J**) TotA structure as determined by NMR. Mapping of ^{1}H-^{15}N heteronuclear NOE onto the NMR structure of TotA, where red hints at more dynamic regions. (**K**) Sequences of TotA from position 57 to 90 containing the Turandot motif (in red) and two variants with this motif deleted (TotAΔ) or alanine-replaced (TotAxA). (**L**) Most representative binding conformation of TotA (orange cartoon) interacting with PS (yellow and red sticks) during the MD simulations. Most relevant charged residues for PS specificity are shown in sticks. (Blue, PE and PC). (**M**) Representative snapshot of the MD simulation showing a lipid bilayer (blue) with some PS lipids (yellow and red spheres) clustering beneath TotA (orange cartoon).

TotA protects host cells from AMPs by sequestering PS

To address the biophysical mechanism underlying AMP inhibition by TotA, we next tested whether TotA could sequester CecA or LL37 in solution. Isothermal titration calorimetry did not reveal any interaction between these AMPs and TotA in solution (**Extended Data Fig. 5a-d**). Therefore, we explored whether TotA could interact with membrane bilayers. Electrophysiology recordings revealed a transient membrane disruption after TotA addition, suggesting a dynamic interaction of TotA with membranes. (**Extended Data Fig. 5e).** We next tested whether TotA could bind to phospholipids using a lipid overlay assay. Strikingly, TotA binding was restricted to negatively charged phospholipids, with the exception of the bacterial lipid phosphatidylglycerol (**Fig. 3.5H**). Accordingly, TotA protein bound to liposomes in a PS-dependent manner, further confirming that TotA interacts with negatively-charged phospholipids (**Fig. 3.5I**).

We then took a structural approach to explore how TotA interacted with membranes. The solution structure of TotA as determined by NMR revealed a four-helix bundle with an internal disordered loop between helix 3 and 4 (**Fig. 3.5J**). This loop was less defined than the rest of the protein, likely because several residues at and around the loop were dynamic across a wide range of timescales. (**Fig. 3.5J and Extended Data Fig. 5f-h**). This flexible loop contains the so-called Turandot motif (*[I/V]-D-G-v-p-x-Q-G-G*), which is shared by all Tot members[4] (**Fig. 3.5K**). We hypothesized that this flexible loop may be important for TotA-mediated AMP inhibition. To test this hypothesis, we designed two protein variants where the loop was deleted (TotAΔ) or entirely replaced with alanines (TotAxA) (**Fig. 3.5K**). Strikingly, both TotA variants were unable to prevent AMP-induced liposome lysis by CecA and

Melittin, in line with the idea that the loop is necessary for AMP inhibition (**Fig. 3.5D and 3.5E**).

We then performed molecular dynamics (MD) simulations of TotA by placing it on the surface of a lipid bilayer model. TotA spontaneously reoriented itself on the membrane, with the Turandot motif loop facing the membrane surface (**Fig. 3.5L and Supplementary Information**). Strikingly, TotA displayed longer residence times around PS when compared to phosphatidylethanolamine (PE) or phosphatidylcholine (PC) lipids, despite PS representing only 10% of the membrane lipid composition (**Extended Data Figure 6a**). Three TotA residues, R59 in helix 2 and R95 and K96 adjacent to the Turandot motif, individually contributed the most to PS binding during the simulations (**Fig. 3.5L**), as assessed by their residence times and occupancy percentage (**Extended Data Figure 6a and b**). This set of interactions triggered a clustering of PS around TotA (**Fig. 3.5M and Supplementary Information**). In contrast TotA did not co-localize as frequently with PC and PE (**Extended Data Figure 6c and 6d)**. Collectively, these results suggest that TotA can sequester PS, thereby preventing their interaction with AMPs and subsequently preserving membrane integrity.

Discussion

In this article, we provide evidence that Turandot proteins promote stress resilience in *Drosophila* by protecting host tissues from AMP-dependent lysis. Strikingly, we observed that TotA neutralizes the pore forming activity of CecA and LL37 on host cells without impacting their microbicidal activity. TotA binds *in vivo* to tracheal cells and can interact with PS-enriched artificial membranes *in vitro*. MD simulations and lipid binding assays show that TotA preferentially interacts with PS, clustering and masking this phospholipid. We hypothesize that PS recruitment and sequestration by TotA shields PS from AMPs, therefore preventing AMP recruitment at the membrane. This would explain the broad protective effect of TotA against phylogenetically distant AMPs. By selectively inhibiting pore formation on eukaryotic cells, Turandot proteins increase AMP selectivity, allowing production of microbicidal AMPs at high concentrations while reducing collateral damage to host tissues.

Surprisingly, Annexin-V staining reveals that tracheal cells constitutively expose high levels of PS in the outer leaflet of the membrane. High PS exposure reduces the asymmetry between the inner and outer leaflet of the membrane and is thought to facilitate cell deformation and prevent shear stress[43,44]. This could be especially important in tracheal branches that are intimately attached to motile tissues, including the muscles and gut, and are constantly exposed to mechanical stress[29]. We believe that Tots emerged through evolution to protect trachea and other tissues that are sensitized to lysis by AMPs due to reduced membrane asymmetry.

Restoration of homeostasis upon stress is energetically costly and requires increased respiration. That lethality of *Tot*-deficient flies with reduced tracheation can be rescued by hyperoxia illustrates that tissue oxygenation by trachea is critical to

survive stress. We suspect that both basal and stress-induced Tot expression by epithelia and the fat body protect the respiratory epithelium. During pupariation, larval trachea undergoes histolysis and adult trachea arise from pupal progenitors. Interestingly, both Tots and AMPs are highly expressed during this stage[4,45]. AMPs are expected to play a prophylactic role during this stage to prevent infection by bacteria escaping the gut during metamorphosis[46]. High Tot expression during metamorphosis would in turn protect trachea from AMPs at this critical stage.

Reports increasingly indicate that AMPs and other cationic peptides can be cytotoxic to host cells in certain contexts[10–12], notably in neurodegeneration[47]. High PS exposure has also been associated with axon degeneration[33], Here we show that exposure of PS[48,49] upon stress or in certain cell types sensitizes them to cationic AMPs. It is therefore tempting to speculate that high PS exposure in neurons could sensitize this tissue to AMP-mediated killing. To our knowledge, our study is the first to identify a class of molecules protecting animal cells from the action of AMPs. Similar mechanisms might exist in other organisms, as suggested by an *in vitro* study showing that two well-known antimicrobial peptides, LL37 and HNP1b, cooperate to kill bacteria more efficiently while minimizing mammalian cell membrane lysis[50]. Identification of factors such as Turandots that protect host cells from AMPs is therefore of therapeutic interest in several contexts, including neurodegeneration.

Extended Data Figures and legends

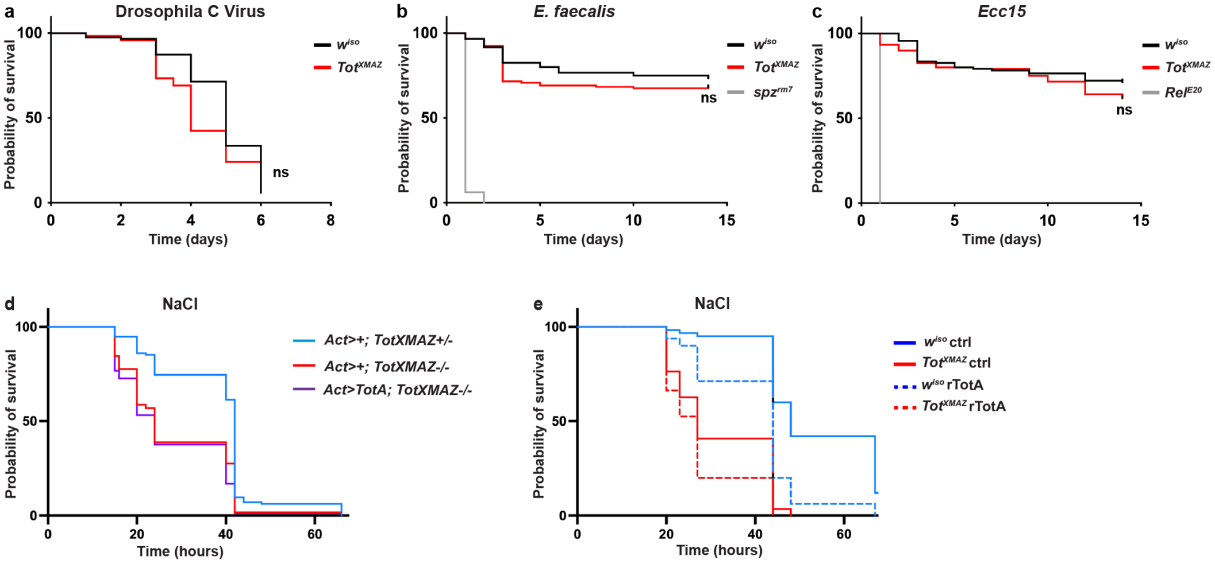

Extended Data Figure 1: **Additional survival phenotypes.** Turandot mutants are not strongly susceptible to microbial infections. w^{iso} (black) or Tot^{XMAZ} (red) female flies were systemically infected with Drosophila C virus (**a**), *Enterococcus faecalis* (**b**) or *Pectobacterium carotovora* (*Ecc15*) (c). $Relish^{E20}$ or spz^{rm7} immune-deficient flies (grey) were used as positive controls in (**b,c**). ns, not significant (Cox-PH test). (**c**) Excessive amounts of TotA reduce resilence to stress. Survival to osmotic stress of *act*>+, Tot^{XMAZ}/+ (red), *act*>+, Tot^{XMAZ} (blue) or upon ubiquitous overexpression of TotA in Tot^{XMAZ} background (*act>totA*, Tot^{XMAZ} purple). (**d**) Survival to osmotic stress of w^{iso} (blue) or Tot^{XMAZ} (red) flies upon injection of PBS (solid lines) or recombinant TotA (dashed lines).

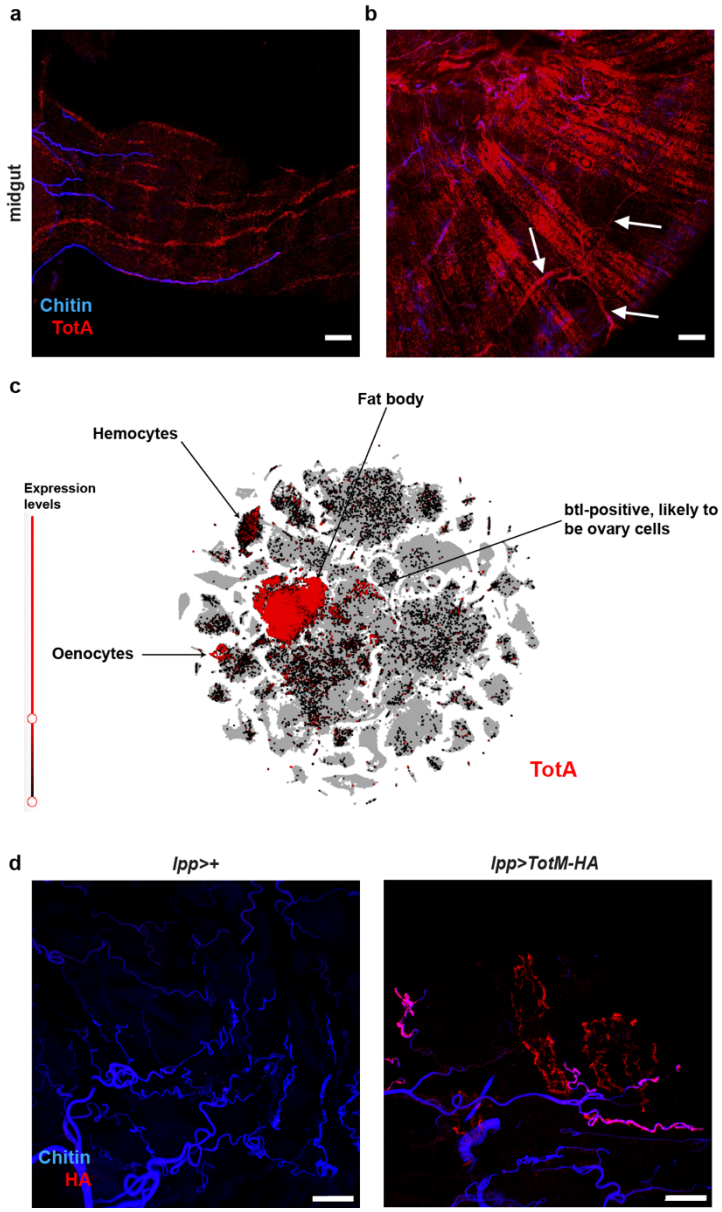

Extended Data Figure 2: **Fat-body-secreted Turandots bind to tracheae and visceral muscles.** (**a,b**) TotA localizes to the visceral muscles. Anti-TotA immunostainings of adult w^{iso} midguts reveal localization to the longitudinal (**a**) and circular (**b**) visceral muscles as well as tracheas (arrows). Blue, chitin; Red, TotA. Scale bar: 20 μm. (**c**) The TotA gene is mostly expressed in the fat body. *t*-distributed stochastic neighbor embedding (t-SNE) plot representing single-cell expression of TotA (red). Shown are TotA expression levels as measured in the 10X Stringent Dataset extracted from FlyCellAtlas ([67]). TotA is mostly expressed in the fat body, in a subset of oenocytes and in hemocytes. Note that some btl-positive cells, which are likely to be ovary cells, express detectable levels of TotA. (**d**) Anti-HA immunostainings of adult *lpp>+* (left) and *lpp>TotM-HA* (right) midguts. Blue, chitin; Red, HA. Scale bar: 20 μm.

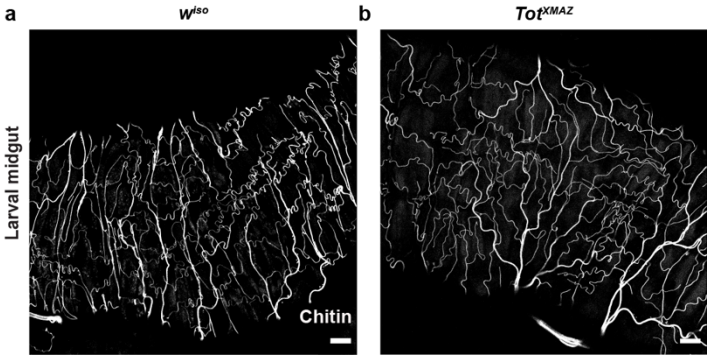

Extended Data Figure 3: Larval gut trachea of w^{iso} and Tot^{XMAZ} larvae have comparable morphologies. Representative pictures of larval gut trachea. Larval tracheas were imaged using chitin autofluorescence (white) of gut trachea of w^{iso} (left) or Tot^{XMAZ} (right) L3 larvae. Scale bar: 20 μm

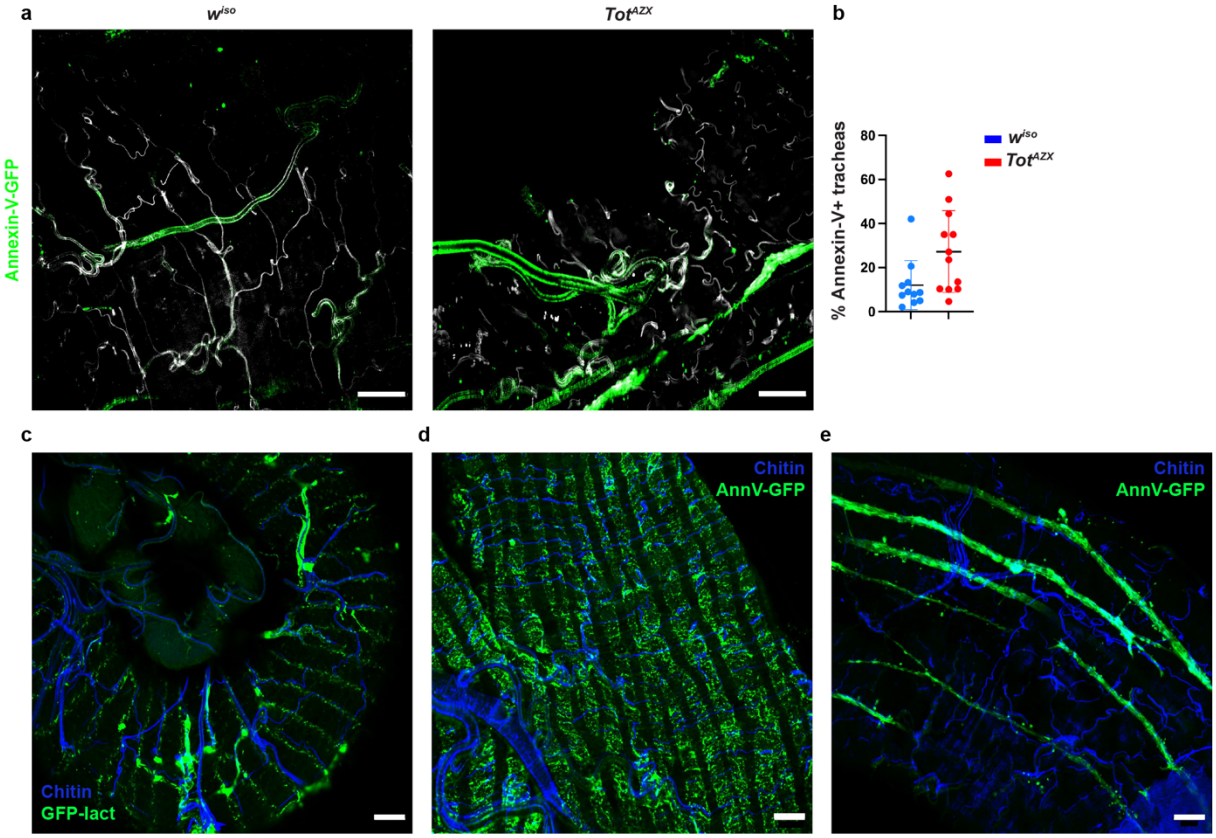

Extended Data Figure 4: Labeling of extracellular phosphatidylserine in adult flies. (a). Anti-GFP (green) immunostaining of trachea from control (left panel, *lpp>AnnexinV-GFP*) or Tot-deficient (right panel, *lpp>AnnexinV-GFP;Tot*^{AZX}) flies exposed to osmotic stress. (**b**) Quantification of the tracheal surface stained by AnnexinV in control (blue) and Tot deficient (red) flies fed NaCl food. (**c,d**)**.** Anti-GFP (green) immunostaining of trachea (**c**) and visceral muscles (**d**) from flies overexpressing the PS-binding protein lactadherin (*lpp>Lact-GFP*). (**e**). Anti-GFP (green) immunostaining revealing Annexin-V binding to the longitudinal visceral muscles in unchallenged wild-type flies (*lpp>AnnexinV-GFP*). Blue, Chitin; Green, GFP; Scale bar: 20μm.

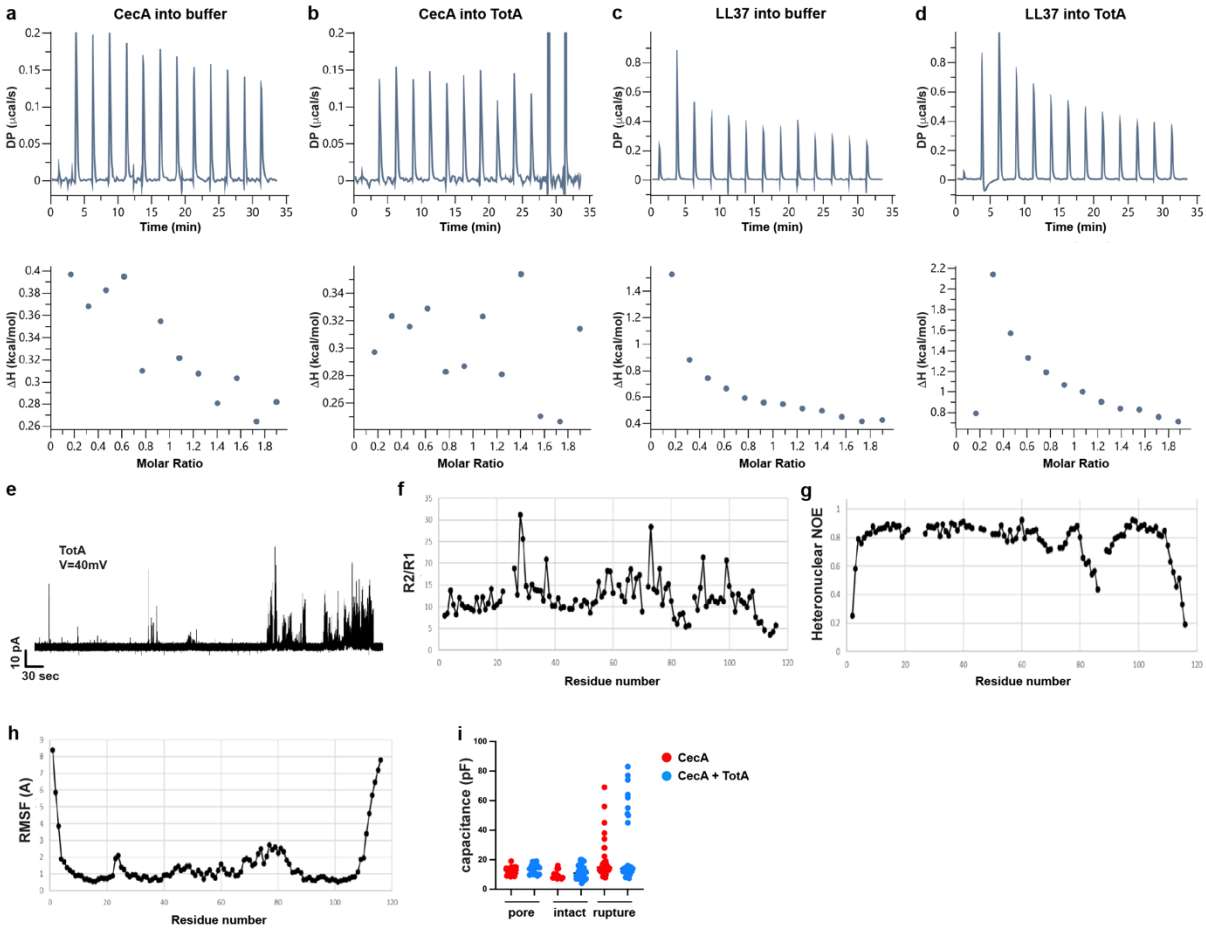

Extended Data Figure 5: Isothermal titration calorimetry and TotA dynamics: Isothermal titration calorimetry experiments reveal no binding of TotA to AMPs. Top panels show Representative raw thermogram plots of Isothermal titration calorimetry experiments. (**a,b**) 2 µL of 2mM CecA were injected 13 times in a chamber containing buffer alone (**a**) or 200 µM TotA (**b**) Lower panels show the integrated data versus molar ratio of peptide to TotA. (**c,d**) 2 µL of 2mM LL37 were injected 13 times in a chamber containing buffer alone (**c**) or 200 µM TotA (**d**). (**e**) Current recordings through lipid bilayer after addition of 4 µM TotA. (**f-h**) Results from ^{15}N relaxation (**g**, R_2/R_1 ratio, **g**, heteronuclear NOE) compared to the flexibility observed in the NMR ensemble (**h**, RMSF to mean structure). In the R_2/R_1 plot, the median reflects a correlation time of 7.45 ns, perfectly consistent with a monomeric, globular, 12 kDa protein as TotA. Positive deviations of the ratio hint at residues experiencing slow exchange, and negative deviations hint at residues undergoing fast dynamics. Likewise, low heteronuclear NOE values indicate fast dynamics, and high RMSF points at flexibility and/or uncertainty in the NMR ensemble. **i**. Capacitances (in pF) of membrane bilayers upon addition of CecA (red) or CecA + TotA (blue) upon pore formation, membrane rupture or when the membrane stayed intact.

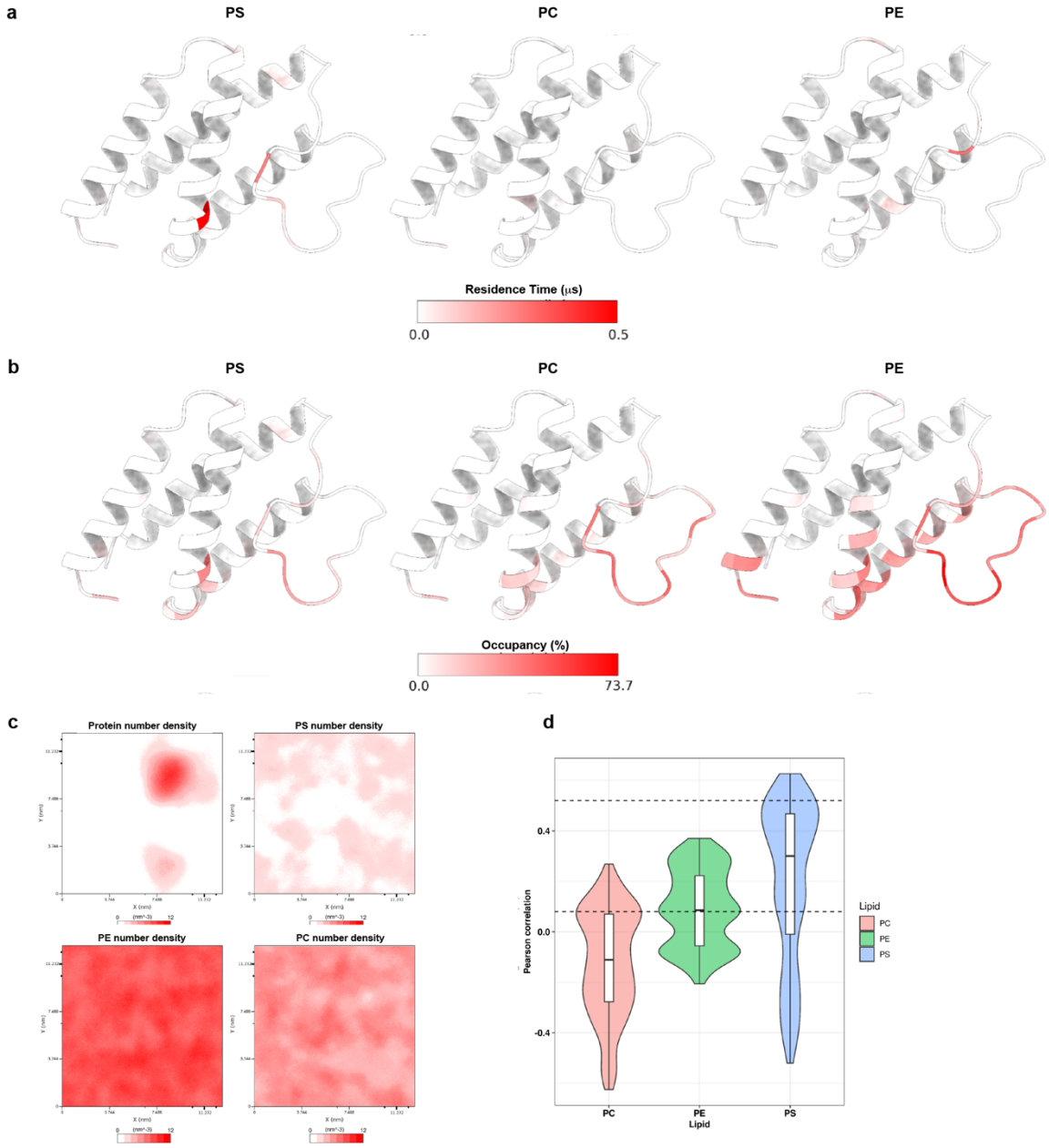

Extended Data Figure 6: Molecular Dynamics (MD) simulations reveal specific binding of TotA to PS: Residue-wise residence times (**a**) and occupancy (**b**) of TotA with PS, PC and PE during the MD simulations. Despite PS displaying the least occupancy as PS is less abundant that the two others (**b**), it does possess the highest residence times during the simulations (**a**). This suggests that TotA has a high specificity towards this lipid. Three TotA residues, R59, R95 and K96, contributed the most to PS specificity based on their residence times (t^{R59} = 0.500 μs, t^{R95} = 0.057 μs, and t^{K96} = 0.154 μs) and occupancy (percentage of simulation time bound to PS, $Occup.^{R59}$ = 39.4%, $Occup.^{R95}$ = 33.6%, and $Occup.^{K96}$ = 36.0%). (**c-d**) TotA and lipid distributions on the XY plane viewed from above the membrane. (**c**) Number density plot of TotA (Protein) and the three lipids during the MD simulations. TotA clustered more to PS when compared to PC and PE. (**d**) Distribution of the correlation between the number density of TotA and the lipid. The position of TotA was more frequently correlated with that of the PS molecules then PC and PE. The dashed lines indicated the mode of the correlation distribution (0.52, for PS, 0.08 for PC and PE).

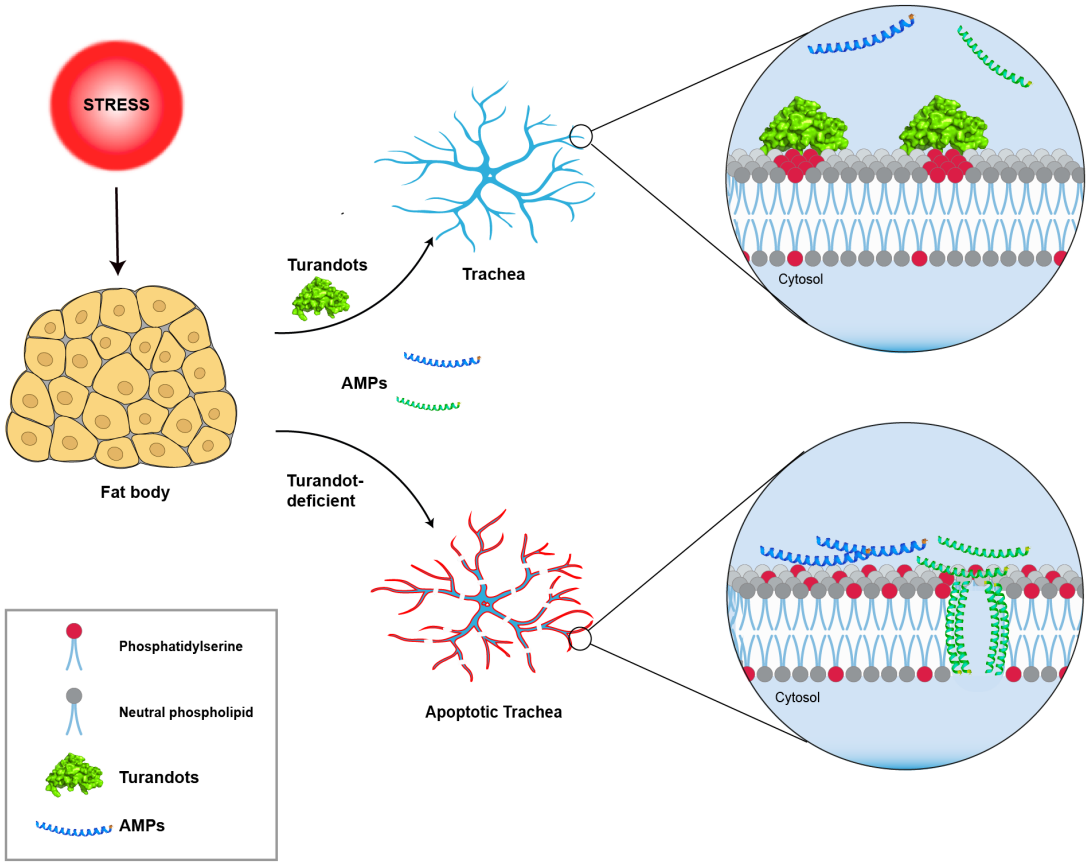

Extended Data Figure 7: Turandots promote stress resilience by protecting *Drosophila* trachea from antimicrobial peptides.
Certain tissues such as trachea expose unusually high amounts of phosphatidylserine even in basal conditions, sensitizing these tissues to cationic antimicrobial peptides. Upon stress exposure, Turandot proteins (green) are secreted into the hemolymph and bind to the membrane of tracheae. (Top) Turandot binding to phosphatidylserine (red) clusters this negatively charged lipid, inhibiting the formation of pores by AMPs (blue and light green), (Bottom) In absence of Turandots, cationic AMPs bind to trachea provoking tracheal apoptosis and lower resilience to stress.

Extended Data Table 1: List of *Drosophila* stocks used in this study

figure	full genotype	short name	origin
figure 1	Iso w^{1118} DrosDel	w iso	Ferreira et al. 2014
	iso;iso;$TotAZ^{SK6}$	TotAZ	this study
	iso;$totM^{JP78}$/CyO	TotM	this study
	iso;$totM^{JP1621}$;$TotX^{JP44}$	TotMX	this study
	iso;$totM^{JP1621}$;$TotAZ^{SK6}$	TotMAZ	this study
	iso;iso;$TotX^{JP44}$, $TotAZ^{SK6}$	TotAZX	this study
	iso;$totM^{JP1621}$;$TotX^{JP44}$, $TotAZ^{SK6}$	TotXMAZ	this study
	iso;iso;$totX^{JP147}$	totX	this study
	iso;$totM^{JP1621}$;iso	TotM	this study
	w^{1118};$totM^{JP1621}$/CyO; lpp-gal4,$TotX^{JP44}$, $TotAZ^{SK6}$/TM3sb	lpp XMAZ	this study
	;UAS-TotA-HA @attP1, $totM^{JP1621}$/CyO; $TotAZ^{SK6}$, $totX^{JP44}$	UAS-totA XMAZ	this study
figure 2	iso w^{1118} DrosDel	w iso	Ferreira et al. 2014
	w;tub-$gal80^{ts}$;lpp-gal4	Lpp>	Brankatschk and Eaton, 2010
	;UAS-HA5UTR-TotA @attP40	UAS-HA-TotA	this study
	iso;$totM^{JP1621}$;$TotX^{JP44}$, $TotAZ^{SK6}$	TotXMAZ	this study
	w^{1118};P(GD6210)v14415	TotA RNAi	VDRC 14415
figure 3	iso w^{1118} DrosDel	w iso	Ferreira et al. 2014
	iso;$totM^{JP1621}$;$TotX^{JP44}$, $TotAZ^{SK6}$	TotXMAZ	this study
	w^{1118};$totM^{JP1621}$/CyO; lpp-gal4,$TotX^{JP44}$, $TotAZ^{SK6}$/TM3sb	lpp XMAZ	this study
	;UAS-TotA-HA @attP1, $totM^{JP1621}$/CyO; $TotAZ^{SK6}$, $totX^{JP44}$	UAS-totA XMAZ	this study
	; ; dsrf-gal4, UAS-PH-GFP, $TotX^{JP44}$, $TotAZ^{SK6}$	dsrf>GFP AZX	Gervais and Casanova 2010 and this study
	w^{1118};; hsp-nls-Timer	timer	Lidsky et al. 2018
	;; hsp-nls-Timer, $TotX^{JP44}$, $TotAZ^{SK6}$	timer AZX	this study
	;btl-gal4,UAS-GFP; tub-$gal80^{ts}$	btl(ts)>GFP	BL8807 and this study
	;btl-gal4, UAS-GFP;$TotAZ^{SK6}$, $totX^{JP44}$, tub-$gal80^{ts}$	btl(ts)>GFP AZX	this study
	w[*]; P{w[+mC]=UAS-p35.H}BH1,TotXJP44, $TotAZ^{SK6}$	p35 AZX	BL5072 and this study
Figure 4	;;UAS-sec-GFP	sec-GFP	Fabrowski et al. 2013 and this study
	;;UAS-sec-GFP,$TotAZ^{SK6}$, $totX^{JP44}$	sec-GFP AZX	Fabrowski et al. 2013 and this study
	;UAS-AnnexinV-GFP	AnnexinV-GFP	Sapar et al. 2018
	;UAS-AnnexinV-GFP;$TotAZ^{SK6}$, $totX^{JP44}$	AnnexinV-GFP AZX	Sapar et al. 2018 and this study
	;btl-gal4, UAS-GFP;$TotAZ^{SK6}$, $totX^{JP44}$, tub-$gal80^{(ts)}$	btl(ts)>GFP AZX	this study
	;scramb1 IR,$TotAZ^{SK6}$, $totX^{JP44}$	scramb1 IR AZX	v107024 and this study
	;btl-gal4, UAS-GFP; tub-$gal80^{(ts)}$	btl(ts)>GFP	BL8807 and this study
	iso;iso;$RelE^{20}$	RelE20	BL55714
	Def^{SK3}, $AttC^{Mi}$, Dro-$AttAB^{SK2}$, Mtk^{R1}, Dpt^{SK1}; Drs^{R1}, CecKOΔA-C, $AttD^{SK1}$	AMP14	Carboni et al. 2022
	;UAS-xkr8/CyoGFP	UAS-xkr8	Sapar et al. 2018
	;btl-gal4, UAS-GFP;	btl>GFP	BL8807
	;btl-gal4, UAS-GFP; $CecKO^{\Delta A-C}$	btl>GFP; CecAC	BL8807 and this study
	;UAS-xkr8/CyoGFP; $CecKO^{\Delta A-C}$	UAS-xkr8; CecAC	Sapar et al. 2018 and this study
	iso;DefSK3, $AttC^{Mi}$, Dro-$AttAB^{SK2}$, Mtk^{R1}, Dpt^{SK1}; iso;iso;$CecKO^{\Delta A-C}$,$TotX^{JP44}$, $TotAZ^{SK6}$	AMP12,AZX	this study
	iso w^{1118} DrosDel	w iso	Ferreira et al. 2014
	iso;iso;$TotX^{JP44}$, $TotAZ^{SK6}$	TotAZX	this study
	w^{1118};; lpp-gal4,$TotX^{JP44}$, $TotAZ^{SK6}$/TM3sb	lpp> AZX	this study
Extended data figure 1	w^{1118};$totM^{JP1621}$, act-gal4/CyO; $TotX^{JP44}$, $TotAZ^{SK6}$/TM3sb	act> XMAZ	BL3853 and this study
	iso w^{1118} DrosDel	w iso	Ferreira et al. 2014
	;UAS-TotA-HA @attP1, $totM^{JP1621}$/CyO; TotAZ, $totX^{JP44}$	UAS-totA XMAZ	this study
	iso;$totM^{JP1621}$;$TotX^{JP44}$, $TotAZ^{SK6}$	TotXMAZ	this study
Extended data figure 2	w;tub-$gal80^{ts}$;lpp-gal4	Lpp>	Brankatschk and Eaton, 2010
	;UAS-TotM-HA@attP1	TotM-HA	this study
	iso w^{1118} DrosDel	w iso	Ferreira et al. 2014
	;UAS-TotA-HA @attP1	TotA-HA	this study
Extended data figure 3	iso w^{1118} DrosDel	w iso	Ferreira et al. 2014
	iso;$totM^{JP1621}$;$TotX^{JP44}$, $TotAZ^{SK6}$	TotXMAZ	this study
Extended data figure 4	w^{1118};tub-$gal80^{ts}$;lpp-gal4	Lpp>	Brankatschk and Eaton, 2010
	w^{1118};; lpp-gal4,$TotX^{JP44}$, $TotAZ^{SK6}$/TM3sb	lpp> AZX	this study
	;UAS-AnnexinV-GFP	AnnexinV-GFP	Sapar et al. 2018
	;UAS-AnnexinV-GFP;$TotAZ^{SK6}$, $totX^{JP44}$	UAS-AnnexinV-GFP;AZX	Sapar et al. 2018 and this study

w^{1118};UAS-GFP-LactC1C2	UAS-lactGFP	Sapar et al. 2018

Extended Data Table 2: NMR and refinement statistics for protein structures

	Protein
NMR distance and dihedral constraints	
Distance constraints	
Total NOE	1061
Intra-residue	225
Inter-residue	836
Sequential ($\|i-j\| = 1$)	352
Medium-range ($\|i-j\| < 4$)	282
Long-range ($\|i-j\| > 5$)	140
Intermolecular	--
Hydrogen bonds	--
Total dihedral angle restraints (from Talos+)	140
ϕ	70
ψ	70
Structure statistics	
Violations (mean and s.d.)	
Distance constraints (Å)	0.5 ± 0.3
Dihedral angle constraints (º)	7.5 ± 2.6
Max. dihedral angle violation (º)	25
Max. distance constraint violation (Å)	1.47
Deviations from idealized geometry	
Bond lengths (Å)	0
Bond angles (º)	0
Impropers (º)	0
Average pairwise r.m.s. deviation* (Å)	
Heavy	3.97 ± 2.37
Backbone	3.28 ± 1.31

* Pairwise r.m.s. deviation was calculated among 20 refined structures throughout the full protein lengths.

Extended Data Table 3: Statistics

			n	test	tailed	correction	group1	group2	pvalue	pvalue_bonferonni
figure 1	A	w	120	coxPH	N/A	N/A			10^{-5}	
		XMAZ	120	coxPH	N/A	N/A				
	B	w	120	coxPH	N/A	N/A			10^{-16}	
		XMAZ	121	coxPH	N/A	N/A				
	C	w	120	coxPH	N/A	N/A			10^{-16}	
		XMAZ	120	coxPH	N/A	N/A				
	E	UAS-totA;XMAZ	60	coxPH	N/A	bonferonni				
		lpp>+;XMAZ	80	coxPH	N/A	bonferonni				
		lpp>totA;XMAZ	80	coxPH	N/A	bonferonni				
		multiple comparisons					UAS-totA;XMAZ	lpp>+;XMAZ	1.19341586034287e-08	7.16049516205724e-08
							UAS-totA;XMAZ	lpp>TotA;XMAZ	1.45061994768379e-18	8.70371968610274e-18
							lpp>+;XMAZ	UAS-totA;XMAZ	1.19341586034287e-08	7.16049516205724e-08
							lpp>+;XMAZ	lpp>TotA;XMAZ	2.92399262162095e-06	1.75439557297257e-05
							lpp>TotA;XMAZ	UAS-totA;XMAZ	1.45061994768379e-18	8.70371968610274e-18
							lpp>TotA;XMAZ	lpp>+;XMAZ	2.92399262162095e-06	1.75439557297257e-05
figure 3	B	w	24	one way ANOVA	one-tailed	dunnett's				
		XMAZ	26	one way ANOVA	one-tailed	dunnett's			<0.0001	
		w nacl	33	one way ANOVA	one-tailed	dunnett's			<0.0001	
		XMAZ nacl	31	one way ANOVA	one-tailed	dunnett's			<0.0001	
	C	w	26	one way ANOVA	one-tailed	dunnett's				
		XMAZ	29	one way ANOVA	one-tailed	dunnett's			0,0032	
		w nacl	34	one way ANOVA	one-tailed	dunnett's			0,06	
		XMAZ nacl	31	one way ANOVA	one-tailed	dunnett's			0,0002	
	E	lpp>w XMAZ+/-	22	one way ANOVA	one-tailed	dunnett's				
		lpp>w XMAZ-/-	21	one way ANOVA	one-tailed	dunnett's			0,0005	
		lpp>TotA-HA XMAZ-/-	22	one way ANOVA	one-tailed	dunnett's			0,2873	
		UAS-TotA-HA XMAZ-/-	7	one way ANOVA	one-tailed	dunnett's			0,009	
	F	hs>nls-timer AZX+/-	12	mann-whitney	two-tailed	N/A			<0.0001	
		hs>nls-timer AZX-/-	9	mann-whitney	two-tailed	N/A			<0.0001	
	G	w	408	Welch two sample t-test		N/A			<0.05	
		XMAZ	303	Welch two sample t-test		N/A			<0.05	
	H	w normoxia	49	coxPH	N/A	bonferonni				
		XMAZ normoxia	80	coxPH	N/A	bonferonni				
		w hypoxia	77	coxPH	N/A	bonferonni				
		XMAZ hypoxia	77	coxPH	N/A	bonferonni				
		multiple comparisons					w normoxia	XMAZ normoxia	2,34E-15	2,81E-14
							w normoxia	w hypoxia (4% O2)	6,84E-10	8,21E-09
							w normoxia	XMAZ hypoxia (4% O2)	7,14E-19	8,57E-18
							XMAZ normoxia	w hypoxia (4% O2)	0,000118997	0,001427969
							XMAZ normoxia	XMAZ hypoxia (4% O2)	3,06E-10	3,68E-09
							w hypoxia (4% O2)	XMAZ hypoxia (4% O2)	1,01E-17	1,21E-16
	I	w normoxia	162	coxPH	N/A	bonferonni				
		XMAZ normoxia	162	coxPH	N/A	bonferonni				
		w hyperoxia	160	coxPH	N/A	bonferonni				
		XMAZ hyperoxia	155	coxPH	N/A	bonferonni				
		multiple comparisons					w normoxia	XMAZ	5.8220943289877e-37	6.98651319478523e-36
							w normoxia	w hyperoxia (40% O2)	0.858922806634268	1
							w normoxia	XMAZ hyperoxia (40%	1.17609999418142e-23	1.41131999301771e-22
							XMAZ	w hyperoxia (40% O2)	1.78262870005903e-32	2.13915444007084e-31
							XMAZ	XMAZ hyperoxia (40%	2.6441909896877e-06	3.17302918762524e-05
							w hyperoxia (40% O	XMAZ hyperoxia (40%	2.03595642176 23e-19	2.44314770611476e-18
	K	w	21	mann-whitney	two-tailed	N/A			<0.0001	
		XMAZ	20	mann-whitney	two-tailed	N/A				
	M	btl(ts)>w AZX +/- ct	15	one way ANOVA	one-tailed	dunnett's				
		btl(ts)>w AZX -/- ct	14	one way ANOVA	one-tailed	dunnett's			0,0002	
		UAS p35 AZX -/- ct	11	one way ANOVA	one-tailed	dunnett's			<0.0001	
		btl(ts)>p35 AZX -/- ct	11	one way ANOVA	one-tailed	dunnett's			0,8899	
		btl(ts)>w AZX +/- ct	58	coxPH	N/A	bonferonni				
		btl(ts)>w AZX -/- ct	44	coxPH	N/A	bonferonni				
		UAS p35 AZX -/- ct	58	coxPH	N/A	bonferonni				
		btl(ts)>p35 AZX -/- ct	62	coxPH	N/A	bonferonni				
	N	multiple comparisons					control	btl(ts)>w AZX -/-	0.00155122498997267	0.018614699879672
							control	btl(ts)>p35 AZX -/-	0.317688812456521	1
							control	UAS p35 AZX -/-	5.23839801496303e-10	6.28607761795564e-09
							btl(ts)>w AZX -/-	btl(ts)>p35 AZX -/-	2.80956090437762e-05	0.000337147308525315
							btl(ts)>w AZX -/-	UAS p35 AZX -/-	0.00238821234797067	0.0286585481756481
							btl(ts)>p35 AZX -/-	UAS p35 AZX -/-	4.69905391510161e-13	5.63886469812194e-12
Figure 4	B	btl(ts)>w AZX +/-	21	one way ANOVA	one-tailed	dunnett's				
		btl(ts)>w AZX -/-	22	one way ANOVA	one-tailed	dunnett's			<0.0001	
		+/scramb1 IR AZX -/-	20	one way ANOVA	one-tailed	dunnett's			<0.0001	
		btl(ts)> scramb1 IR AZX -/-	21	one way ANOVA	one-tailed	dunnett's			0,0231	
	C	btl(ts)>w AZX +/-	101	coxPH	N/A	bonferonni				
		btl(ts)>w AZX -/-	98	coxPH	N/A	bonferonni				
		+/scramb1 IR AZX -/-	99	coxPH	N/A	bonferonni				
		btl(ts)> scramb1 IR AZX -/-	100	coxPH	N/A	bonferonni				
		multiple comparisons					+/scramb1 IR;AZX -/	btl(ts)>w AZX +/-	3.65123058756842e-16	1.09536917627052e-14
							+/scramb1 IR;AZX -/	btl(ts)>w AZX -/-	2.22769354595678e-06	6.68308063787034e-05
							+/scramb1 IR;AZX -/	btl(ts)>scramb1 IR;AZ)	1.00358027556739e-24	3.01074082670218e-23
							btl(ts)>w AZX +/-	btl(ts)>w AZX -/-	1.845478336133e-05	0.00055364350608399
							btl(ts)>w AZX +/-	btl(ts)>scramb1 IR;AZ)	0.676638942442102	1
							btl(ts)>scramb1 IR;A	btl(ts)>w AZX -/-	1.52113068748423e-08	4.56339206245268e-07
	D	btl(ts)>GFP, w	22	mann-whitney	two-tailed	N/A			<0.0001	
		btl(ts)>GFP, xkr8	22	mann-whitney	two-tailed	N/A				
	E	btl(ts)>GFP, w	130	coxPH	N/A	N/A			6.19887959845118e-14	
		btl(ts)>GFP, xkr8	183	coxPH	N/A	N/A				
	F	w ct	32	one way ANOVA	one-tailed	dunnett's				
		w HK	31	one way ANOVA	one-tailed	dunnett's				<0.0001
		rel	23	one way ANOVA	one-tailed	dunnett's				0,9916
		rel HK	23	one way ANOVA	one-tailed	dunnett's				0,9934
		AMP14 ct	16	one way ANOVA	one-tailed	dunnett's				0,9997
		AMP14 HK	16	one way ANOVA	one-tailed	dunnett's				0,9994
	G	btl>GFP, w	36	one way ANOVA	one-tailed	dunnett's				
		btl>GFP, xkr8	32	one way ANOVA	one-tailed	dunnett's				<0.0001
		btl>GFP, w cecAC	20	one way ANOVA	one-tailed	dunnett's				0,1856
		btl>GFP, xkr8 cecAC	21	one way ANOVA	one-tailed	dunnett's				0,9983
		btl>GFP, w	95	coxPH	N/A	bonferonni				
		btl>GFP, xkr8	103	coxPH	N/A	bonferonni				
		btl>GFP, w cecAC	129	coxPH	N/A	bonferonni				
		btl>GFP, xkr8 cecAC	129	coxPH	N/A	bonferonni				
	H	multiple comparisons					btl>w	btl>xkr8	4.44221922561541e-06	0.000186573207475847
							btl>w	btl >w CecAC -/-	1.15191745813471e-06	4.83805332416579e-05
							btl>w	btl >xkr8 CecAC -/-	0.757618830871803	1
							btl>xkr8	btl >w CecAC -/-	1.40810770537736e-20	5.91405236258491e-19
							btl>xkr8	btl >xkr8 CecAC -/-	1.28256149937143e-07	5.38675829736001e-06
							btl >w CecAC -/-	btl >xkr8 CecAC -/-	7.17595891903314e-10	3.01390274599392e-08
	I	w	23	one way ANOVA	one-tailed	dunnett's				
		AZX-/-	20	one way ANOVA	one-tailed	dunnett's				0,0005
		AMP2; CecAC, TotAZX	19	one way ANOVA	one-tailed	dunnett's				0,1776
	J	w	79	coxPH	N/A	bonferonni				
		AZX-/-	121	coxPH	N/A	bonferonni				
		AMP2; CecAC, TotAZX	118	coxPH	N/A	bonferonni				
		multiple comparisons					w	TotAZX	5.42521802542149e-17	3.25513081525289e-16
							w	AMP2; CecAC, TotAZX	0.281449057946893	1
							TotAZX	AMP2; CecAC, TotAZX	3.77152156397125e-15	2.26291293838276e-14
Figure 5	A	ctrl	9	one way ANOVA	one-tailed	Holm-Šídák's				
		LL37	3	one way ANOVA	one-tailed	Holm-Šídák's				<0.0001
		LL37 + TotA	3	one way ANOVA	one-tailed	Holm-Šídák's				<0.0001
	B	ctrl	9	one way ANOVA	one-tailed	Holm-Šídák's				
		LL37	9	one way ANOVA	one-tailed	Holm-Šídák's				<0.0001
		LL37 + TotA	9	one way ANOVA	one-tailed	Holm-Šídák's				0,0415

REFERENCES

1. Hanson, M. A. & Lemaitre, B. New insights on Drosophila antimicrobial peptide function in host defense and beyond. *Current Opinion in Immunology* **62**, 22–30 (2020).
2. Lazzaro, B. P., Zasloff, M. & Rolff, J. Antimicrobial peptides: Application informed by evolution. *Science* **368**, (2020).
3. Gosztyla, M. L., Brothers, H. M. & Robinson, S. R. Alzheimer's Amyloid-β is an Antimicrobial Peptide: A Review of the Evidence. *Journal of Alzheimer's Disease* **62**, 1495–1506 (2018).
4. Ekengren, S., Tryselius, Y., Dushay, M. S. & Liu, G. A humoral stress response in Drosophila. 5.
5. Ekengren, S. & Hultmark, D. A Family of Turandot-Related Genes in the Humoral Stress Response of Drosophila. *Biochemical and Biophysical Research Communications* **284**, 998–1003 (2001).
6. Pakos-Zebrucka, K. *et al.* The integrated stress response. *EMBO reports* **17**, 1374–1395 (2016).
7. Medzhitov, R., Schneider, D. S. & Soares, M. P. Disease Tolerance as a Defense Strategy. *Science* **335**, 936–941 (2012).
8. Dantzer, R., Cohen, S., Russo, S. J. & Dinan, T. G. Resilience and immunity. *Brain, Behavior, and Immunity* **74**, 28–42 (2018).
9. Zasloff, M. Antimicrobial peptides of multicellular organisms. *Nature* **415**, 389–395 (2002).
10. Bacalum, M. & Radu, M. Cationic Antimicrobial Peptides Cytotoxicity on Mammalian Cells: An Analysis Using Therapeutic Index Integrative Concept. *International Journal of Peptide Research and Therapeutics* **21**, 47–55 (2015).
11. Parvy, J.-P. *et al.* The antimicrobial peptide defensin cooperates with tumour necrosis factor to drive tumour cell death in Drosophila. *eLife* **8**, (2019).
12. Iwasaki, T. *et al.* Selective cancer cell cytotoxicity of enantiomeric 9-mer peptides derived from beetle defensins depends on negatively charged phosphatidylserine on the cell surface. *Peptides* **30**, 660–668 (2009).
13. Vance, J. & Steenbergen, R. Metabolism and functions of phosphatidylserine. *Progress in Lipid Research* **44**, 207–234 (2005).
14. Birge, R. B. *et al.* Phosphatidylserine is a global immunosuppressive signal in efferocytosis, infectious disease, and cancer. *Cell Death & Differentiation* **23**, 962–978 (2016).
15. Imler, J.-L. & Bulet, P. Antimicrobial Peptides in Drosophila: Structures,Activities and Gene Regulation. in *Chemical Immunology and Allergy* (eds. Kabelitz, D. & Schröder, J.-M.) 1–21 (KARGER, 2005). doi:10.1159/000086648.
16. Marra, A., Hanson, M. A., Kondo, S., Erkosar, B. & Lemaitre, B. Drosophila Antimicrobial Peptides and Lysozymes Regulate Gut Microbiota Composition and Abundance. **12**, (2021).
17. Overend, G. *et al.* The receptor guanylate cyclase Gyc76C and a peptide ligand, NPLP1-VQQ, modulate the innate immune IMD pathway in response to salt stress. *Peptides*

34, 209–218 (2012).
18. Zheng, W. *et al.* Dehydration triggers ecdysone-mediated recognition-protein priming and elevated anti-bacterial immune responses in Drosophila Malpighian tubule renal cells. *BMC Biology* **16**, (2018).
19. Agaisse, H., Petersen, U.-M., Boutros, M., Mathey-Prevot, B. & Perrimon, N. Signaling Role of Hemocytes in Drosophila JAK/STAT-Dependent Response to Septic Injury. *Developmental Cell* **5**, 441–450 (2003).
20. Brun, S. *et al.* The MAPKKK Mekk1 regulates the expression of Turandot stress genes in response to septic injury in Drosophila. *Genes to Cells* **11**, 397–407 (2006).
21. West, C. & Silverman, N. p38b and JAK-STAT signaling protect against Invertebrate iridescent virus 6 infection in Drosophila. *PLOS Pathogens* **14**, e1007020 (2018).
22. Amstrup, A. B., Bæk, I., Loeschcke, V. & Givskov Sørensen, J. A functional study of the role of Turandot genes in Drosophila melanogaster: An emerging candidate mechanism for inducible heat tolerance. *Journal of Insect Physiology* **143**, 104456 (2022).
23. Manenti, T., Loeschcke, V. & Jesper Givskov Sørensen. Constitutive up-regulation of Turandot genes rather than changes in acclimation ability is associated with the evolutionary adaptation to temperature fluctuations in Drosophila simulans. *Journal of Insect Physiology* **104**, 40–47 (2018).
24. Linneweber, G. A. *et al.* Neuronal Control of Metabolism through Nutrient-Dependent Modulation of Tracheal Branching. *Cell* **156**, 69–83 (2014).
25. Nussbaumer, U., Halder, G., Groppe, J., Affolter, M. & Montagne, J. Expression of the blistered/DSRF gene is controlled by different morphogens during Drosophila trachea and wing development. *Mechanisms of Development* **96**, 27–36 (2000).
26. Leader, D. P., Krause, S. A., Pandit, A., Davies, S. A. & Dow, J. A. T. FlyAtlas 2: a new version of the Drosophila melanogaster expression atlas with RNA-Seq, miRNA-Seq and sex-specific data. *Nucleic Acids Research* **46**, D809–D815 (2018).
27. Perochon, J. *et al.* Dynamic adult tracheal plasticity drives stem cell adaptation to changes in intestinal homeostasis in Drosophila. *Nature Cell Biology* **23**, 485–496 (2021).
28. Tamamouna, V. *et al.* Remodelling of oxygen-transporting tracheoles drives intestinal regeneration and tumorigenesis in Drosophila. *Nature Cell Biology* **23**, 497–510 (2021).
29. Hayashi, S. & Kondo, T. Development and Function of the *Drosophila* Tracheal System. *Genetics* **209**, 367–380 (2018).
30. Lidsky, P. V. *et al.* Genetically-encoded fluorescent probe for imaging of oxygenation gradients in living *Drosophila*. *Development* (2018) doi:10.1242/dev.156257.
31. Vucic, D., Kaiser, W. J., Harvey, A. J. & Miller, L. K. Inhibition of Reaper-induced apoptosis by interaction with inhibitor of apoptosis proteins (IAPs). *Proceedings of the National Academy of Sciences* **94**, 10183–10188 (1997).
32. Tanaka, K., Fujimura-Kamada, K. & Yamamoto, T. Functions of phospholipid flippases. *Journal of Biochemistry* **149**, 131–143 (2011).
33. Sapar, M. L. *et al.* Phosphatidylserine Externalization Results from and Causes Neurite Degeneration in Drosophila. *Cell Reports* **24**, 2273–2286 (2018).
34. Tornesello, A. L., Borrelli, A., Buonaguro, L., Buonaguro, F. M. & Tornesello, M. L. Antimicrobial Peptides as Anticancer Agents: Functional Properties and Biological Activities. *Molecules* **25**, 2850 (2020).

35. Hedengren, M. *et al.* Relish, a Central Factor in the Control of Humoral but Not Cellular Immunity in Drosophila. *Molecular Cell* **4**, 827–837 (1999).
36. Carboni, A. L., Hanson, M. A., Lindsay, S. A., Wasserman, S. A. & Lemaitre, B. Cecropins contribute to *Drosophila* host defense against a subset of fungal and Gram-negative bacterial infection. *Genetics* **220**, (2022).
37. Kylsten, P., Samakovlis, C. & Hultmark, D. The cecropin locus in Drosophila; a compact gene cluster involved in the response to infection. *The EMBO Journal* **9**, 217–224 (1990).
38. Cerón, J. M. *et al.* The antimicrobial peptide cecropin A induces caspase-independent cell death in human promyelocytic leukemia cells. *Peptides* **31**, 1494–1503 (2010).
39. Gazit, E., Boman, A., Boman, H. G. & Shai, Y. Interaction of the Mammalian Antibacterial Peptide Cecropin P1 with Phospholipid Vesicles. *Biochemistry* **34**, 11479–11488 (1995).
40. Suttmann, H. *et al.* Antimicrobial peptides of the Cecropin-family show potent antitumor activity against bladder cancer cells. *BMC Urology* **8**, (2008).
41. Raghuraman, H. & Chattopadhyay, A. Melittin: a Membrane-active Peptide with Diverse Functions. *Bioscience Reports* **27**, 189–223 (2007).
42. Fabisiak, A., Murawska, N. & Fichna, J. LL-37: Cathelicidin-related antimicrobial peptide with pleiotropic activity. *Pharmacological Reports* **68**, 802–808 (2016).
43. Shiomi, A. *et al.* Extreme deformability of insect cell membranes is governed by phospholipid scrambling. *Cell Reports* **35**, 109219 (2021).
44. Nagao, K. & Umeda, M. Cellular function of (a)symmetric biological membranes. *Emerging Topics in Life Sciences* **7**, 47–54 (2022).
45. Tryselius, Y., Samakovlis, C., Kimbrell, D. A. & Hultmark, D. CecC, a cecropin gene expressed during metamorphosis in Drosophila pupae. *European Journal of Biochemistry* **204**, 395–399 (1992).
46. Nunes, C., Koyama, T. & Sucena, É. Co-option of immune effectors by the hormonal signalling system triggering metamorphosis in Drosophila melanogaster. *PLOS Genetics* **17**, e1009916 (2021).
47. Smith, K. J. & Gwyer Findlay, E. Expression of antimicrobial host defence peptides in the central nervous system during health and disease. *Discovery Immunology* **1**, (2022).
48. Park, Y.-J. *et al.* Phosphatidylserine synthase plays an essential role in glia and affects development, as well as the maintenance of neuronal function. *iScience* **24**, 102899 (2021).
49. Kim, H.-Y., Huang, B. X. & Spector, A. A. Phosphatidylserine in the brain: Metabolism and function. *Progress in Lipid Research* **56**, 1–18 (2014).
50. Drab, E. & Sugihara, K. Cooperative Function of LL-37 and HNP1 Protects Mammalian Cell Membranes from Lysis. *Biophysical Journal* **119**, 2440–2450 (2020).

Material and methods

Drosophila stocks and genetics

Flies were raised on Yeast-Cornmeal food (6% cornmeal, 6% yeast, 0.62% agar, 0.1% fruit juice, that was supplemented with 10.6g/L Moldex and 4.9ml/L propionic acid) at 25°C. Experiments were performed on 5-10 days old animals at 25°C, unless otherwise stated. Animals were bred and maintained at a low population density in vials and flipped twice a week. Isogenic w^{1118} Drosdel flies[51] (w^{iso}) were used as wild-type. *TotM* and *TotX* mutants were generated as previously described[52]. Briefly, w^{iso} embryos were injected with a mixture of recombinant Cas9 (Invitrogen) and a gRNA targeting the *TotM* coding sequence (ACTTATCGTAGAAAGTGACCAGG) or the *TotX* coding sequence (GTTCAAGTTATGAGGAACACAGG), respectively. $TotAZ^{sk6}$ line was created as previously described in[53]. This mutation was subsequently backcrossed in the w^{iso} background. To generate Tot^{AZX} stock, $TotAZ^{sk6}$ embryos were injected with a mixture of recombinant Cas9 (Invitrogen) and a gRNA targeting TotX coding sequence (GTTCAAGTTATGAGGAACACAGG). Tot^{AZX} mutations were then combined with *TotM* mutation (on the second chromosome) to create the Tot^{XMAZ} line. All Tot^{AZX} mutations were located on the third chromosome and this mutant almost phenocopied Tot^{XMAZ}. Additionally, most of the transgenes and genomic deletions used in our genetic analysis were located on the second chromosome. We therefore decided to use Tot^{AZX} instead of Tot^{XMAZ} in this study in order to simplify the genetic schemes. U*AS-TotA-HA* and *UAS-HA-TotA* lines were generated by phiC3-mediated recombineering. Stocks used in this study are listed in **Extended Data Table 1**.

Cloning and DNA constructs

Cloning was performed by Gibson assembly (New England Biolabs), following the manufacturer's instructions. *TotA* coding sequence was cloned into the pUASt-attb-GFP vector and a HA tag was added in C-term. A sequence containing the TotA 5'UTR, TotA signal peptide, 3 times a HA-tag and TotA CDS was ordered from Genewiz and subsequently cloned into the pUASt-attb-GFP vector to create the UAS-HA-TotA construct. For recombinant protein expression, a codon-optimized version of TotA fused to a Tobacco Etch Virus (TEV) protease cleavage site was ordered from Twist Bioscience and cloned into the pET29b vector. TotAxA and TotAΔ were made by GenScript, using pET29b-TotA as a template.

Recombinant protein and antibody production

TotA, TotAxA and TotAΔ were expressed overnight at 18°C in Rosetta2 *E. coli* (DE3, Novagen). Cells were lysed by sonication in 700 mM NaCl;20 mM HEPES 7.5 containing 1 protease inhibitor tablet (Roche) + 5ul Turbonuclease. TotA was purified using HisPur Ni-NTA Resin beads (ThermoFisher). MBP protein was cut using super TEV protease and both proteins were removed using HisPur Ni-NTA Resin beads. TotA was further purified by incubation with Amylose Resin (New England Biolabs) followed by size-exclusion chromatography on a HiLoad superdex75 16/60 column

(GE healthcare) and concentrated in 150 mM NaCl; 20 mM HEPES 7.5. TotA was used as immunogen to produce rabbit anti-TotA antibody (made by GenScript).

Microbial cultures

Bacteria were cultured overnight on a shaking plate at 180 RPM. The following morning, they were pelleted by centrifugation (4000 RPM at 4°C) and the bacterial pellets were diluted to the desired optical density at 600 nm (OD_{600}). *Pectobacterium carotovorum carotovorum 15* (*Ecc15*) and *Micrococcus luteus* were grown in LB medium at 29°C. *Enterococcus faecalis* was grown in GHI medium at 37°C. For experiments with heat killed bacteria, bacterial pellets were cyclically (4 times) heated at 95°C and frozen at -20°C. *Drosophila C Virus* (*DCV*) stock was kindly provided by Prof. Carla Saleh.

Survival experiments

All experiments were done on 5- to 7-days old adult female flies. Systemic infections with *Ecc15*, *M. luteus* and *E. faecalis* were performed as follow[54]: flies were pricked in the thorax with a needle previously dipped into a concentrated bacterial pellet at OD_{600}:200 (*Ecc15* and *M. luteus*) or OD_{600}:5 (*E. faecalis*). Infected flies were maintained at 25°C (*E. faecalis*) or 29°C (*Ecc15* and *M. luteus*) and survival was recorded daily. Flies were flipped into fresh vials every 2-3 days. Systemic infections with DCV were performed by injecting 50 nL of $2*10^5$ $TCID_{50}$/mL into the thorax of female adult flies using a nanoinjector (Drummond) and glass capillary needles.

Survivals to abiotic stresses were performed as followed: osmotic stress experiments were performed by feeding fly food supplemented with NaCl (final concentration: 4%). Flies carrying Gal4 or $Gal4^{ts}$ overexpressing transgenes were raised at 25°C, kept for 3days at 25°C, transferred for 2-4days at 29°C and exposed to an osmotic stress at 29°C. Starvation experiments were performed by keeping flies on 1.8% agar. For heat stress experiments, flies were kept in a 34°C incubator. For hypoxic/hyperoxic experiments, flies were maintained in an incubator with controlled oxygen levels (5% O_2 for hypoxia of 60% O_2 for hyperoxia).

Western Blot

Total hemolymph was harvested by bleeding ten L3 wandering larvae in 100 μL of Phosphate Buffer Saline (PBS) supplemented with Complete Inhibitor (Roche, diluted 1/50), PMSF (1 mM) and PTU (1 μM). A step of centrifugation (5 minutes at 500 x g) was done to discard hemocytes. 10 μg of proteins was denatured (2 minutes at 80°C) and then separated on a Novex 10-20% precast Tricine Gel, and transferred to a nitrocellulose membrane (Invitrogen iBlot). The membrane was blocked in 5% non-fat dry milk in PBS containing 0.1% Tween-20 for 1 hour and then incubated overnight at 4°C with a rabbit anti-TotA (1:1000 dilution) antibody. Goat anti-rabbit-HRP secondary antibody (Jackson ImmunoResearch) diluted at 1:15000 was incubated for 1h at room temperature. Bound antibodies were detected using

SURESIGNAL Western Substrate (lubioScience). The membrane was imaged on a ChemiDoc XRS+ (BioRad).

Immunostaining and trachea imaging

Guts were dissected in PBS and fixed in 8% paraformaldehyde for 15 minutes at room temperature. The tissues were subsequently rinsed two times with PBS containing 0.1% Triton X-100, blocked for 1 hour in PBS containing 1% of goat serum and 2% BSA, and incubated at 4°C in the blocking solution containing an anti-GFP (2hours, 1:3000), anti-HA (overnight, 1:500) or anti-cleaved Caspase3 primary antibody (overnight, 1:500). The tissues were subsequently washed and incubated with a secondary antibody (1:4000) for 1 hour at room temperature. After extensive washes, tissues were mounted in glycerol. Anti-TotA staining was done following a similar protocol without adding Triton X-100. To image AnnevinV-GFP, guts were dissected in AnnexinV buffer (Hepes 10mM, NaCl 150mM, KCl 5mM, $MgCl_2$ 5mM, $CaCl_2$ 1.8 mM) and subsequently stained following the abovementioned protocol. Anti-TotA staining of fat bodies was performed on dissected carcasses. Tissues were fixed for 45 min, permeabilized in PBS-0.1% Triton X-100 for 1 hour, blocked for 1 hour in PBS containing 1% of goat serum and 2% BSA, and incubated overnight at 4°C in the blocking solution containing anti-TotA antibody (1:3000). The tissues were subsequently washed and incubated with a secondary antibody (1:4000) for 1 hour at room temperature. After extensive washes, tissues were mounted in glycerol. Tracheation of guts was assessed by imaging the autofluorescent chitin lining the tracheal lumen. The dityrosine bonds chitin fluoresce under UV excitation, allowing chitin to be imaged using a DAPI filter set. Flies were starved for two hours before guts were dissected and fixed in 8% paraformaldehyde for 45 minutes at room temperature. Guts were subsequently washed 3 times 15min in PBS and mounted in glycerol. Guts were imaged on a LSM700 microscope (Zeiss) using the DAPI channel.

Tunel Staining

Guts from adult female flies were dissected in PBS and fixed in 4% paraformaldehyde for 15 minutes at room temperature. The guts were subsequently rinsed three times with PBS and permeabilized for 2 minutes in PBS+0.1% Triton X-100 + 0.1% Sodium citrate tribasic dihydrate, and rinsed three times in PBS. Guts were then incubated for 1 hour with reagents from the *In Situ Cell Death Detection Kit, TMR red* (Roche). Tissues were washed three times and mounted in Dako Fluorescence Mounting Medium (Agilent).

Tissue oxygenation determination

Oxygenation of Drosophila tissues was determined using a genetically-encoded fluorescent probe (nls-timer) as described[30]. Guts and Malpighian tubules were dissected and fixed in 4% paraformaldehyde for 45 minutes and mounted in glycerol. Images were acquired in the GFP and RFP channels on a Leica M205 FA fluorescent stereomicroscope. Ratiometric analysis of red and green nuclei fluorescence was performed using ImageJ to determine tissue oxygenation.

Image analysis and TTC quantification

Image quantifications were performed using ImageJ software. Trachea coverage was determined by measuring the surface of trachea divided by the area of the R2 gut region. Terminal tracheal cells cellular bodies, as defined by the characteristic shape of the chitinous lumen, were manually counted in the R2 region of the midgut.

Respirometry

Respiration in flies was measured using a stop-flow gas-exchange system (Q-Box RP1LP Low Range Respiration, Qubit Systems, Ontario, Canada, K7M 3L5). Eight female flies were put into an airtight glass tube and supplied with food. Each tube was provided with CO_2-free air while 'spent' air was simultaneously flushed through the system and analyzed for its CO_2 and O_2 content. In this way, evolved CO_2 and consumed O_2 were measured for each tube every ~ 44 minutes for a duration of 12h-16h.

NMR spectroscopy

Recombinant proteins for NMR spectroscopy were prepared with the isotope enrichment scheme appropriate for each experiment in MES buffer pH 6 with 100 mM NaCl and 10% ^2H_2O. Protein concentrations were around 300 μM for NMR titrations and close to 1 mM for experiments aimed at resonance assignment, structure determination, and ^{15}N relaxation analysis. All NMR experiments were carried out in a 18.8 T (800 MHz ^1H Larmor frequency) Bruker spectrometer equipped with a CPTC ^1H,^{13}C,^{15}N 5 mm cryoprobe and an Avance Neo console. Backbone (H, N, CA, and C) and CB resonances were assigned using a standard procedure based in conventional 3D HNCA, HN(CO)CA, HNCO, HN(CA)CO, CBCA(CO)NH and HNCACB spectra, further assisted by ^{15}N-resolved TOCSY and NOESY[55]. Experiments for sidechain assignment and structure calculation entailed ^{15}N-resolved NOESY, ^{15}N-resolved TOCSY, HCCH-TOCSY, ^{13}C-resolved NOESY, HNHA, 2D TOCSY and 2D NOESY spectra. All spectra were acquired and processed using Bruker's Topsin 4.0 software. Backbone and sidechain assignments were obtained through manual spectral analysis assisted by the program CARA[56]. Analysis of NOESY spectra and structure calculations were performed semiautomatically using UNIO's ATNOS/CANDID module coupled to Cyana[57,58] using NOEs and dihedral angles derived from chemical shifts with Talos-n[59]. NMR structure statistics are provided in **Extended Data Table 2**. The solved protein structure was deposited in the PDB under ID 8PBV and NMR chemical shifts at the BMRB under ID 34825.

For studies of ^{15}N relaxation, heteronuclear ^1H-^{15}N NOEs were measured using an interleaved, phase-sensitive gradient-enhanced version; and ^{15}N T_1 and T_2 were measured via conventional pseudo-3D experiments that apply respectively inversion recovery or CPMG sequences onto an HSQC spectrum, both using gradient selection, water suppression, and decoupling during acquisition. All spectra for measurement of ^{15}N relaxation were acquired with 256 increments in the indirect dimension and 3 seconds of relaxation delay. For T_1 measurements we used delays of 20, 50, 100,

200, 300, 400, 500, 700, 1000, 1200, 1500, 2000, 3000 and 4000 ms. For T_2 measurements we used delays of 17, 34, 51, 68, 85, 102, 119, 136, 170, 204, 238, 272 and 340 ms. Relaxation rates were fitted from exponential decay models using the ad hoc module from the Sparky-NMRfam program[60] on the peaks derived from our backbone assignment.

Peptides

Purified CecA and Melittin (Sigma) were used in leakage experiments. Synthetic CecA and LL37 were purchased from GenicBio (purity> 95%).

Isothermal Titration calorimetry

ITC experiments were performed on a Microcal PEAQ-ITC (Malvern Instruments). 13 injections of 2uL of a 10mM HEPES pH7.5 150mM NaCl solution of 2mM CecA or LL37 were injected 13 times in the chamber containing 200 μM TotA and heats of reaction were recorded. Control experiments were run where peptides were titrated in the buffer solution alone.

Liposome preparation, binding and leakage experiments

Lipids (3 mg) were resuspended in chloroform and mixed at a 3:1:0.4 ratio (DOPE:DOPC:DOPS) with the exception of experiments involving melittin, in which DOPS was omitted, as this lipid inhibits the membranolytic activity of melittin. Chloroform was evaporated under a nitrogen stream and the lipid film was hydrated with 600 μL of 50 mM Tris pH=8, 100 mM NaCl containing 70 mM Calcein. After 5 freeze-thaw cycles, liposomes were extruded 20 times through a 0.2 μm pore-size filter. To remove un-entrapped calcein, liposomes were passed through two HiTrap columns at low flow rate. Fractions containing calcein-loaded liposomes were pooled, diluted 4 times and used for subsequent assays. For calcein leakage experiments, 10 μl liposomes were incubated in 90 μl 50 mM Tris pH=8, 100 mM NaCl containing 0.5 μM TotA, TotAxA or TotAΔ, together with CecropinA and Melittin (Sigma-Aldrich , at a concentration of 1 μM and 8.5 nM, respectively) and fluorescence was recorded on an Infinite M Nano fluorospectrophotometer (Tecan) for 1 hour. Maximum release of Calcein was determined by addition of 0.1% triton-X100 and data were normalized as percentage of full release. For binding assays, 3 μM TotA was incubated with180 μL 1mg/mL liposomes containing DOPC and increasing amounts of DOPS for 30 minutes at room temperature and centrifuged at 100000 x g in a discontinuous sucrose gradient (35%:20%:10%) for 1 hour. Liposome fraction and soluble fractions were subjected to anti-TotA immunoblotting.

Lipid overlay assay

Membrane lipid strips (Echelon Bioscience) were incubated with 0.5μg/mL TotA in PBS-0.1% Tween, 3%BSA for 1 hour at room temperature. TotA was then probed with an anti-totA antibody as described above.

Single-channel bilayer experiments

1,2-diphytanoyl-*sn*-glycero-3-phosphocholine (DPhPC) and 1,2-diphytanoyl-*sn*-glycero-3-phospho-L-serine powder (DPhPS) (Avanti Polar Lipids Inc.,) were dissolved in octane (Sigma-Aldrich) to a final concentration of 8 mg/mL and either used pure or in mixture as specified in the figure caption. Single-channel recording experiments were performed on an Orbit 16 TC instrument (Nanion). Phospholipid membranes were formed across a MECA 16 recording chip that contains 16 circular microcavities (100 µm diameter) in a highly inert polymer. Each cavity contains an individual integrated Ag/AgCl microelectrode and can record 16 artificial lipid bilayers in parallel. The buffer (10 mM HEPES, 200 mM KCl, pH=7.4), the concentration of CecA and TotA was 8 µM and the temperature was set to 25°C for all experiments. Membranes were formed and their capacitance were recorded (**Extended Data Figure 5i**). The traces were recorded in Elements Data Reader (Elements) and further analyzed by Clampfit (Molecular device). Data was collected at 20 kHz sampling rate with a 10 kHz low-pass filter. Results, fitting, and graphs were produced in Prism (GraphPad) and figures were generated in Adobe Illustrator 2022 (Adobe).

Killing Assays

A culture of *E. coli* grown overnight was diluted to OD600=0.001 and allowed to regrow for 2hrs at 29°C. 1 µl of this culture was diluted in 100µL LB containing 2µM LL37 in the absence or presence of 2.5 µM TotA. The plate was incubated at 25°C under intermittent agitation and OD was recorded every 10 minutes. For eukaryotic cell killing assay, 10000 HL60 cells were seeded in 100µL of RPMI supplemented with heat-inactivated FBS, HEPES and antibiotics in half-area 96-well plates (corning). The next day, 50 µL of supernatant was removed and LL37 and TotA were added at 40 and 80 µM final concentration, respectively. After 1h incubation at 37°C, 5 µL of MTT (Biotium) was dispensed in each well and further incubated at 37°C for 1h. 100 µL DMSO were then added and thoroughly mixed to dissolve crystals. Absorbance was read at 570nm and 630nm on an Infinite M nano spectrofluorometer (Tecan).

Molecular Dynamics simulation

We obtained the structure of TotA from the AlphaFold Protein Structure Database (AFDB) [61,62] under the UniProt accession code Q8IN44 [63]. The models available in AFDB are computed based on the entire sequence of the target proteins, so it was necessary to remove the sequence peptide of TotA (residues 1 to 21) from the structure prior to preparing the simulation setup.

We processed the TotA model in the CHARMM-GUI web server[64] to generate the input files for the MD simulation, using the CHARMM-GUI Membrane Builder tool[65] . We used the Positioning of Proteins in Membrane (PPM) tool from Orientations of Proteins and Membranes (OPM) database to orient TotA with respect to the membrane[66]. We generated a tetragonal box with TotA and a symmetric lipid bilayer with 10% DOPS, 30% DOPC, and 60% DOPE, resulting in a membrane with an area of 131 × 131 Å2. We solvated the system with TIP3P water[67] and neutralized its liquid

charges with counterions corresponding to a 0.15 M NaCl solution. Lastly, we generated all the necessary files to run the MD simulations with the CHARMM36m forcefield[68].

We used GROMACS[69] version 2022.1 to run and analyze the MD simulations. In all stages of the procedure, the cut-off radius for short-range electrostatic and van der Waals interactions was 12 Å; we used the particle mesh Ewald algorithm (PME)[70] to calculate long-range electrostatic interactions. We restrained the length of covalent bonds involving hydrogen atoms using the LINCS algorithm[71]. Periodic boundary conditions were applied in all directions.

In the first stage of the simulation protocol, we minimized the potential energy of the system using the steepest descent algorithm, employing a 1000 kJ mol-1 nm-1 maximum force constant on the atoms as a convergence criterion. After minimization, we subjected the system to thermal equilibration in the canonical ensemble (NVT)[72], to accommodate water and counterions around the protein and membrane. Initial atomic velocities were determined following a Maxwell-Boltzmann distribution corresponding to a temperature of 300 K and we equilibrated the system under these conditions for 0.25 ns with a 1 fs time step using the Berendsen thermostat[73]. During the equilibration stage, we restrained heavy-atom positions using a harmonic potential, with force constants of 4000 (backbone) and 2000 (sidechain) kJ mol-1 nm-2, respectively. The phosphorus atoms of the lipid molecules were also restrained on the Z-axis (direction of the normal vector at the membrane surface), as well as the dihedral angles of the double bonds in the fatty acid chains, with force constants of 1000 kJ mol-1 nm -2 and 1000 kJ mol-1 rad-2, respectively.

After controlling the temperature, we stabilized pressure and density in the isothermal-isobaric ensemble (NPT)[74]. The pressure was maintained at 1 bar using the Berendsen barostat[73] with semi-isotropic pressure coupling and a 5 ps time constant. The systems were equilibrated for 1.625 ns, with position restraints released gradually.

The production dynamics were also performed in the NPT ensemble, changing only the thermostat used for Nosé-Hoover[75,76] and the barostat to Parrinello-Rahman[77,78]. This stage lasted 1 μs, with a time step of 2 fs. All simulations had five replicas and only the last 500 ns of each simulation were used for the analyses.

We performed all lipid interaction analyses with the Python package PyLipID[79]. The distance cutoff for lipid interactions was set to 0.3 nm, and only residence times calculated with an estimated R2 > 0.97 were reported.

We used the Visual Molecular Dynamics (VMD)[80] software for visual inspection of the simulations and recording of the movies. All protein and membrane images were generated with ChimeraX[81]. Density and violin plots were generated with the R programming language in RStudio[80,81].

Statistical analysis

Each experiment was repeated independently at least three times. Survival curves included experiments with at least one cohort of 20 flies per condition. Survival

analyses were performed using a Cox proportional hazards (CoxPH) model, with Bonferonni corrections for *P*-values when multiple comparisons were done. In this case, Statistics were represented using a compact letter display (CLD) graphical method: groups were assigned the same letter if they were not significantly different ($p > 0.05$). Quantification data were analyzed using a Mann-Whitney test, Welch two sample t-test, student t-test or ordinary one-way ANOVA with Dunnett's multiple comparisons test, as stated in the figure legends. Error bars represent the standard deviation of the mean of replicate experiments (SD). *p*-values are represented in the figures by the following symbols: ns for $p \geq 0.05$, * for *P* between 0.01 and 0.05; ** for *P* between 0.001 and 0.01, *** for *P* between 0.0001 and 0.001, **** for $p \leq 0.0001$. Survival statistics were represented using a compact letter display graphical technique: groups were assigned the same letter if they were not significantly different ($P > 0.05$). All survival statistics are summarized in **Extended Data Table 3**.

Methods references

51. Ferreira, Á. G. *et al.* The Toll-Dorsal Pathway Is Required for Resistance to Viral Oral Infection in Drosophila. *PLoS Pathogens* **10**, e1004507 (2014).

52. Rommelaere, S., Boquete, J.-P., Piton, J., Kondo, S. & Lemaitre, B. The Exchangeable Apolipoprotein Nplp2 Sustains Lipid Flow and Heat Acclimation in Drosophila. *Cell Reports* **27**, 886-899.e6 (2019).

53. Kondo, S. & Ueda, R. Highly Improved Gene Targeting by Germline-Specific Cas9 Expression in *Drosophila*. *Genetics* **195**, 715–721 (2013).

54. Neyen, C., Bretscher, A. J., Binggeli, O. & Lemaitre, B. Methods to study Drosophila immunity. *Methods* **68**, 116–128 (2014).

55. Sattler, M. Heteronuclear multidimensional NMR experiments for the structure determination of proteins in solution employing pulsed field gradients. *Progress in Nuclear Magnetic Resonance Spectroscopy* **34**, 93–158 (1999).

56. Keller, R. L. J. The Computer Aided Resonance Assignment Tutorial.

57. Herrmann, T., Güntert, P. & Wüthrich, K. Protein NMR Structure Determination with Automated NOE Assignment Using the New Software CANDID and the Torsion Angle Dynamics Algorithm DYANA. *Journal of Molecular Biology* **319**, 209–227 (2002).

58. Gottstein, D., Kirchner, D. K. & Güntert, P. Simultaneous single-structure and bundle representation of protein NMR structures in torsion angle space. *Journal of Biomolecular NMR* **52**, 351–364 (2012).

59. Shen, Y. & Bax, A. Protein backbone and sidechain torsion angles predicted from NMR chemical shifts using artificial neural networks. *Journal of Biomolecular NMR* **56**, 227–241 (2013).

60. Lee, W., Tonelli, M. & Markley, J. L. NMRFAM-SPARKY: enhanced software for biomolecular NMR spectroscopy. *Bioinformatics* **31**, 1325–1327 (2015).

61. Varadi, M. *et al.* AlphaFold Protein Structure Database: massively expanding the structural coverage of protein-sequence space with high-accuracy models. *Nucleic Acids Research* **50**, D439–D444 (2022).

62. Jumper, J. *et al.* Highly accurate protein structure prediction with AlphaFold. *Nature*

596, 583–589 (2021).
63. The UniProt Consortium. UniProt: a worldwide hub of protein knowledge. *Nucleic Acids Research* **47**, D506–D515 (2019).
64. Jo, S., Kim, T., Iyer, V. G. & Im, W. CHARMM-GUI: A web-based graphical user interface for CHARMM. *Journal of Computational Chemistry* **29**, 1859–1865 (2008).
65. Lee, J. *et al.* CHARMM-GUI *Membrane Builder* for Complex Biological Membrane Simulations with Glycolipids and Lipoglycans. *Journal of Chemical Theory and Computation* **15**, 775–786 (2019).
66. Lomize, M. A., Pogozheva, I. D., Joo, H., Mosberg, H. I. & Lomize, A. L. OPM database and PPM web server: resources for positioning of proteins in membranes. *Nucleic Acids Research* **40**, D370–D376 (2012).
67. Jorgensen, W. L., Chandrasekhar, J., Madura, J. D., Impey, R. W. & Klein, M. L. Comparison of simple potential functions for simulating liquid water. *The Journal of Chemical Physics* **79**, 926–935 (1983).
68. Huang, J. *et al.* CHARMM36m: an improved force field for folded and intrinsically disordered proteins. *Nature Methods* **14**, 71–73 (2017).
69. GROMACS - A PARALLEL COMPUTER FOR MOLECULAR-DYNAMICS SIMULATIONS — the University of Groningen research portal. https://research.rug.nl/en/publications/gromacs-a-parallel-computer-for-molecular-dynamics-simulations.
70. Darden, T., York, D. & Pedersen, L. Particle mesh Ewald: An $N \cdot \log(N)$ method for Ewald sums in large systems. *The Journal of Chemical Physics* **98**, 10089–10092 (1993).
71. Hess, B., Bekker, H., Berendsen, H. J. C. & Fraaije, J. G. E. M. LINCS: A linear constraint solver for molecular simulations. *Journal of Computational Chemistry* **18**, 1463–1472 (1997).
72. Nosé, S. A molecular dynamics method for simulations in the canonical ensemble. *Molecular Physics* **52**, 255–268 (1984).
73. Berendsen, H. J. C., Postma, J. P. M., van Gunsteren, W. F., DiNola, A. & Haak, J. R. Molecular dynamics with coupling to an external bath. *The Journal of Chemical Physics* **81**, 3684–3690 (1984).
74. Andersen, H. C. Molecular dynamics simulations at constant pressure and/or temperature. *The Journal of Chemical Physics* **72**, 2384–2393 (1980).
75. Nosé, S. A unified formulation of the constant temperature molecular dynamics methods. *The Journal of Chemical Physics* **81**, 511–519 (1984).
76. Hoover, W. G. Canonical dynamics: Equilibrium phase-space distributions. *Physical Review A* **31**, 1695–1697 (1985).
77. Parrinello, M. & Rahman, A. Polymorphic transitions in single crystals: A new molecular dynamics method. *Journal of Applied Physics* **52**, 7182–7190 (1981).
78. Nosé, S. & Klein, M. L. Constant pressure molecular dynamics for molecular systems. *Molecular Physics* **50**, 1055–1076 (1983).
79. PyLipID: A Python Package for Analysis of Protein–Lipid Interactions from Molecular Dynamics Simulations. https://pubs.acs.org/doi/epdf/10.1021/acs.jctc.1c00708 doi:10.1021/acs.jctc.1c00708.
80. Humphrey, W., Dalke, A. & Schulten, K. VMD: visual molecular dynamics. *J Mol*

Graph **14**, 33–8, 27–8 (1996).
81. Goddard, T. D. *et al.* UCSF ChimeraX: Meeting modern challenges in visualization and analysis. *Protein Science* **27**, 14–25 (2018).

Acknowledgements

We thank the Bloomington Stock Center in the USA and the Vienna Drosophila Resource Center for fly stocks; Jordi Casanova, Stefano de Renzis and Chun Han for providing fly strains; the BioImaging & Optics Platform (BIOP) in EPFL for confocal microscopy; the Protein Production & Structure Core Facility (PTPSP) for TotA production and NMR analysis; Hannah Westlake and Florent Masson for comments and editing on the manuscript. This work was supported by Sinergia SNSF grant CRSII5_186397, the SNSF project grant 310030_215073, PR00P3_193090 205321_192371 to Matteo Dal Peraro and Novartis Foundation 532114 awarded to Bruno Lemaitre, 532589 to Chan Cao.

Authors Contributions

SR and BL designed the study and wrote the manuscript with inputs from all the authors. SR, AC, JBJ, LAA, CV, VR designed and performed experiments and analyzed data. JPB performed experiments and generated mutant and transgenic stocks. LAA performed the NMR experiments, solved TotA structure and wrote the manuscript. FM ran and analyzed the MD simulations. CV generated and analyzed respirometry data. SK provided mutants. MSD and MDP acquired funding and provide feedbacks. CC acquired funding and supervised experiments. BL acquired funding and supervised the project.

Competing Interests Statement

The authors have no competing interests to declare.

Supplementary Information is available for this paper.

Correspondence and requests for materials should be addressed to Samuel Rommelaere (samuel.rommelaere@epfl.ch).

Reprints and permissions information is available at www.nature.com/reprints.

Chapter 4: Functional characterization of immune-induced Dnases in *Drosophila* innate immunity

Note: This Chapter is based on a study in preparation for publication.

Authors: Alexia Carboni, Jean-Philippe Boquete, Shu Kondo and Bruno Lemaitre.

Contribution of Alexia Carboni: Designed the study, performed all experiments and analysis, wrote the manuscript.

INTRODUCTION

Endogenous immune elicitors refer to immunostimulatory molecules that are naturally produced within the body and are able to stimulate or modulate the immune system. Extracellular Damage-Associated Molecular Patterns (DAMPs) are typically molecules within the cells, which are discharged to the extracellular space in response to damage due to trauma or a pathogen (Roh and Sohn 2018). Once released from the cell, extracellular DAMPs bind to specific Pattern Recognition Receptors (PRRs) at the surface of cells, and promote a non-infectious immune activation. Intracellular DAMPs are immunogenic molecules which are released from specific organelles (e.g., lysosomes that digest apoptotic cells) into the cytosol. These activate another class of PRRs which are cytosolic (e.g. the cytosolic receptor cGAS in mammals). In the 1960s, immunologists showed for the first time that host nucleic acids, which are normally sequestered inside the nucleus, can be recognized by and modulate the innate immune system (Isaacs *et al.* 1963). In the early 2000s, more extensive work showed that DNA could activate the innate immune system when found in circulation (Hanayama *et al.* 2004). Moreover, pioneer studies showed that the accumulation of undegraded DNA inside the cells stimulates the production of IFN-β in mice, a factor that stimulates pathways homologous to NF-κB pathways of *Drosophila* (Yoshida *et al.* 2005; Okabe *et al.* 2005). Therefore, enzymes such as deoxyribonucleases (DNases), which are able to degrade intra- and extra-cellular DNA, can maintain homeostasis and prevent a "sterile" activation of innate immunity.

Apoptosis is defined by a list of hallmarks, one of which is the degradation of chromosomal DNA. In a mouse model, McIlroy et al. (2000) identified a Caspase-Activated Dnase (CAD), which is complexed in the cell cytosol with its inhibitor, ICAD. McIlroy et al. (2000) found that when apoptosis is triggered, caspases (3 and 7) cleave ICAD, which releases CAD to translocate into the nucleus and degrade DNA into nucleosomal units. Subsequently, the apoptotic cell is recognized by macrophages which engulf it by phagocytosis. Finally, another intracellular caspase-independent deoxyribonuclease named DNase II is activated inside the lysosome of the macrophage to complete the degradation of DNA from the engulfed apoptotic cell.

The same group published a follow-up study on the role of DNase II, but this time focusing on *Drosophila melanogaster* immunity (Mukae *et al.* 2002). Using a linker-mediated PCR method during embryogenesis and oogenesis, they showed the absence of DNA fragments in

CAD/ICAD mutants, while DNase II hypomorphic mutants accumulate degraded chromosomal DNA. These results confirm their previous hypothesis that CAD and DNase II work independently to degrade chromosomal DNA. Finally, they showed that an hypomorphic mutation of the *DNase II* gene*, Dnase II* ^{lo}*,* caused the constitutive expression of the antimicrobial peptide genes *Diptericin* and *Attacin*, that are regulated by the Imd pathway, suggesting that endogenous *Drosophila* DNA, when not degraded by DNase enzymes, activates innate immunity. A role for Dnase II in *Drosophila* immunity was supported by Seong et al. (2006) who showed that *DNase II* hypomorphic mutants were more susceptible to both Gram-positive and Gram-negative bacteria. However, they did not analyze how a deficiency in *Dnase II* causes an immune susceptibility. Collectively, these results suggest that death of infected *DNase II* mutants is due to ineffective degradation of debris generated by pathogen clearance, rather than combatting the pathogen itself. Finally, a more recent study identified a novel stress induced Dnase (SID) in *Drosophila*, where the authors suggested that SID also protects flies from the toxicity of accumulated DNA (Seong *et al.* 2014). These pioneer studies left many questions unanswered. It has been shown that *DNase II* mutants show higher levels of *Diptericin* and *Attacin* transcripts in unchallenged conditions. However, there was no genetic demonstration that the Imd pathway specifically is activated. As extensive cross-talk occurs between immune pathways, it is essential to identify which intracellular and extracellular sensors are activated by DNA, and which downstream pathway(s) is/are activated. Notably, the recent description of cGas-STING pathway homologs in *Drosophila* uncovers new candidates for consideration.

In this study, we use a full knockout approach to understand the consequences of the loss of Dnase II on the activation of innate immunity in *Drosophila melanogaster*. We show that *Dnase II* mutant flies have a delay in development, reduced lifespan, strong locomotor defect and an overloaded microbiota at early adult stage. Curiously, *Dnase II* mutant or wild type flies are not susceptible to microbial or *Drosophila* DNA injection, refuting the idea that DNA is immunogenic. However, *Dnase II* mutant flies are susceptible to Gram-negative and Gram-positive systemic bacterial infection, suggesting a role for *Dnase II* in disease tolerance. *Dnase II* mutant larvae also show a higher IMD pathway response after pinching (a clean injury), which can be rescued by *Relish* or *STING* knock-out. After injury, we observe the accumulation of apoptotic bodies in hemocytes of *DNAse II* deficient larvae. This suggests an incapacity to digest phagocytosed apoptotic bodies. Collectively, our work provides the first functional

characterization of *Dnase II* in *Drosophila melanogaster* immunity using a full knock-out approach. We present in this manuscript the results we have so far obtained on the on-going characterization of *Dnase II*.

MATERIAL AND METHODS

Drosophila stocks and rearing conditions

All fly stocks were maintained on standard fly medium (6% cornmeal, 6% yeast, 0.6% agar, 0.1% fruit juice, 10.6 g/L moldex and 4.9 mL/L propionic acid) at 25°C. Experiments were performed on 5-7 days old adult animals, or third instar wandering larvae (L3) were selected 110-120 hours after egg laying. Isogenic w^{1118} Drosdel flies (w^{iso}) were used as control. *Dnase* II^{sk4} mutants was generated as previously described (Kondo and Ueda 2013). The $Bom^{\Delta 55C}$ and *iso* $Relish^{E20}$ flies were the same as used in (Carboni *et al.* 2022). The $Sting^{JLI}$ line was the same as used in (Cai *et al.* 2020).

Microbial cultures

Bacteria were cultured overnight on a shaking plate at 180 RPM. The following morning, they were pelleted by centrifugation (4000 RPM at 4°C) and the bacterial pellets were diluted to the desired optical density at 600 nm (OD_{600}). *Pectobacterium carotovorum carotovorum 15* (*Ecc15*) and *Micrococcus luteus* were grown in LB media at 29°C. *Enterococcus faecalis* was grown in GHI media at 37°C.

Survival experiments

All experiments were done on 3- to 5-day old adult mated female flies. Systemic infections with *P. carotovorum carotovorum 15* (*Ecc15*), *M. luteus* and *E. faecalis* were performed as followed: flies were pricked in the thorax with a 100 μm thick needle previously dipped into a concentrated bacterial pellet at a desired OD_{600}. Infected flies were then maintained at 25°C (*E. faecalis*) or 29°C (*Ecc15 and M. luteus*) and survivals were recorded daily. Flies were flipped into fresh vials every 2-3 days.

Climbing assay

Flies were gently tapped to the bottom of a tube and filmed with a digital camera. The percentage of flies climbing above 7 cm within 10 seconds was calculated.

DNA injection experiments

DNA was extracted from *E. coli* or *Drosophila* using the High quality DNA extraction for RT-PCR and Sequencing kit (Qiagen). Briefly, a bacterial pellet or 5 flies were lysed on ice using the kit lysis solution. Samples were heated to 65°C for 15 minutes, and 100 μL of Protein precipitation solution (PPS) was added. The samples were centrifuged and the supernatants containing DNA were harvested. The DNA was precipitated using isopropanol, and washed two times with ethanol. DNA was re-hydrated with MiliQ water. The samples were diluted to the desired concentration, and subsequently injected using a nanoinjector and glass capillary needles.

Larval pinching and *in vivo* phagocytosis assay

To generate apoptosis *in vivo*, third instar wandering larvae (L3) were collected and placed in a grape juice collection plate using a paintbrush. Using forceps, the posterior end of the larvae was carefully pinched without damaging the posterior spiracles. The larvae were then kept on the grape juice collection plate supplemented with 200 μL of water, and placed in a humid chamber (to avoid dehydration) for one, two or three hours to allow phagocytosis of apoptotic corpses *in vivo*.

Immunostaining and TUNEL staining

For TUNEL and phalloidin staining of hemocytes, L3 larvae were bled in Schneider medium on slides and hemocytes were left to adhere for 45 minutes. Cells were then fixed for 15 minutes in PBS, 0.1% Triton X-100 (PBT) and 4% paraformaldehyde at room temperature. The cells were subsequently rinsed three times with PBS and permeabilized for 2 minutes in PBS + 0.1% Triton X-100 + 0.1% sodium citrate tribasic dihydrate, and rinsed three times in PBS. Cells were then incubated for 1 hour with reagents from the In Situ Cell Death Detection Kit, TMR red (Roche). Cells were subsequently washed, and incubated for 1 hour with Alexia Fluor TM 488 phalloidin at a dilution of 1/100 (Thermo Fisher Scientific, A12379), and DAPI at a dilution

of 1/20000 for 10 minutes. Cells were then washed three times and mounted in Dako Fluorescence Mounting Medium (Agilent).

Apoptotic cells preparation

S2 cells were cultured in Schneider's insect medium (Sigma-Aldrich) supplemented with 10% FBS (GibcoTM) and Penicillin/Streptomycin (Sigma-Aldrich) at a concentration of 100 U/mL. To induce apoptosis, cycloheximide (Sigma-Aldrich) was added to the cell culture at a final concentration of 50μg/mL for 24h. The remaining intact cells were pelleted by centrifugation at 400G for 5 minutes and removed. The supernatant was harvested and stained for apoptotic bodies with CFSE 5(6)-CFDA/SE, Molecular Probes™ at a final concentration of 5μM for 15 minutes in the dark at room temperature.

***Ex vivo* larval hemocyte phagocytosis assay**

Ex vivo phagocytosis assay of apoptotic bodies or Alexia FluorTM 488 *S. aureus* BioparticulesTM conjugate for phagocytosis (Invitrogen) were performed as previously described (Petrignani *et al.* 2021). Briefly, five L3 wandering larvae carrying the HmlGal4,UAS-GFP macrophage marker were vortexed for 5 seconds and bled in 150 μL of Schneider medium supplemented with 1 μM Phenylthiourea (Sigma-Aldrich). After 1 minute 30 seconds, the macrophage suspension was transferred to a 1.5 mL low-bind tube (Eppendorf). The hemocytes were incubated with $1x10^6$ apoptotic bodies or $1x10^5$ Alexa Fluor 488 *S. aureus* Bioparticles for 60 minutes to enable phagocytosis, and subsequently placed on ice to stop the reaction. In order to quantify the fraction of cells phagocytosing and their fluorescence intensity, a flow cytometer was used (CytoFLEX, Beckman Coulter). 60 μL volume was read for two minutes at medium speed (30μL/Min). The macrophages were first gated using the HmlGal4,UAS-GFP hemocytes alone. The Red signal of apoptotic cells or Alexa Fluor™ 488 *S. aureus* Bioparticles™ (Invitrogen), indicative of macrophages with effective phagocytosis, was monitored with 488 nm laser and 585/40 standard filter.

The phagocytic index was calculated as followed:

$$\textbf{Fraction of hemocytes phagocytosing (f)} = \frac{[number\ of\ hemocytes\ in\ fluorescence\ positive\ gate]}{[total\ number\ of\ hemocytes]}$$

$$\textbf{Phagocytic index (PI)} = [Mean\ fluorescence\ intensity\ of\ hemocytes\ in\ fluorescence\ positive\ gate]\ x\ f$$

Gene expression levels by RT-qPCR

Gene expression measurements were performed by RT-qPCR as previously described (Carboni *et al.* 2022). Briefly, 5 wholes flies/larvae were homogenized and their RNA was extracted using TRIzol reagent and resuspended in RNase-free water. Reverse transcription was performed using PrimeScript RT kit (TAKARA) with random hexamers and oligo dTs. Quantitative PCRs were performed on a LightCycler 480 (Roche) using PowerUp SYBR Green Master Mix.

Statistical analysis

Survival experiments were performed using a Cox proportional hazards (CoxPH) regression model in R 1.4.1103. Each experiment was repeated independently three times unless otherwise indicated. Quantitative PCR data were compared by one-way ANOVA with *Holm-Šidak* multiple test correction in Prism. Error bars represent the standard error of the mean of replicate experiments (SEM). Data were analyzed using an appropriate statistical test as indicated in legends. P values are represented in the figures by the following symbols: ns for $p \geq 0.05$, * for *P* between 0.01 and 0.05; ** for *P* between 0.001 and 0.01, *** for *P* between 0.0001 and 0.001, **** for $p \leq 0.0001$.

RESULTS

Characterization of *Dnase II*^{sk4} null mutants

Dnase II is a gene which is strongly expressed in the larval fat body (Chintapalli *et al.* 2007). It is upregulated upon systemic infection (De Gregorio *et al.* 2002), indicating a possible function in host defense (**Fig. 4.1A**). In order to characterize the function of *Dnase II* in *Drosophila* immunity, we generated a null mutant line by CRISPR-Cas9 editing method, referred to as

Dnase II^{sk4}. *Dnase II^{sk4}* flies were homozygous viable but the mutant showed a delay and significant lethality during development, suggesting a role for *Dnase II* in larval tissue reorganization. *Dnase II^{sk4}* mutant flies also showed a drastically reduced lifespan (**Fig. 4.1B**) and displayed a reduced locomotor activity, as shown by a defect in climbing (**Fig. 4.1C**). This might indicate a role for *Dnase II* in neuronal functions or development of the nervous system. Finally, *Dnase II^{sk4}* mutant showed an overloaded microbiota at early adult stage (20 days old flies), suggesting a role for *Dnase II* in regulating the density or diversity of the microbiome (**Fig. 4.1D**). Considering the tri-directional communication between the central nervous system, the enteric nervous system and the microbiota, we wondered if removing the microbiota from *Dnase II^{sk4}* mutant flies could improve their locomotor activity. However, axenic *Dnase II^{sk4}* mutant flies displayed a similar climbing defect, refuting the hypothesis of a disrupted gut-brain axis. Altogether, these results suggest a role for *Dnase II* in larval development, aging and brain health and gut homeostasis.

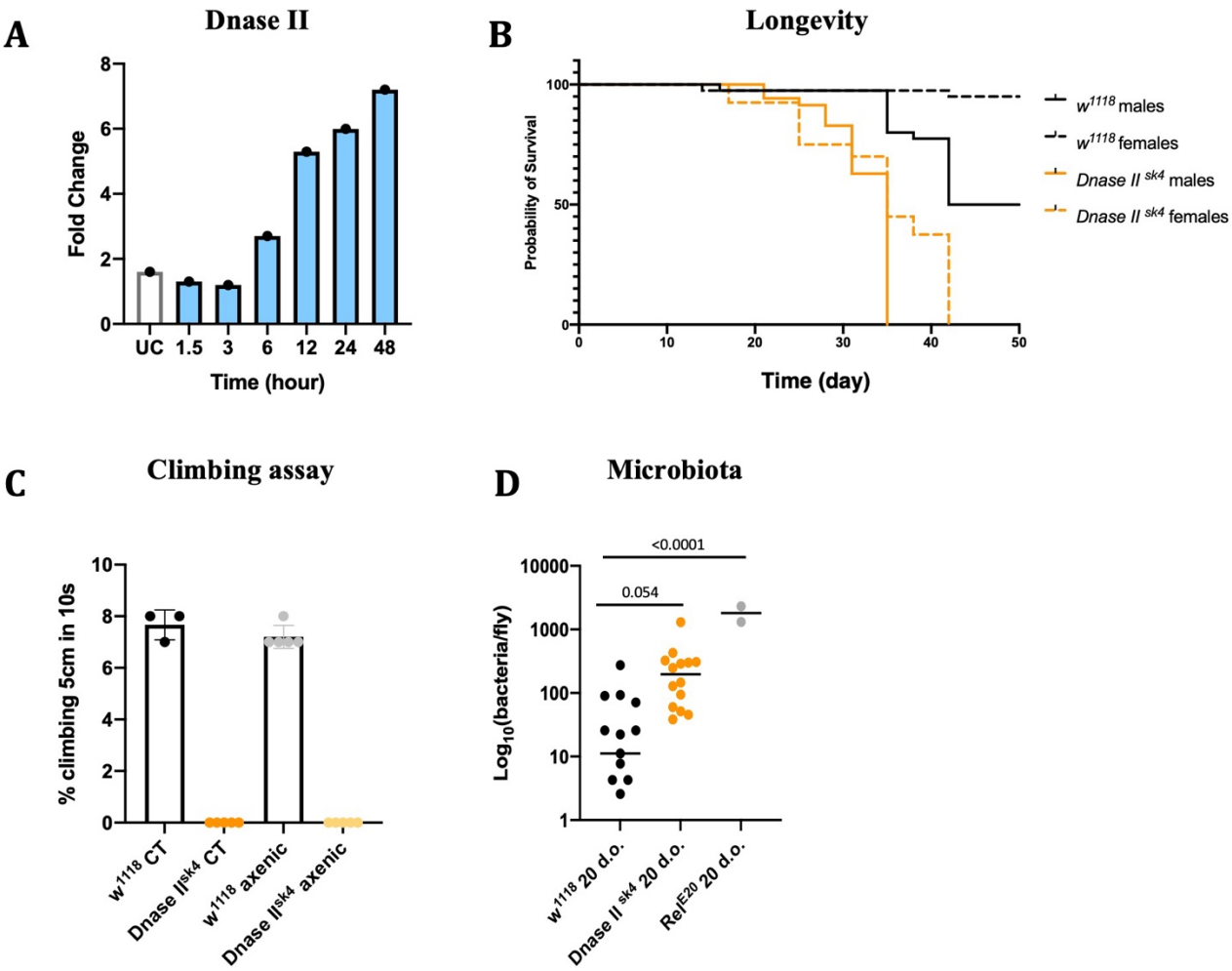

Figure 4.1. Characterization of Dnase II^{sk4} null mutants

(A) kinetics of *Dnase II* induction after septic injury with a mixture of the Gram-negative bacterium *Ecc15* and the Gram-positive bacterium *M. luteus*; these data was extracted from (De Gregorio et *al.* 2002) **(B)** Lifespan of wildtype (w^{1118}) and *Dnase II^{sk4}* mutant flies kept at 25°C on standard food. **(C)** 5-7 days old wild type (w^{1118}) and *Dnase II^{sk4}* mutant flies reared in in standard or axenic conditions were tested using a standard climbing assay **(D)** Colony Forming Units of the total microbiome (all species combined) in 20 days old wild type (w^{1118}), *Dnase II^{sk4}* mutant and *Relish^{E20}* mutant flies.

Dnase II mutant flies are susceptible to Gram-negative and Gram-positive systemic bacterial infection

We next explored the contribution of *Dnase II* to host defense. We observed that *Dnase II^{sk4}* mutant flies were susceptible to Gram-negative (*Ecc15*) and Gram-positive (*E. faecalis*) bacterial infections. Interestingly, they succumbed to these systemic infections with a different kinetics than classical immunodeficient mutant lines (*Relish^{E20}* and *Bom$^{\Delta 55C}$*) (**Fig. 4.2A ,B**). This susceptibility was not related to a dysfunctional Toll or Imd pathways, as indicated by wild-type level of expressions of respective readouts of these pathways after infection (**Fig.4.2C,D**). Moreover, bacterial load measurements performed on flies 7 days post infection revealed a wild-type ability of *Dnase II^{sk4}* mutants to eliminate invading pathogens after infection (**Fig. 4.2E**). Altogether, these results suggest a role for *Dnase II* in disease tolerance and not direct antimicrobial activity.

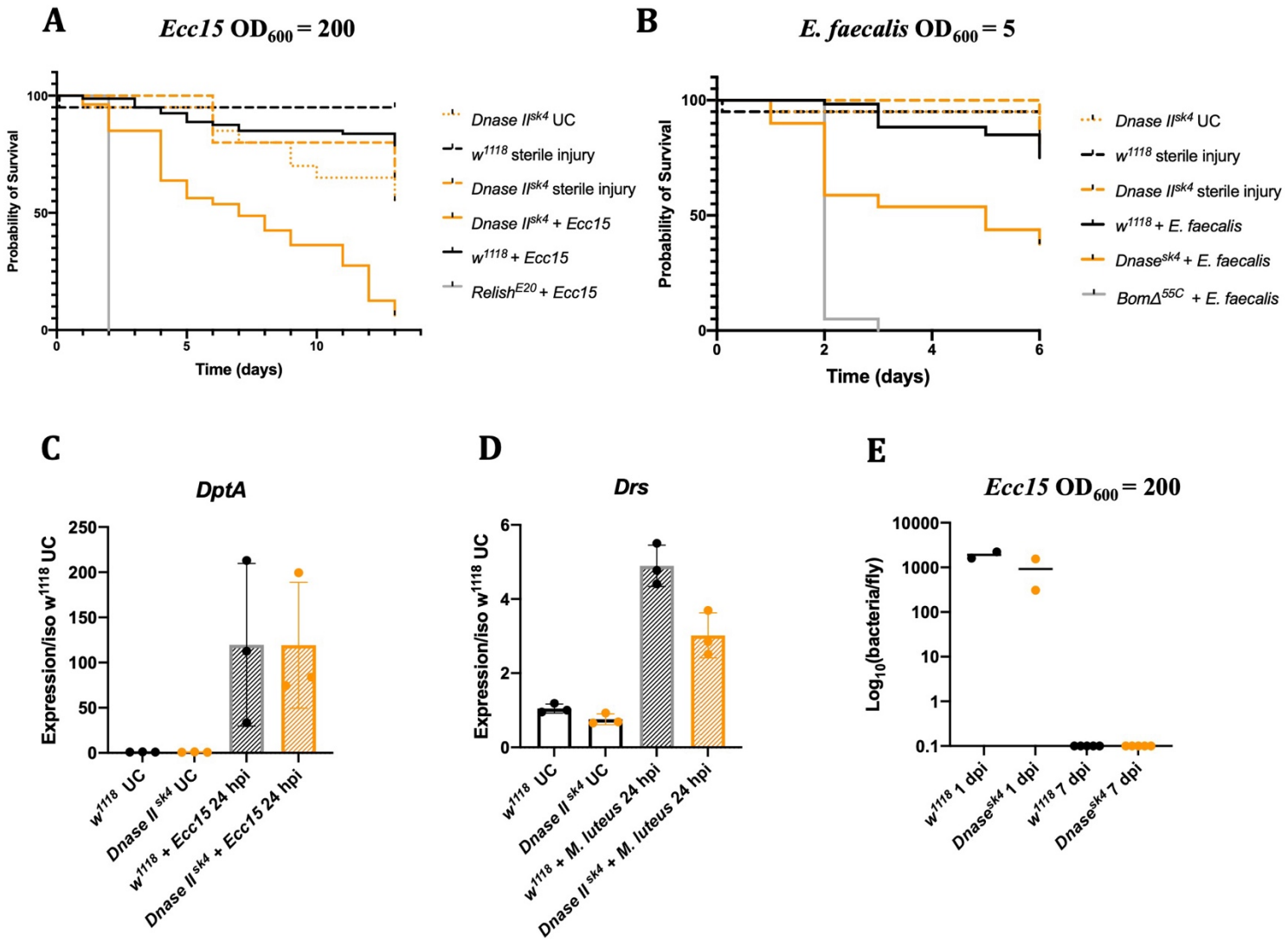

Figure 4.2. Dnase II^{sk4} mutant flies are susceptible to Gram-negative and Gram-positive bacterial infection

(A,B) Survival of wildtype (*w^{1118}*) and *Dnase II^{sk4}* flies upon infection with **(A)** *Ecc15* and **(B)** with *E. faecalis*. **(C,D)** qRT-PCR of measurement of **(C)** *DptA*, a readout for the Imd pathway and **(D)** *Drosomycin*, a readout for the Toll pathway in wildtype (*w^{1118}*) and *Dnase II^{sk4}* mutant flies 24 hours post infection with **(C)** *Ecc15* or **(D)** *M. luteus* **(E)** bacterial load measurements at 1 day or 7 days post *Ecc15* infection in wildtype (*w^{1118}*) and *Dnase II^{sk4}* mutant flies.

Hemocytes of *DNAse II^{sk4}* deficient larvae show a defect in the phagocytosis of apoptotic bodies.

We next decided to test the ability of larval macrophages to engulf labeled apoptotic corpses or labeled bacterial bioparticles using an *ex vivo* phagocytosis assay. Larval hemocytes from wild type, *Dnase II^{sk4}* mutants and the double mutant *NimC1;Eater* (used as a positive control for impaired phagocytosis (Melcarne *et al.* 2019)) were incubated with either apoptotic

bodies or bacterial bioparticles. We found a reduced phagocytic capacity of apoptotic bodies, but not of *S. aureus* bioparticles for *Dnase II*^{sk4} mutant macrophages, suggesting a specific role for *Dnase II* in efferocytosis (**Fig. 4.3A,B**). To investigate this hypothesis, we collected larval hemocytes for immunohistochemistry and microscopy analyses. Using a TUNEL assay, we assessed the phagocytosis of apoptotic DNA by hemocytes of larvae collected 2 hours after clean injury/pinching, in order to increase the events of phagocytosis. As presented in Fig. **4.3C**, we saw an accumulation of apoptotic DNA in *Dnase II*^{sk4} mutant hemocytes, suggesting that phagocytes could engulf, but not digest apoptotic bodies. In the same context, we also observed an increased cell size of *Dnase II*^{sk4} hemocytes as well as a weak TUNEL staining in hemocytes nuclei, suggesting that the inability to digest engulfed apoptotic DNA might result in the death of phagocytes.

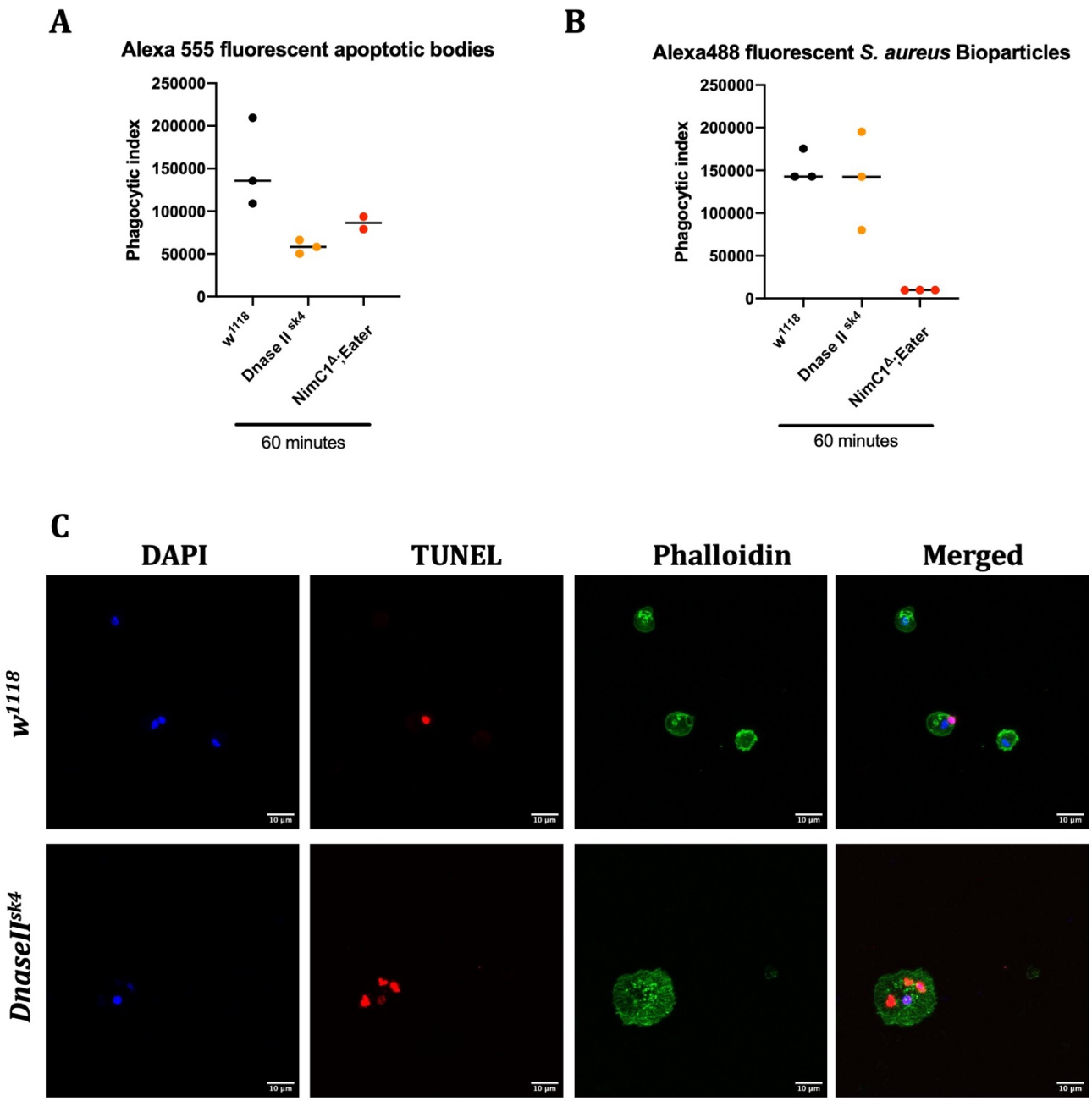

Figure 4.3. Impaired phagocytosis of apoptotic bodies in Dnase II^{sk4} mutant hemocytes

(A) Ex vivo phagocytosis assay using Alexa555 fluorescent apoptotic bodies. Wildtype (*w^{1118}*), *Dnase II^{sk4}* and *NimC1;Eater* mutant macrophages from L3 wandering larvae were incubated with Alexa555 fluorescent apoptotic bodies for 60 minutes at room temperature. Phagocytosis was quantified by flow cytometry. **(B)** *Ex vivo* phagocytosis assay using Alexa488 fluorescent *S. aureus* bioparticles. Wildtype (*w^{1118}*), *Dnase II^{sk4}* mutant, and *NimC1;Eater* mutant macrophages from L3 wandering larvae were incubated with Alexa488 fluorescent *S. aureus* bioparticles for 60 minutes at room temperature. Phagocytosis was quantified by flow cytometry. **(C)** Representative images of immunostaining of hemocytes from wildtype (upper panels) and *Dnase II^{sk4}* mutant (lower panels) hemocytes collected 2 hours after larval injury by pinching with forceps. Blue: DAPI ; Red: Tunel ; Green: Phalloidin. Scale bar: 10 µM.

DNA is not immunogenic

We next wondered if this impaired phagocytosis could consequently cause an activation of *Drosophila* innate immune pathways. It has previously been shown that the hypomorphic mutation of the *DNase II* gene (*Dnase II* ^{lo}) caused a constitutive activation the Imd pathway, suggesting that endogenous *Drosophila* DNA, when not degraded by the DNase II enzyme, activates innate immunity (Mukae *et al.* 2002). In unchallenged conditions, we confirmed that the expression levels of Diptericin A (a readout for the Imd pathway) in the hypomorphic *Dnase II* adult mutant (*Dnase II* ^{lo}) was significantly higher than wild type, although much lower than levels observed upon septic injury. However, we could not see a similar induction in the *Dnase II* ^{sk4} null mutant, nor the transheterozygote mutant (*Dnase II* ^{lo}*/Dnase II* ^{sk4}). We then decided to change the chromosomes I and II in the *Dnase II*^{lo} mutant line (referred to as *+;+;Dnase II* ^{lo}), in order to discard potential artifactual effects of the genetic background. In line with the results obtained with *Dnase II* ^{sk4} mutant, this new *DNase II* ^{lo} mutant line lost its constitutive induction of *DptA* **(Fig.4.4A).** These results suggest that higher *Dpt* expression in the original *Dnase II*^{lo} mutants used by Mukae et *al.* (2002) is due to a second site mutation on the first or second chromosome. We then decided to inject wild-type, *Dnase II* ^{lo} and *Dnase II* ^{sk4} mutant flies with either self-DNA (from *Drosophila*) or bacterial DNA (from *E. coli*). Interestingly, *DNase II* ^{lo} and *Dnase II* ^{sk4} mutant flies were not susceptible to DNA injections **(Fig.4.4B,D)**. Moreover, similar *Diptericin A* expression levels were measured after PBS or DNA injection in wild-type and *Dnase II*^{lo} mutants **(Fig.4.4C)**. Altogether, these results suggest that lacking *Dnase II* has no effect on the activation of immunity in unchallenged adult flies, and that the injection of naked DNA into the hemolymph of wild-type and *Dnase II* ^{sk4} mutant flies is not immunogenic. Nevertheless, the consequences of the impaired phagocytosis of apoptotic bodies in *Dnase II* ^{sk4} mutant hemocytes might be revealed in other contexts.

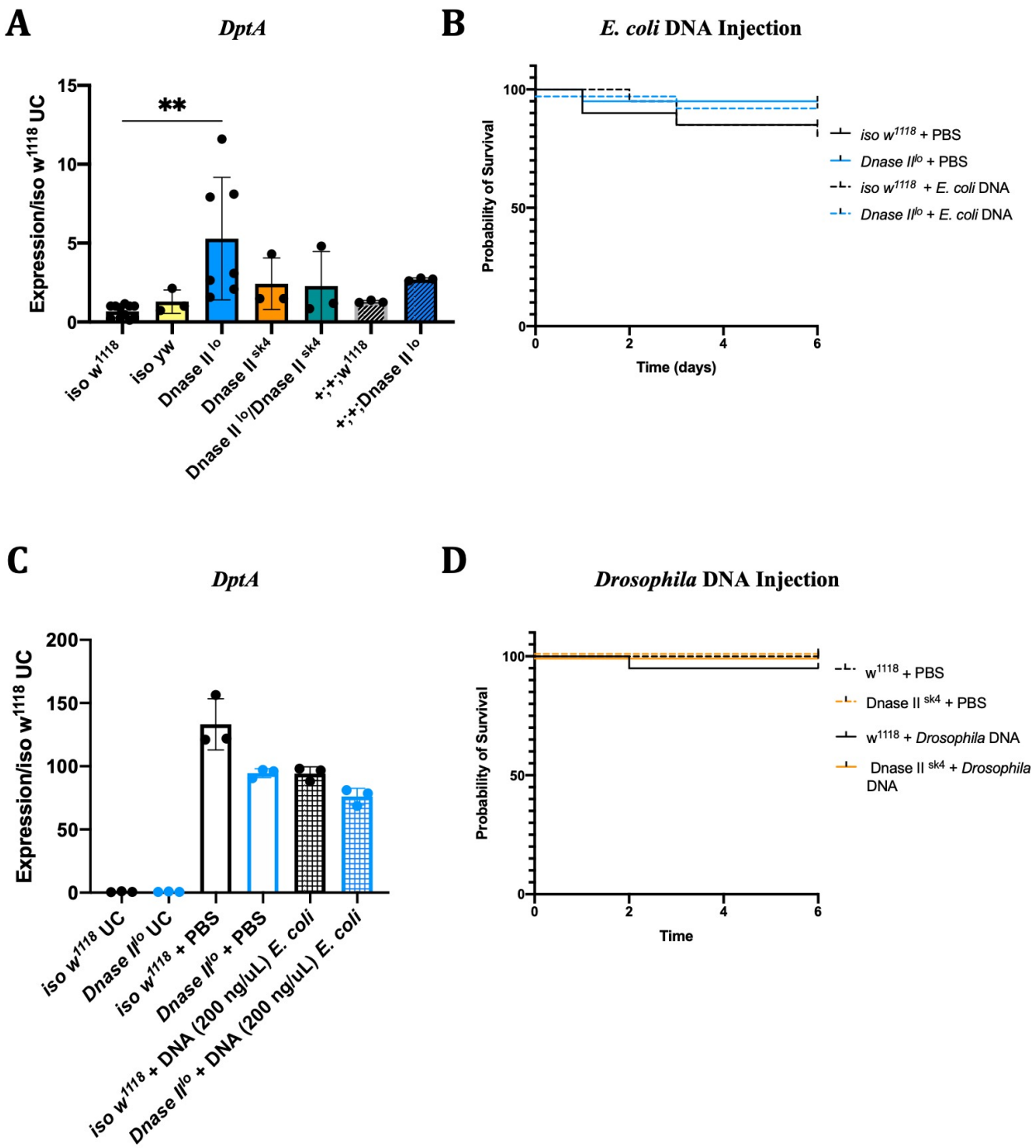

Figure 4.4. DNA is not immunogenic

(A) qRT-PCR of *DptA* expression in unchallenged adult flies of the following genotypes: wildtype (*iso* w^{1118}, *iso yw*), *DnaseII*^{lo} hypomorphic mutant, *Dnase II*^{sk4} mutant, *DnaseII*^{lo}/*DnaseII*^{sk4} transheterozygote mutant, wild-type with change of chromosome I and II, and *Dnase II* ^{lo} hypomorphic mutant with changed chromosome I and II **(B)** Survival experiments of wild-type (w^{1118}) or *Dnase II* ^{lo} flies upon injection of PBS (control) or *E. coli* DNA **(C)** qRT-PCT of *DptA* expression in wildtype (w^{1118}) or *Dnase II* ^{lo} hypomorphic mutant adult flies in unchallenged conditions, after PBS injection or after injection of DNA from *E. coli*. The injection of DNA does not lead to higher induction of *DptA* than injection of PBS. **(D)** Survival experiments upon injection of PBS (control) or *Drosophila* DNA in wild-type (w^{1118}) or *Dnase II* ^{sk4} mutant flies

Dnase II^{sk4}* mutant larvae show an enhanced activation of IMD signalling after injury, which required *Relish* and *Sting

To investigate the consequences of *Dnase II* absence in an apoptotic setting, we established an *in vivo* assay. We collected L3 wandering larvae and gently pinched their posterior cuticle using forceps, in order to generate apoptotic corpses within their body cavity, but without causing an infection. When then measured the expression levels of *DptA* and *DptB*, two readouts for the activation of the Imd pathway, in whole larvae (**Fig. 4.5A,B**). Our results showed that both *DptA* and *DptB* were induced in wild-type flies after pinching. Strikingly, this induction was significantly higher in *Dnase II^{sk4}* mutant larvae 2 hours after injury, compared to wild type larvae. Interestingly, this over-activation of Imd signalling after injury in the *Dnase II^{sk4}* mutants could be rescued by inactivating not only *Relish* but also *Sting* genes (**Fig. 4.5A,B**). These results show that the overactivation of the Imd pathway after injury caused by the absence of *Dnase II* is *Relish* and *Sting* dependent.

We then wondered if any other immune pathway was affected after larval pinching in our *Dnase II^{sk4}* mutants. Strikingly, we observed a constitutive activation of the JNK pathway in unchallenged *Dnase II^{sk4}* mutant larvae, as indicated by the high expression levels of *Puckered*, a readout for the JNK pathway (**Fig. 4.5C**). This activation was not affected by injury, and did not depend on *Sting*, indicating the existence of two distinct and independent phenotypes (**Fig. 4.5D**).

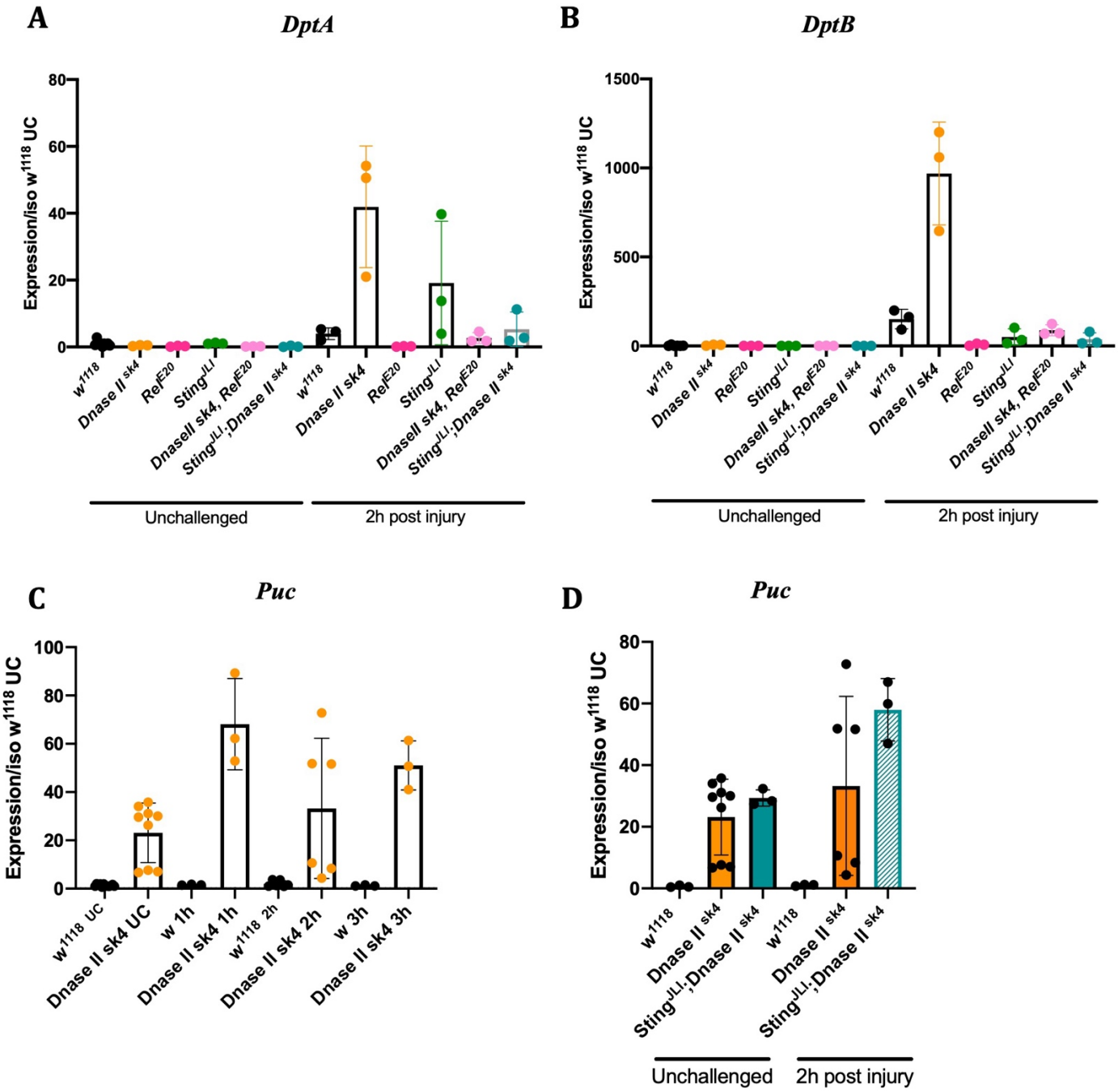

Figure 4.5. Dnase IIsk4 mutant larvae show an activated IMD signalling after injury

(A,B) qRT-PCR of **(A)** *DptA* and **(B)** *DptB* expression in unchallenged larvae or in larvae 2 hours after pinching with forceps in the following genotypes : wildtype (w^{1118}), *Dnase II*^{sk4} mutant, *Relish*^{E20} mutant, *Sting*^{JLI} and *DnaseII*^{sk4},*Relish*^{E20} double mutant, *DnaseII*^{sk4},*Sting*^{JLI} double mutants. **(C,D)** qRT-PCR of puckered in unchallenged larvae or 1 to 3 hours after injury by larval pinching with forceps in the following genotypes: **(C)** wildtype (w^{1118}) and *Dnase II*^{sk4} mutant, and **(D)** wildtype (w^{1118}), *Dnase II*^{sk4} mutant and *DnaseII*^{sk4},*Sting*^{JLI} double mutant.

DISCUSSION

In this study, we generated the first null mutant for *Dnase II*. In agreement with previous studies (Seong *et al.* 2006; Tarayrah-Ibraheim *et al.* 2021), *Dnase II*^{sk4} mutant flies show a strong delay and a significant lethality during development, and a reduced lifespan. Moreover, *Dnase II*^{sk4} mutants show similar locomotor defect. Such locomotor defect are also observed in *Draper*, *SIMU* and *NimB4* single mutants and has been associated with defective clearance of apoptotic cells during embryonic or larval brain development (MacDonald *et al.* 2006; Kurant *et al.* 2008; Petrignani *et al.* 2021). This led us to speculate that Dnase II could play a major role in the clearance of apoptotic cells by degrading DNA during efferocytosis. *Dnase II*^{sk4} mutants also display a higher susceptibility to bacterial systemic infections. However, they display a wild-type ability to express AMPs after infection, indicating effective humoral immune responses. Moreover, the slow and gradual susceptibility of *Dnase II*^{sk4} mutants to systemic infection differs from that of classical immunodeficient mutants. These findings align with the constitutive activation of the JNK pathway in *Dnase II*^{sk4} mutants, associated with enhanced cellular stress responses. Altogether, these data indicate that *Dnase II* is not directly antimicrobial, but rather suggest a role in disease tolerance.

It was previously thought that the absence of *DNase II* in adult flies leads to a constitutive activation of the Imd pathway in response to undigested DNA accumulation (Mukae *et al.* 2002). In our study, we contradict their results, as we show that changing the genetical background of the hypomorphic *Dnase II*^{lo} line abolishes its phenotype. We could also not show a deleterious effect of DNA injection in wild-type nor *Dnase II* deficient flies. It should be pointed out that our experiments were performed using naked DNA (DNA which is not associated with proteins). It remains possible that the proteins associated with DNA to form nucleosomes, the histones, but not the DNA strands themselves, are immunogenic. To answer these hypotheses, we plan to inject apoptotic bodies in wild-type and *Dnase II*^{sk4} mutant flies and record their viability.

By performing *in vivo* phagocytosis assays in larvae, we showed the accumulation of apoptotic DNA in intracellular vesicles of *Dnase II* mutant hemocytes after injury. This is consistent with a role of *Dnase II* in efferocytosis. We consequently showed that injuring larvae leads to an enhanced upregulation of *Diptericin A* and *Diptercin B* transcripts in *Dnase II*^{sk4} mutants 2h

later. Not surprisingly, this higher expression of *Dpt* in *Dnase II* deficient flies relies on *Relish*, the transcription factor of the Imd pathway. Strikingly, we observed that this higher expression of Dpt in *Dnase II* deficient flies upon pinching relies on *Sting*, the secondary messenger of the cGAS-STING pathway. These results raised the hypothesis that Sting could be activated in the *Dnase II* mutant upon detection of undegraded double stranded DNA by a cytosolic sensor. Future work will focus on the role of cGAS-like Receptors (dm-cGLRs), recently identified in *Drosophila* to activate the STING-Relish pathway. A recent study conducted *in vitro* showed that Dm-cGLR1 is able to bind double stranded RNA, while Dm-cGLR2 to viral nucleic acids. To date, Dm-cGLR3 has no identified binding partner (Holleufer *et al.* 2021; Slavik *et al.* 2021) and could be involved in sensing DNA. We would like to investigate whether one of the three cGLRs could bind double stranded DNA or DNA-associated proteins such as histones, and act downstream of *Dnase II* in *Dpt* activation. Future work in vivo will also focus on deciphering the pathway linking the accumulation of apoptotic DNA in hemocytes of *Dnase II* mutant larvae and the upregulation of the Imd pathway after injury through *Sting* activation.

In this study, we show for the first time a role for *Dnase II* in preventing an Imd-dependent upregulation of innate immunity after sterile injury in larvae. Future work should also focus on the tissue specificity of *DNase II* activity, and reveal whether it is restricted to phagocytic macrophages, or if it is also essential in other tissues such as the fat body. We could unfortunately not reproduce our key results by knocking down specifically *Dnase II* in the hemocytes (*hmlGal4>UAS-DnaseII-IR*), suggesting an activity for *Dnase II* which is not restricted to plasmatocytes. Phylogenetic analyses highlight the existence of another Dnase, named *Dnase I*, in all species except insects. *Dnase II* is defined as an intracellular protein, while *Dnase I* as a secreted extracellular protein. As insect species specifically lost *Dnase I* during evolution, we wonder if *Dnase II* endorsed the molecular role of *Dnase I* and is also, to some extent, secreted. In this study, we did not observe any induction of the Toll and Imd pathway by external DNA, and it remains unclear if *Drosophila* possess a pattern-recognition receptor involved in the sensing of DNA. Future ongoing work in our lab should better delineate the role of *Dnase II* in *Drosophila* immune response. Results obtained in *Drosophila* might shed light on the conserved role of Dnases in development and immunity.

REFERENCES

Cai H., A. Holleufer, B. Simonsen, J. Schneider, A. Lemoine, *et al.*, 2020 2'3'-cGAMP triggers a STING- and NF-κB–dependent broad antiviral response in Drosophila. Sci. Signal. 13. https://doi.org/10.1126/scisignal.abc4537

Carboni A. L., M. A. Hanson, S. A. Lindsay, S. A. Wasserman, and B. Lemaitre, 2022 Cecropins contribute to Drosophila host defense against a subset of fungal and Gram-negative bacterial infection. Genetics 220: iyab188. https://doi.org/10.1093/genetics/iyab188

Chintapalli V. R., J. Wang, and J. A. T. Dow, 2007 Using FlyAtlas to identify better Drosophila melanogaster models of human disease. Nat Genet 39: 715–720. https://doi.org/10.1038/ng2049

De Gregorio E., P. T. Spellman, P. Tzou, G. M. Rubin, and B. Lemaitre, 2002 The Toll and Imd pathways are the major regulators of the immune response in Drosophila. The EMBO Journal 21: 2568–2579. https://doi.org/10.1093/emboj/21.11.2568

Hanayama R., M. Tanaka, K. Miyasaka, K. Aozasa, M. Koike, *et al.*, 2004 Autoimmune disease and impaired uptake of apoptotic cells in MFG-E8-deficient mice. Science 304: 1147–1150. https://doi.org/10.1126/science.1094359

Holleufer A., K. G. Winther, H. H. Gad, X. Ai, Y. Chen, *et al.*, 2021 Two cGAS-like receptors induce antiviral immunity in Drosophila. Nature 597: 114–118. https://doi.org/10.1038/s41586-021-03800-z

Isaacs A., R. A. Cox, and Z. Rotem, 1963 FOREIGN NUCLEIC ACIDS AS THE STIMULUS TO MAKE INTERFERON. The Lancet 282: 113–116. https://doi.org/10.1016/S0140-6736(63)92585-6

Kondo S., and R. Ueda, 2013 Highly Improved Gene Targeting by Germline-Specific Cas9 Expression in Drosophila. Genetics 195: 715–721. https://doi.org/10.1534/genetics.113.156737

Kurant E., S. Axelrod, D. Leaman, and U. Gaul, 2008 Six-microns-under acts upstream of Draper in the glial phagocytosis of apoptotic neurons. Cell 133: 498–509. https://doi.org/10.1016/j.cell.2008.02.052

MacDonald J. M., M. G. Beach, E. Porpiglia, A. E. Sheehan, R. J. Watts, *et al.*, 2006 The Drosophila Cell Corpse Engulfment Receptor Draper Mediates Glial Clearance of Severed Axons. Neuron 50: 869–881. https://doi.org/10.1016/j.neuron.2006.04.028

McIlroy D., M. Tanaka, H. Sakahira, H. Fukuyama, M. Suzuki, *et al.*, 2000 An auxiliary mode of apoptotic DNA fragmentation provided by phagocytes. Genes Dev. 14: 549–558. https://doi.org/10.1101/gad.14.5.549

Melcarne C., E. Ramond, J. Dudzic, A. J. Bretscher, É. Kurucz, *et al.*, 2019 Two Nimrod receptors, NimC1 and Eater, synergistically contribute to bacterial phagocytosis in Drosophila melanogaster. The FEBS Journal 286: 2670–2691. https://doi.org/10.1111/febs.14857

Mukae N., H. Yokoyama, T. Yokokura, Y. Sakoyama, and S. Nagata, 2002 Activation of the innate immunity in Drosophila by endogenous chromosomal DNA that escaped apoptotic degradation. Genes Dev 16: 2662–2671. https://doi.org/10.1101/gad.1022802

Okabe Y., K. Kawane, S. Akira, T. Taniguchi, and S. Nagata, 2005 Toll-like receptor-independent gene induction program activated by mammalian DNA escaped from apoptotic DNA degradation. J Exp Med 202: 1333–1339. https://doi.org/10.1084/jem.20051654

Petrignani B., S. Rommelaere, K. Hakim-Mishnaevski, F. Masson, E. Ramond, *et al.*, 2021 A secreted factor NimrodB4 promotes the elimination of apoptotic corpses by phagocytes in Drosophila. EMBO reports 22: e52262. https://doi.org/10.15252/embr.202052262

Roh J. S., and D. H. Sohn, 2018 Damage-Associated Molecular Patterns in Inflammatory Diseases. Immune Netw 18: e27. https://doi.org/10.4110/in.2018.18.e27

Seong C.-S., A. Varela-Ramirez, and R. J. Aguilera, 2006 DNase II deficiency impairs innate immune function in Drosophila. Cellular Immunology 240: 5–13. https://doi.org/10.1016/j.cellimm.2006.05.007

Seong C.-S., A. Varela-Ramirez, X. Tang, B. Anchondo, D. Magallanes, *et al.*, 2014 Cloning and Characterization of a Novel Drosophila Stress Induced DNase. PLOS ONE 9: e103564. https://doi.org/10.1371/journal.pone.0103564

Slavik K. M., B. R. Morehouse, A. E. Ragucci, W. Zhou, X. Ai, *et al.*, 2021 cGAS-like receptors sense RNA and control 3’2’-cGAMP signalling in Drosophila. Nature 597: 109–113. https://doi.org/10.1038/s41586-021-03743-5

Tarayrah-Ibraheim L., E. C. Maurice, G. Hadary, S. Ben-Hur, A. Kolpakova, *et al.*, 2021 DNase II mediates a parthanatos-like developmental cell death pathway in Drosophila primordial germ cells. Nat Commun 12: 2285. https://doi.org/10.1038/s41467-021-22622-1

Yoshida H., Y. Okabe, K. Kawane, H. Fukuyama, and S. Nagata, 2005 Lethal anemia caused by interferon-beta produced in mouse embryos carrying undigested DNA. Nat Immunol 6: 49–56. https://doi.org/10.1038/ni1146

Chapter 5: General discussion and perspectives

The aim of this PhD thesis was to understand the complexity and diversity underlying *Drosophila melanogaster* innate immune responses. Indeed, we characterized the function of three immune-related gene families and their involvement in different processes associated with the immune response. All three chapters of this thesis could be conducted thanks to the powerful genetic techniques possible in *Drosophila melanogaster,* allowing us to investigate various molecular processes, and more specifically, innate immune mechanisms.

Our first study (Carboni *et al.* 2022) focused on a family of antimicrobial peptides named the Cecropins. We showed a role for Cecropins in the defense against certain Gram-negative bacterial species (more specifically against *Gammaproteobacteria*), and against fungi, consistent with in vitro data ((Hultmark *et al.* 1980; Steiner *et al.* 1981, 1988). These results show how *Drosophila* elicits a humoral immune response in response to the detection of specific microbes, and selectively enhances the production of multiple immune effectors, some of them with high specificity (Hanson *et al.* 2019). By performing the first *in vivo* functional characterization of Cecropins in *Drosophila* immune defense, this study contributes to the rapid progress in understanding the role of immune effectors in *Drosophila*. Recent research has greatly advanced this field, notably with the new ability to produce mutations in small genes and to combine them in compound mutants, uncovering specific roles of genes which cannot be detected by single mutations. This study adds support for the amendment of the previous "cocktail" model of action for AMPs, which postulated that AMPs are generalist effectors which are required as a combination to fight infection. Indeed, our study reveals the specific role of Cecropin activity against certain microbes. When examining the role of AMPs from an immune perspective, we are probably only scratching the surface on their importance in *Drosophila* physiology.

A second part of this doctoral thesis focused on the effects of environmental – or abiotic – factors on *Drosophila* innate immune genes. Indeed, we showed that stressful environmental conditions could increase the expression of antimicrobial peptides, which can be cytotoxic to host cells. More specifically, the tracheal system shows an intrinsic vulnerability to the action of AMPs due to the high levels of phosphatidylserine exposure on tracheal cell membranes.

We showed that a family of stress induced peptides, the Turandots, protect *Drosophila* tracheas from AMP-dependent killing. In this study, we showed for the first time an example of a humoral mechanism used to promote resilience to stress, by limiting collateral damages of immune effectors. The combination of *in vitro* and *in vivo* experiments allowed us to delineate the mode of action of Turandots. Turandots are secreted into the hemolymph of flies and subsequently bind to host cells exposing high levels of phosphatidylserines, masking them from cationic pore forming AMPs. Consistent with this, deleting AMPs rescued the susceptibility of *Turandot* mutants to various stresses.

Finally, the third part of this thesis characterized the role of Dnases in *Drosophila* host defense. We investigated the hypothesis that nucleic acids, if not properly digested by professional enzymes called Dnases, can be recognized as a danger signal by the innate immune system and induce "sterile" activation of immunity. Our study finds multiple roles for Dnase II in efferocytosis and disease tolerance.

5.1. The interconnection between immune resistance and disease tolerance

Although the complexity of immune responses varies between species, all living organisms possess some form of immune system. Even prokaryotes, the earliest and most primitive forms of life on Earth, have protective mechanisms against invading pathogens, such as the use of restriction enzymes, bacteriocidins and CRISPR systems. This ability to limit pathogen burden has been more precisely defined as "immune resistance". Nevertheless, this protection mechanism, essential for organism survival, is tied to associated risks and consequences. A major risk of an active immune system lies in the possibility of mounting immune responses against harmless self-molecules, cells or tissues. The repercussions of an immune response are characterized by detrimental effects to body functions or structures, that come with or follow an infection. Therefore, multiple mechanisms have evolved in addition to immune defense to cope with the side effects of infection, without having any effect on pathogen load. These mechanisms, known as "disease tolerance", are defined as the ability to protect host tissues during or after an infection, by tissue repair or detoxification mechanisms. More precisely, disease tolerance can be categorized into two different

strategies. On one hand, organisms have evolved mechanisms to tolerate damage on host tissues directly caused by the pathogen itself (e.g., pathogen virulence factors). On the other hand, organisms also rely on mechanisms aiming at limiting damage caused by their own immune response, i.e., at limiting "immunopathologies" **(Fig.5.1.)**. This doctoral thesis consistently aims to illuminate fine interconnections between immune resistance and disease tolerance, which are central mechanisms of the innate immunity. We show a potent immune resistance mechanism through our work on the Cecropin antimicrobial peptides. Indeed, these peptides are described as immune effectors that play a crucial role in combating bacterial and fungal infections. Through the prism of host defense, the antimicrobial activity of immune effectors, such as AMPs, is essential to survive infection. However, by taking a step back to gain a broader and more global perspective, we show that these activated effectors might have detrimental repercussions on host healthy cells and tissues. Thus we have studied another family of proteins, the Turandots, which evolved to promote resilience to stress by preventing AMP-dependent pore formation to some tissues such as tracheas. Indeed, our study revealed negative consequences of the secretion of high concentrations of AMPs in response to stress on the respiratory system, which is critical to survive stress. Interestingly, removing only the four *Cecropin* genes was sufficient to protect the tracheae of *Turandot*-deficient flies or flies genetically modified to increase membrane PS exposure. Thus, the evolution of Turandots represents an crucial innovation in *Drosophila* that allows mitigation of the toxicity of AMPs towards self tissues while maintaining a potent immune response for host defense, therefore improving their efficacy.

Over the last decade, many studies have pointed out the coupling of immune resistance and disease tolerance not only in *Drosophila melanogaster*, but also in other model organisms. The first example of a key mechanism that limits immunopathology resulting from an immune response is common to all organisms: the evolution of catalases, key enzymes that protect cells from oxidative damage by the antimicrobial reactive oxygen species (ROS) (Radyuk *et al.* 2009; Lee *et al.* 2009). Another conserved tolerance mechanism relies on the evolution of negative regulators of immune pathways. These evolved to prevent damage by overactivation of the immune system, ultimately mitigating the development of immunopathologies. This is the case for *PGRP-LB* in the Imd pathway or *Puckered* in the JNK pathway in *Drosophila*. Furthermore, a pioneer study showed how genes controlling the metabolic stress response, such as *FOXO* or *Akt*, increase *Drosophila* survival to infection without interfering with

pathogen load (Dionne *et al.* 2006). Another study conducted in flies identified a group of genes which reduce endurance (another term used for tolerance at that time) to *Listeria monocytogenes* infection, without affecting the bacterial load of infected flies (Ayres *et al.* 2008). In flies, the bacterial endosymbiont *Wolbachia* has been shown to be responsible in the disease tolerance to *Flock House Virus* (*FHV*) or *Insect Iridescent Virus 6* (*IIV-6*) infections (Teixeira *et al.* 2008).

In mammals, the first demonstration and interpretation of disease tolerance mechanisms were performed in the context of *Plasmodium* infection. Indeed, a pioneer study used a rodent-Malaria infection model to demonstrate that resistance and tolerance were genetically negatively correlated, suggesting that these two mechanisms are traded off against each other (Råberg *et al.* 2007). In the same context, another study described the first molecular mechanism promoting disease tolerance to infection, without any effect on parasite burden (Seixas *et al.* 2009). Indeed, infection with *Plasmodium* is associated with hemolysis, leading to the release of hemoglobin into circulation, which can be oxidized and produce deleterious free heme. The heme-catabolizing enzyme HO-1 is responsible for the degradation of heme, thus reducing tissue damage following *Plasmodium* infection. The same year, another study, conducted on *Drosophila* and mice, showed an essential role of ATP-sensitive potassium (K_{ATP}) channels in protection against viral infections, without any effect on pathogen loads (Croker *et al.* 2007). In the following years, novel studies pointed out deleterious effects of activated programmed cell death on host tissues during or following infection. Therefore, it was suggested that deleting master regulator genes of different cell death programs (apoptosis, necroptosis) is sufficient to confer disease tolerance to microbial or viral infections in mice. This was shown by deleting the genes *RIP Kinase 3* (*RIPK3*) or *cIAP2*, which are essentials for necroptosis signaling (Duprez *et al.* 2011; Rodrigue-Gervais *et al.* 2014).

Interestingly, the mechanisms governing disease tolerance are closely interconnected with those of biological resilience, and the two concepts are often used interchangeably. On one hand, disease tolerance represents a defense mechanism by which an organism limits tissue damage that comes with or follows an infection. Biological resilience, on the other hand, is defined as the ability of an organism to recover after prolonged exposure to extreme environmental parameters. It is carried out through the activation of various stress responses which are able to limit cell or tissue damage. These two mechanisms have thus evolved with

the same objective: maintain and restore homeostasis after stress, whether it is biotic or abiotic. In our study, we define for the first time proteins which are at the interplay between disease tolerance and biological resilience. Indeed, we show that Turandot proteins promote biological resilience to environmental stressors, as Tot mutants die to stress exposure. Additionally, we show that Turandots are key humoral molecules for the protection of host tissues (more specifically, tracheae) against antimicrobial peptide killing. Therefore, they are essential to counteract collateral damages of an activated immune response, conferring them a role in disease tolerance.

In the future, it would be of interest to investigate the metabolic adaptation of *Tot* mutants to stress exposure. Indeed, metabolic adaptation represents a main outcome of the stress response which aims at preserving essential cellular and physiological functions to avoid tissue failure and death. Several studies have shown the importance of the tracheal system remodeling in response to stress exposure in flies, which reflect a need for increased oxygen supply in response to increased metabolic needs, thus metabolic adaptation. It would also be interesting to investigate the effect of *Tot* mutation on other *Drosophila* tissues which are known to expose some PS, like the muscles or the neurons (Park *et al.* 2021). Indeed, numerous recent studies have pointed out a role for AMPs in neurodegenerative diseases (Arora and Ligoxygakis 2020). In this context, the Turandot proteins represent promising molecules in protecting the central nervous system and preventing aging or neurodegeneration. The identification of novel factors such as the Turandots, protecting host cells from immune-induced damage and thus immunopathologies, opens the door to novel applications in therapeutic and clinical contexts.

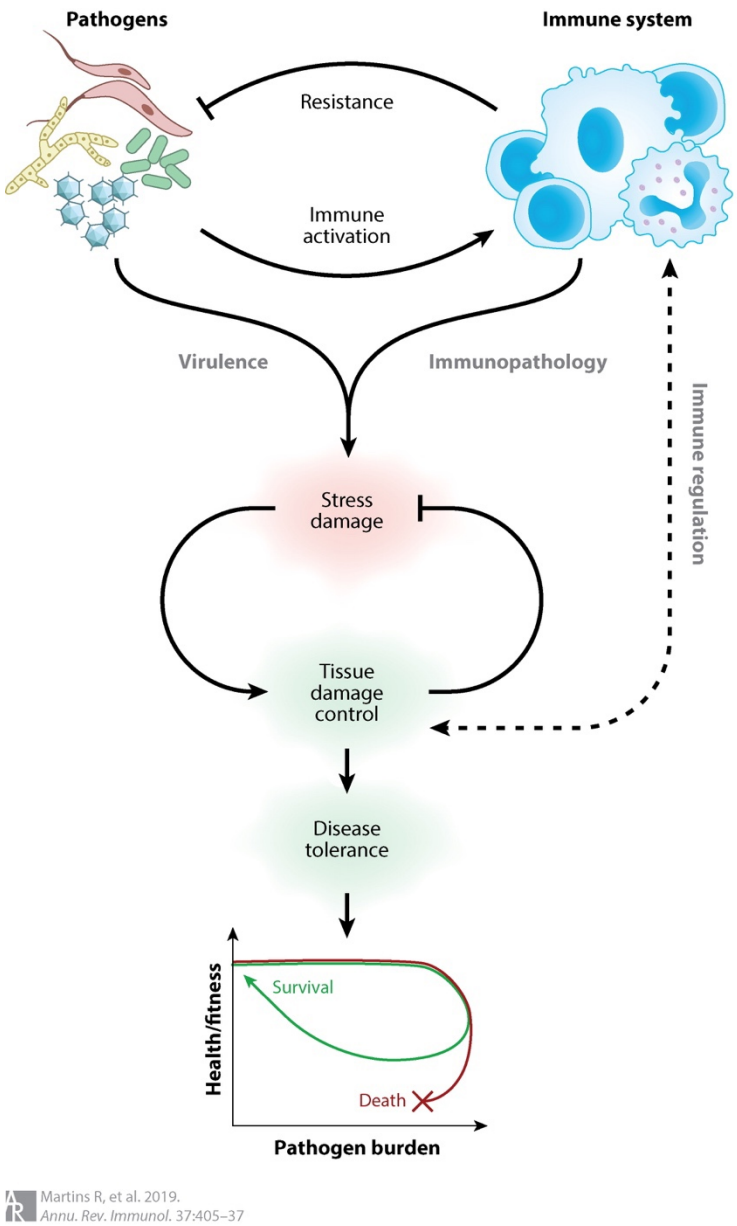

Figure 5.1. The fitness cost resulting from host-pathogen interactions.
Invasion of pathogens triggers an immune response in the host, providing resistance to infection. However, the virulence of the pathogens, combined with immune-driven resistance mechanisms (immunopathology), lead to different forms of stresses and damage on host tissues. The control of tissue damage relies on the establishement of disease tolerance mechanisms, which increases host health/survival without any effect on the pathogen load (from (Martins *et al.* 2019)).

5.2. Sterile inflammation as part of innate immunity

Immune resistance mechanisms are associated with risks and consequences. The main risks of an active immune system lie in the possibility of mounting immune responses in the

absence of pathogenic microorganisms, as a sustained activated immune response, being extremely costly, might become detrimental for the organism. The inflammation that results from traumatic events, such as an injury, is called “sterile inflammation”. There is ongoing debate regarding the classification of “sterile inflammation” as a component of the immune response. Indeed, it challenges the traditional definition of inflammation as a physiological response triggered by the recognition of foreign invading pathogens. However, some argue that, even though the molecular patterns triggering the immune activation are different, the downstream signaling pathways and mechanisms are the same. In this chapter, we will present a state-of-the-art of the concept of “sterile inflammation” in different model organisms, and discuss its inclusion as a component of *Drosophila* innate immunity.

Sterile inflammation can be initiated by different aseptic injuries: mechanical trauma, chemicals, toxins, or even harmless antigens. It has been suggested that these injuries induce the accumulation of inflammatory particles in the circulation: dead cells, but also Damaged-Associated Molecular Patterns (DAMPs) (Chen and Nuñez 2010). The accumulation of pro-inflammatory factors is thought to initiate the activation of immunity through the binding of DAMPs to specific membrane receptors. In mammals, DAMPs are known to bind to Toll Like Receptors (TLRs), the Receptor for Advanced Glycation End products (RAGE), and possibly other unidentified receptors. This binding induces nuclear translocation of NF-κB, which stimulates the production of pro-inflammatory cytokines, such as Tumor Necrosis Factor (TNF) and Interleukin-1 (IL-1), notably through the activation of the intracellular inflammasome complex. This secretion of inflammatory cytokines additionally results in the recruitment of immune cells, such as neutrophils and macrophages. Thus, sterile inflammation is characterized by the activation of signaling pathways that are parts of the innate immune response.

One well-characterized activation of sterile inflammation in mammals occurs through the detection of the DAMP ‘High Mobility Group Box 1’ (HMGB1) by the receptor RAGE. HMGB1 is a chromatin protein, which interacts with histones, nucleosomes and transcription factors. In 1999, it was shown that this protein can be released into the circulation upon cytokine stimulation and subsequently act as a cytokine itself (Wang *et al.* 1999). There are more than 700 publications characterizing the implication of HMGB1 binding to RAGE, the majority describing the subsequent activation of NF-κB and stimulation of cytokines, resulting in

diverse immunopathologies (Sims *et al.* 2010). These findings strongly support the concept of sterile inflammation as an immune response to DAMPs in mammals.

As *Drosophila* lacks adaptative immune responses, it has been described as a good model to study the primary defense against DAMPs (Shaukat *et al.* 2015). Several studies have indeed defined 'impaired apoptosis' as a trigger of sterile inflammation in *Drosophila*. As extensively discussed in Chapter 4, our study reveals that loss of *Dnase II* leads to the accumulation of endogenous DNA. We however observe that the loss of *Dnase II* does not lead to high activation of the Imd pathway, but only potentiates the immune response. Indeed, we observed higher expression of the Imd pathway readouts, Diptericins A and B, two hours after injuring Dnase II mutant larvae, compared to wild type. Thus, our study does not confirm previous observations of (Mukae *et al.* 2002) which suggested that the absence of Dnase II led to DNA escape, activating immunity. Interestingly, another study has linked apoptosis dysfunction to Toll signaling pathway: a deficiency in *Dronc*, an initiator caspase, leads to active cleavage of Spz, leading to the canonical activation of the Toll pathway (Ming *et al.* 2014). Additionally, using a *Rasv12* oncogenic model, other studies suggested that cells with tumor-like properties elicit sterile signals which activate both the humoral and cellular branches of innate immunity (Parisi *et al.* 2014; Hauling *et al.* 2014). Another recent study also demonstrated the existence of DAMP-initiated immune signaling in *Drosophila*. They showed that the detection of alpha-actinin, via an unidentified receptor, induces a Src-family kinase dependent cascade, leading to JAK/STAT activation and production of Turandot proteins ((Srinivasan *et al.* 2016; Gordon *et al.* 2018). Finally, another recent study demonstrated that pinching larvae with forceps induces a humoral immune response, more precisely the upregulation of *Drosomycin* in the fat body (Kenmoku *et al.* 2017). Altogether, these studies have demonstrated an activation of innate immune signaling pathways in the absence of microorganisms. However, proper identification of a causative agent (a DAMP) binding to a specific receptor (membrane-bound or cytosolic) remains elusive. To date, there has been no molecular demonstration confirming the existence of a sterile inflammation mechanism in *Drosophila* immunity.

As sterile inflammation responses have been linked to severe immunopathologies in mammals, it is crucial to better understand how they are induced and orchestrated. Although the list of identified DAMPs and their respective receptors remains elusive, specifically in *Drosophila*, this research domain shows great future potential. Gaining comprehensive

understanding of the fundamental mechanisms driving and resulting from sterile inflammation could open prospects to novel therapeutic approaches and applications.

References

Agaisse H., and N. Perrimon, 2004 The roles of JAK/STAT signaling in Drosophila immune responses. Immunol Rev 198: 72–82. https://doi.org/10.1111/j.0105-2896.2004.0133.x

Arora S., and P. Ligoxygakis, 2020 Beyond Host Defense: Deregulation of Drosophila Immunity and Age-Dependent Neurodegeneration. Front. Immunol. 11. https://doi.org/10.3389/fimmu.2020.01574

Arthur J. S. C., and S. C. Ley, 2013 Mitogen-activated protein kinases in innate immunity. Nat Rev Immunol 13: 679–692. https://doi.org/10.1038/nri3495

Ayala A., M. F. Muñoz, and S. Argüelles, 2014 Lipid Peroxidation: Production, Metabolism, and Signaling Mechanisms of Malondialdehyde and 4-Hydroxy-2-Nonenal. Oxidative Medicine and Cellular Longevity 2014: e360438. https://doi.org/10.1155/2014/360438

Ayres J. S., N. Freitag, and D. S. Schneider, 2008 Identification of Drosophila Mutants Altering Defense of and Endurance to Listeria monocytogenes Infection. Genetics 178: 1807–1815. https://doi.org/10.1534/genetics.107.083782

Bach E. A., S. Vincent, M. P. Zeidler, and N. Perrimon, 2003 A sensitized genetic screen to identify novel regulators and components of the Drosophila janus kinase/signal transducer and activator of transcription pathway. Genetics 165: 1149–1166. https://doi.org/10.1093/genetics/165.3.1149

Basset A., R. S. Khush, A. Braun, L. Gardan, F. Boccard, *et al.*, 2000 The phytopathogenic bacteria Erwinia carotovora infects Drosophila and activates an immune response. PNAS 97: 3376–3381. https://doi.org/10.1073/pnas.97.7.3376

Benfield A. H., and S. T. Henriques, 2020 Mode-of-Action of Antimicrobial Peptides: Membrane Disruption vs. Intracellular Mechanisms. Frontiers in Medical Technology 2.

Benguettat O., R. Jneid, J. Soltys, R. Loudhaief, A. Brun-Barale, *et al.*, 2018 The DH31/CGRP enteroendocrine peptide triggers intestinal contractions favoring the elimination of opportunistic bacteria. PLoS Pathog 14: e1007279. https://doi.org/10.1371/journal.ppat.1007279

Bergmann A., D. Stein, R. Geisler, S. Hagenmaier, B. Schmid, *et al.*, 1996 A gradient of cytoplasmic Cactus degradation establishes the nuclear localization gradient of the

dorsal morphogen in Drosophila. Mechanisms of Development 60: 109–123. https://doi.org/10.1016/S0925-4773(96)00607-7

Binggeli O., C. Neyen, M. Poidevin, and B. Lemaitre, 2014 Prophenoloxidase Activation Is Required for Survival to Microbial Infections in Drosophila. PLOS Pathogens 10: e1004067. https://doi.org/10.1371/journal.ppat.1004067

Bolhassani A., and E. Agi, 2019 Heat shock proteins in infection. Clin Chim Acta 498: 90–100. https://doi.org/10.1016/j.cca.2019.08.015

Borch Jensen M., Y. Qi, R. Riley, L. Rabkina, and H. Jasper, 2017 PGAM5 promotes lasting FoxO activation after developmental mitochondrial stress and extends lifespan in Drosophila, (U. Banerjee, Ed.). eLife 6: e26952. https://doi.org/10.7554/eLife.26952

Böröczky K., A. Wada-Katsumata, D. Batchelor, M. Zhukovskaya, and C. Schal, 2013 Insects groom their antennae to enhance olfactory acuity. Proceedings of the National Academy of Sciences 110: 3615–3620. https://doi.org/10.1073/pnas.1212466110

Buchon N., N. A. Broderick, M. Poidevin, S. Pradervand, and B. Lemaitre, 2009 Drosophila Intestinal Response to Bacterial Infection: Activation of Host Defense and Stem Cell Proliferation. Cell Host & Microbe 5: 200–211. https://doi.org/10.1016/j.chom.2009.01.003

Buchon N., N. Silverman, and S. Cherry, 2014 Immunity in Drosophila melanogaster--from microbial recognition to whole-organism physiology. Nat Rev Immunol 14: 796–810. https://doi.org/10.1038/nri3763

Cai H., C. Meignin, and J.-L. Imler, 2022 cGAS-like receptor-mediated immunity: the insect perspective. Current Opinion in Immunology 74: 183–189. https://doi.org/10.1016/j.coi.2022.01.005

Caldwell R. M., J. F. Schafer, L. E. Compton, and F. L. Patterson, 1958 Tolerance to Cereal Leaf Rusts. Science 128: 714–715. https://doi.org/10.1126/science.128.3326.714

Cao Y., N. Ohwatari, T. Matsumoto, M. Kosaka, A. Ohtsuru, *et al.*, 1999 TGF-β1 mediates 70-kDa heat shock protein induction due to ultraviolet irradiation in human skin fibroblasts. Pflügers Arch 438: 239–244. https://doi.org/10.1007/s004240050905

Capo F., A. Wilson, and F. Di Cara, 2019 The Intestine of Drosophila melanogaster: An Emerging Versatile Model System to Study Intestinal Epithelial Homeostasis and Host-Microbial Interactions in Humans. Microorganisms 7: 336. https://doi.org/10.3390/microorganisms7090336

Carboni A. L., M. A. Hanson, S. A. Lindsay, S. A. Wasserman, and B. Lemaitre, 2022 Cecropins contribute to Drosophila host defense against a subset of fungal and Gram-negative bacterial infection. Genetics 220: iyab188. https://doi.org/10.1093/genetics/iyab188

Carton Y., M. Poirié, and A. J. Nappi, 2008 Insect immune resistance to parasitoids. Insect Science 15: 67–87. https://doi.org/10.1111/j.1744-7917.2008.00188.x

Castillo J. C., U. Shokal, and I. Eleftherianos, 2013 Immune gene transcription in Drosophila adult flies infected by entomopathogenic nematodes and their mutualistic bacteria. J Insect Physiol 59: 179–185. https://doi.org/10.1016/j.jinsphys.2012.08.003

Chen G. Y., and G. Nuñez, 2010 Sterile inflammation: sensing and reacting to damage. Nat Rev Immunol 10: 826–837. https://doi.org/10.1038/nri2873

Chihara C. J., D. J. Silvert, and J. W. Fristrom, 1982 The cuticle proteins of Drosophila melanogaster: Stage specificity. Developmental Biology 89: 379–388. https://doi.org/10.1016/0012-1606(82)90326-8

Chung Y.-S. A., and C. Kocks, 2011 Recognition of Pathogenic Microbes by the Drosophila Phagocytic Pattern Recognition Receptor Eater*. Journal of Biological Chemistry 286: 26524–26532. https://doi.org/10.1074/jbc.M110.214007

Clemmons A. W., S. A. Lindsay, and S. A. Wasserman, 2015 An effector Peptide family required for Drosophila toll-mediated immunity. PLoS Pathog 11: e1004876. https://doi.org/10.1371/journal.ppat.1004876

Cohen L. B., S. A. Lindsay, Y. Xu, S. J. H. Lin, and S. A. Wasserman, 2020 The Daisho Peptides Mediate Drosophila Defense Against a Subset of Filamentous Fungi. Front. Immunol. 11. https://doi.org/10.3389/fimmu.2020.00009

Croker B., K. Crozat, M. Berger, Y. Xia, S. Sovath, *et al.*, 2007 ATP-sensitive potassium channels mediate survival during infection in mammals and insects. Nat Genet 39: 1453–1460. https://doi.org/10.1038/ng.2007.25

D'Autréaux B., and M. B. Toledano, 2007 ROS as signalling molecules: mechanisms that generate specificity in ROS homeostasis. Nat Rev Mol Cell Biol 8: 813–824. https://doi.org/10.1038/nrm2256

Davis R. J., 2000 Signal Transduction by the JNK Group of MAP Kinases. Cell 103: 239–252. https://doi.org/10.1016/S0092-8674(00)00116-1

Davis M. M., and Y. Engström, 2012 Immune Response in the Barrier Epithelia: Lessons from the Fruit Fly Drosophila melanogaster. J Innate Immun 4: 273–283. https://doi.org/10.1159/000332947

De Gregorio E., P. T. Spellman, P. Tzou, G. M. Rubin, and B. Lemaitre, 2002 The Toll and Imd pathways are the major regulators of the immune response in Drosophila. The EMBO Journal 21: 2568–2579. https://doi.org/10.1093/emboj/21.11.2568

Decout A., J. D. Katz, S. Venkatraman, and A. Ablasser, 2021 The cGAS–STING pathway as a therapeutic target in inflammatory diseases. Nat Rev Immunol 21: 548–569. https://doi.org/10.1038/s41577-021-00524-z

Delaney J. R., S. Stöven, H. Uvell, K. V. Anderson, Y. Engström, *et al.*, 2006 Cooperative control of Drosophila immune responses by the JNK and NF-κB signaling pathways. The EMBO Journal 25: 3068–3077. https://doi.org/10.1038/sj.emboj.7601182

Dionne M. S., L. N. Pham, M. Shirasu-Hiza, and D. S. Schneider, 2006 Akt and FOXO dysregulation contribute to infection-induced wasting in Drosophila. Curr Biol 16: 1977–1985. https://doi.org/10.1016/j.cub.2006.08.052

Dostert C., E. Jouanguy, P. Irving, L. Troxler, D. Galiana-Arnoux, *et al.*, 2005 The Jak-STAT signaling pathway is required but not sufficient for the antiviral response of drosophila. Nat Immunol 6: 946–953. https://doi.org/10.1038/ni1237

Dudzic J. P., M. A. Hanson, I. Iatsenko, S. Kondo, and B. Lemaitre, 2019 More Than Black or White: Melanization and Toll Share Regulatory Serine Proteases in Drosophila. Cell Reports 27: 1050-1061.e3. https://doi.org/10.1016/j.celrep.2019.03.101

Duprez L., N. Takahashi, F. Van Hauwermeiren, B. Vandendriessche, V. Goossens, *et al.*, 2011 RIP Kinase-Dependent Necrosis Drives Lethal Systemic Inflammatory Response Syndrome. Immunity 35: 908–918. https://doi.org/10.1016/j.immuni.2011.09.020

Ekengren S., and D. Hultmark, 2001 A Family of Turandot-Related Genes in the Humoral Stress Response of Drosophila. Biochemical and Biophysical Research Communications 284: 998–1003. https://doi.org/10.1006/bbrc.2001.5067

Elrod-Erickson M., S. Mishra, and D. Schneider, 2000 Interactions between the cellular and humoral immune responses in Drosophila. Curr Biol 10: 781–784. https://doi.org/10.1016/s0960-9822(00)00569-8

Ferrandon D., A. c. Jung, M.-C. Criqui, B. Lemaitre, S. Uttenweiler-Joseph, *et al.*, 1998 A drosomycin–GFP reporter transgene reveals a local immune response in Drosophila that is not dependent on the Toll pathway. The EMBO Journal 17: 1217–1227. https://doi.org/10.1093/emboj/17.5.1217

Foley E., and P. H. O'Farrell, 2003 Nitric oxide contributes to induction of innate immune responses to gram-negative bacteria in Drosophila. Genes Dev 17: 115–125. https://doi.org/10.1101/gad.1018503

Garland T., 2014 Trade-offs. Curr Biol 24: R60–R61. https://doi.org/10.1016/j.cub.2013.11.036

Gendrin M., A. Zaidman-Rémy, N. A. Broderick, J. Paredes, M. Poidevin, *et al.*, 2013 Functional Analysis of PGRP-LA in Drosophila Immunity. PLOS ONE 8: e69742. https://doi.org/10.1371/journal.pone.0069742

Georgel P., S. Naitza, C. Kappler, D. Ferrandon, D. Zachary, *et al.*, 2001 Drosophila Immune Deficiency (IMD) Is a Death Domain Protein that Activates Antibacterial Defense and Can Promote Apoptosis. Developmental Cell 1: 503–514. https://doi.org/10.1016/S1534-5807(01)00059-4

Ghabrial A., S. Luschnig, M. M. Metzstein, and M. A. Krasnow, 2003 Branching morphogenesis of the Drosophila tracheal system. Annu Rev Cell Dev Biol 19: 623–647. https://doi.org/10.1146/annurev.cellbio.19.031403.160043

Gobert V., M. Gottar, A. A. Matskevich, S. Rutschmann, J. Royet, *et al.*, 2003 Dual Activation of the Drosophila Toll Pathway by Two Pattern Recognition Receptors. Science 302: 2126–2130. https://doi.org/10.1126/science.1085432

Gold K. S., and K. Brückner, 2015 Macrophages and cellular immunity in Drosophila melanogaster. Seminars in Immunology 27: 357–368. https://doi.org/10.1016/j.smim.2016.03.010

Gordon O., C. M. Henry, N. Srinivasan, S. Ahrens, A. Franz, *et al.*, 2018 α-actinin accounts for the bioactivity of actin preparations in inducing STAT target genes in Drosophila melanogaster, (B. Lemaître, T. Taniguchi, and B. Lemaître, Eds.). eLife 7: e38636. https://doi.org/10.7554/eLife.38636

Gottar M., V. Gobert, T. Michel, M. Belvin, G. Duyk, *et al.*, 2002 The Drosophila immune response against Gram-negative bacteria is mediated by a peptidoglycan recognition protein. Nature 416: 640–644. https://doi.org/10.1038/nature734

Gottar M., V. Gobert, A. A. Matskevich, J.-M. Reichhart, C. Wang, *et al.*, 2006 Dual detection of fungal infections in Drosophila via recognition of glucans and sensing of virulence factors. Cell 127: 1425–1437. https://doi.org/10.1016/j.cell.2006.10.046

Ha E.-M., C.-T. Oh, Y. S. Bae, and W.-J. Lee, 2005 A direct role for dual oxidase in Drosophila gut immunity. Science 310: 847–850. https://doi.org/10.1126/science.1117311

Hanson M. A., A. Dostálová, C. Ceroni, M. Poidevin, S. Kondo, *et al.*, 2019 Synergy and remarkable specificity of antimicrobial peptides in vivo using a systematic knockout approach. eLife 8. https://doi.org/10.7554/eLife.44341

Hanson M. A., and B. Lemaitre, 2020 New insights on Drosophila antimicrobial peptide function in host defense and beyond. Current Opinion in Immunology 62: 22–30. https://doi.org/10.1016/j.coi.2019.11.008

Hanson M. A., L. B. Cohen, A. Marra, I. Iatsenko, S. A. Wasserman, *et al.*, 2021 The Drosophila Baramicin polypeptide gene protects against fungal infection. PLOS Pathogens 17: e1009846. https://doi.org/10.1371/journal.ppat.1009846

Hauling T., R. Krautz, R. Markus, A. Volkenhoff, L. Kucerova, *et al.*, 2014 A Drosophila immune response against Ras-induced overgrowth. Biology Open 3: 250–260. https://doi.org/10.1242/bio.20146494

Hecht P. M., and K. V. Anderson, 1993 Genetic characterization of tube and pelle, genes required for signaling between Toll and dorsal in the specification of the dorsal-ventral pattern of the Drosophila embryo. Genetics 135: 405–417. https://doi.org/10.1093/genetics/135.2.405

Hedengren M., BengtÅsling, M. S. Dushay, I. Ando, S. Ekengren, *et al.*, 1999 Relish, a Central Factor in the Control of Humoral but Not Cellular Immunity in Drosophila. Molecular Cell 4: 827–837. https://doi.org/10.1016/S1097-2765(00)80392-5

Holleufer A., K. G. Winther, H. H. Gad, X. Ai, Y. Chen, *et al.*, 2021 Two cGAS-like receptors induce antiviral immunity in Drosophila. Nature 597: 114–118. https://doi.org/10.1038/s41586-021-03800-z

Hultmark D., H. Steiner, T. Rasmuson, and H. G. Boman, 1980 Insect Immunity. Purification and Properties of Three Inducible Bactericidal Proteins from Hemolymph of Immunized Pupae of Hyalophora cecropia. European Journal of Biochemistry 106: 7–16. https://doi.org/10.1111/j.1432-1033.1980.tb05991.x

Iatsenko I., J.-P. Boquete, and B. Lemaitre, 2018 Microbiota-Derived Lactate Activates Production of Reactive Oxygen Species by the Intestinal NADPH Oxidase Nox and Shortens Drosophila Lifespan. Immunity 49: 929-942.e5. https://doi.org/10.1016/j.immuni.2018.09.017

Iatsenko I., A. Marra, J.-P. Boquete, J. Peña, and B. Lemaitre, 2020 Iron sequestration by transferrin 1 mediates nutritional immunity in Drosophila melanogaster. Proceedings of the National Academy of Sciences 117: 7317–7325. https://doi.org/10.1073/pnas.1914830117

Imler J.-L., and P. Bulet, 2005 Antimicrobial Peptides in Drosophila: Structures,Activities and Gene Regulation. Mechanisms of Epithelial Defense 86: 1–21. https://doi.org/10.1159/000086648

Ip Y. T., M. Reach, Y. Engstrom, L. Kadalayil, H. Cai, *et al.*, 1993 Dif, a dorsal-related gene that mediates an immune response in Drosophila. Cell 75: 753–763. https://doi.org/10.1016/0092-8674(93)90495-C

Ishikawa H., and G. N. Barber, 2008 STING is an endoplasmic reticulum adaptor that facilitates innate immune signalling. Nature 455: 674–678. https://doi.org/10.1038/nature07317

Janeway C. A., and R. Medzhitov, 2002 Innate immune recognition. Annu Rev Immunol 20: 197–216. https://doi.org/10.1146/annurev.immunol.20.083001.084359

Jang I.-H., N. Chosa, S.-H. Kim, H.-J. Nam, B. Lemaitre, *et al.*, 2006 A Spätzle-Processing Enzyme Required for Toll Signaling Activation in Drosophila Innate Immunity. Developmental Cell 10: 45–55. https://doi.org/10.1016/j.devcel.2005.11.013

Johansson M. E. V., D. Ambort, T. Pelaseyed, A. Schütte, J. K. Gustafsson, *et al.*, 2011 Composition and functional role of the mucus layers in the intestine. Cell Mol Life Sci 68: 3635–3641. https://doi.org/10.1007/s00018-011-0822-3

Jones R. M., L. Luo, C. S. Ardita, A. N. Richardson, Y. M. Kwon, *et al.*, 2013 Symbiotic lactobacilli stimulate gut epithelial proliferation via Nox-mediated generation of reactive oxygen species. The EMBO Journal 32: 3017–3028. https://doi.org/10.1038/emboj.2013.224

Kallio J., A. Leinonen, J. Ulvila, S. Valanne, R. A. Ezekowitz, *et al.*, 2005 Functional analysis of immune response genes in Drosophila identifies JNK pathway as a regulator of antimicrobial peptide gene expression in S2 cells. Microbes Infect 7: 811–819. https://doi.org/10.1016/j.micinf.2005.03.014

Karpac J., A. Younger, and H. Jasper, 2011 Dynamic coordination of innate immune signaling and insulin signaling regulates systemic responses to localized DNA damage. Dev Cell 20: 841–854. https://doi.org/10.1016/j.devcel.2011.05.011

Kenmoku H., A. Hori, T. Kuraishi, and S. Kurata, 2017 A novel mode of induction of the humoral innate immune response in Drosophila larvae. Disease Models & Mechanisms 10: 271–281. https://doi.org/10.1242/dmm.027102

Kobler J. M., F. J. Rodriguez Jimenez, I. Petcu, and I. C. Grunwald Kadow, 2020 Immune Receptor Signaling and the Mushroom Body Mediate Post-ingestion Pathogen Avoidance. Curr Biol 30: 4693-4709.e3. https://doi.org/10.1016/j.cub.2020.09.022

Kocks C., J. H. Cho, N. Nehme, J. Ulvila, A. M. Pearson, *et al.*, 2005 Eater, a Transmembrane Protein Mediating Phagocytosis of Bacterial Pathogens in Drosophila. Cell 123: 335–346. https://doi.org/10.1016/j.cell.2005.08.034

Kranzusch P. J., S. C. Wilson, A. S. Y. Lee, J. M. Berger, J. A. Doudna, *et al.*, 2015 Ancient Origin of cGAS-STING Reveals Mechanism of Universal 2',3' cGAMP Signaling. Mol Cell 59: 891–903. https://doi.org/10.1016/j.molcel.2015.07.022

Lambeth J. D., and A. S. Neish, 2014 Nox enzymes and new thinking on reactive oxygen: a double-edged sword revisited. Annu Rev Pathol 9: 119–145. https://doi.org/10.1146/annurev-pathol-012513-104651

Lanot R., D. Zachary, F. Holder, and M. Meister, 2001 Postembryonic hematopoiesis in Drosophila. Dev Biol 230: 243–257. https://doi.org/10.1006/dbio.2000.0123

Lee K.-S., K. Iijima-Ando, K. Iijima, W.-J. Lee, J. H. Lee, *et al.*, 2009 JNK/FOXO-mediated neuronal expression of fly homologue of peroxiredoxin II reduces oxidative stress and extends life span. J Biol Chem 284: 29454–29461. https://doi.org/10.1074/jbc.M109.028027

Lemaitre B., E. Nicolas, L. Michaut, J.-M. Reichhart, and J. A. Hoffmann, 1996 The Dorsoventral Regulatory Gene Cassette spätzle/Toll/cactus Controls the Potent Antifungal Response in Drosophila Adults. Cell 86: 973–983. https://doi.org/10.1016/S0092-8674(00)80172-5

Lemaitre B., and J. Hoffmann, 2007 The Host Defense of Drosophila melanogaster. Annual Review of Immunology 25: 697–743. https://doi.org/10.1146/annurev.immunol.25.022106.141615

Leulier F., A. Rodriguez, R. S. Khush, J. M. Abrams, and B. Lemaitre, 2000 The Drosophila caspase Dredd is required to resist Gram-negative bacterial infection. EMBO reports 1: 353–358. https://doi.org/10.1093/embo-reports/kvd073

Li X., S. Rommelaere, S. Kondo, and B. Lemaitre, 2020 Renal Purge of Hemolymphatic Lipids Prevents the Accumulation of ROS-Induced Inflammatory Oxidized Lipids and Protects Drosophila from Tissue Damage. Immunity 52: 374-387.e6. https://doi.org/10.1016/j.immuni.2020.01.008

Ligoxygakis P., N. Pelte, J. A. Hoffmann, and J.-M. Reichhart, 2002 Activation of Drosophila Toll During Fungal Infection by a Blood Serine Protease. Science 297: 114–116. https://doi.org/10.1126/science.1072391

Liu F., G. Baggerman, W. D'Hertog, P. Verleyen, L. Schoofs, *et al.*, 2006 In Silico Identification of New Secretory Peptide Genes in Drosophila melanogaster*. Molecular & Cellular Proteomics 5: 510–522. https://doi.org/10.1074/mcp.M400114-MCP200

Liu Y., B. Gordesky-Gold, M. Leney-Greene, N. L. Weinbren, M. Tudor, *et al.*, 2018 Inflammation-Induced, STING-Dependent Autophagy Restricts Zika Virus Infection in

the Drosophila Brain. Cell Host Microbe 24: 57-68.e3. https://doi.org/10.1016/j.chom.2018.05.022

Lopes E. S. S., and H. M. Araujo, 2004 The maternal JAK/STAT pathway of Drosophila regulates embryonic dorsal-ventral patterning. Braz J Med Biol Res 37: 1811–1818. https://doi.org/10.1590/s0100-879x2004001200006

Martin M., A. Hiroyasu, R. M. Guzman, S. A. Roberts, and A. G. Goodman, 2018 Analysis of Drosophila STING Reveals an Evolutionarily Conserved Antimicrobial Function. Cell Reports 23: 3537-3550.e6. https://doi.org/10.1016/j.celrep.2018.05.029

Martins R., A. R. Carlos, F. Braza, J. A. Thompson, P. Bastos-Amador, *et al.*, 2019 Disease Tolerance as an Inherent Component of Immunity. Annual Review of Immunology 37: 405–437. https://doi.org/10.1146/annurev-immunol-042718-041739

Masuzzo A., G. Manière, Y. Grosjean, L. Kurz, and J. Royet, 2022 Bacteria-Derived Peptidoglycan Triggers a Noncanonical Nuclear Factor-κB-Dependent Response in Drosophila Gustatory Neurons. J Neurosci 42: 7809–7823. https://doi.org/10.1523/JNEUROSCI.2437-21.2022

Matz J. M., M. J. Blake, H. M. Tatelman, K. P. Lavoi, and N. J. Holbrook, 1995 Characterization and regulation of cold-induced heat shock protein expression in mouse brown adipose tissue. American Journal of Physiology-Regulatory, Integrative and Comparative Physiology 269: R38–R47. https://doi.org/10.1152/ajpregu.1995.269.1.R38

McCarville J., and J. Ayres, 2018 Disease tolerance: concept and mechanisms. Curr Opin Immunol 50: 88–93. https://doi.org/10.1016/j.coi.2017.12.003

Meister M., and M. Lagueux, 2003 Drosophila blood cells. Cellular Microbiology 5: 573–580. https://doi.org/10.1046/j.1462-5822.2003.00302.x

Melcarne C., E. Ramond, J. Dudzic, A. J. Bretscher, É. Kurucz, *et al.*, 2019a Two Nimrod receptors, NimC1 and Eater, synergistically contribute to bacterial phagocytosis in Drosophila melanogaster. The FEBS Journal 286: 2670–2691. https://doi.org/10.1111/febs.14857

Melcarne C., B. Lemaitre, and E. Kurant, 2019b Phagocytosis in Drosophila: From molecules and cellular machinery to physiology. Insect Biochem Mol Biol 109: 1–12. https://doi.org/10.1016/j.ibmb.2019.04.002

Ming M., F. Obata, E. Kuranaga, and M. Miura, 2014 Persephone/Spätzle Pathogen Sensors Mediate the Activation of Toll Receptor Signaling in Response to Endogenous Danger Signals in Apoptosis-deficient Drosophila*. Journal of Biological Chemistry 289: 7558–7568. https://doi.org/10.1074/jbc.M113.543884

Mishima Y., J. Quintin, V. Aimanianda, C. Kellenberger, F. Coste, *et al.*, 2009 The N-terminal Domain of Drosophila Gram-negative Binding Protein 3 (GNBP3) Defines a Novel Family of Fungal Pattern Recognition Receptors*. Journal of Biological Chemistry 284: 28687–28697. https://doi.org/10.1074/jbc.M109.034587

Morehouse B. R., A. A. Govande, A. Millman, A. F. A. Keszei, B. Lowey, *et al.*, 2020 STING cyclic dinucleotide sensing originated in bacteria. Nature 586: 429–433. https://doi.org/10.1038/s41586-020-2719-5

Morisato D., and K. V. Anderson, 1994 The spätzle gene encodes a component of the extracellular signaling pathway establishing the dorsal-ventral pattern of the Drosophila embryo. Cell 76: 677–688. https://doi.org/10.1016/0092-8674(94)90507-X

Mukae N., H. Yokoyama, T. Yokokura, Y. Sakoyama, and S. Nagata, 2002 Activation of the innate immunity in Drosophila by endogenous chromosomal DNA that escaped apoptotic degradation. Genes Dev 16: 2662–2671. https://doi.org/10.1101/gad.1022802

Myllymäki H., and M. Rämet, 2014 JAK/STAT Pathway in Drosophila Immunity. Scandinavian Journal of Immunology 79: 377–385. https://doi.org/10.1111/sji.12170

Naitza S., C. Rossé, C. Kappler, P. Georgel, M. Belvin, *et al.*, 2002 The Drosophila Immune Defense against Gram-Negative Infection Requires the Death Protein dFADD. Immunity 17: 575–581. https://doi.org/10.1016/S1074-7613(02)00454-5

Nappi A., M. Poirié, and Y. Carton, 2009 The role of melanization and cytotoxic by-products in the cellular immune responses of Drosophila against parasitic wasps. Adv Parasitol 70: 99–121. https://doi.org/10.1016/S0065-308X(09)70004-1

Parisi F., R. K. Stefanatos, K. Strathdee, Y. Yu, and M. Vidal, 2014 Transformed Epithelia Trigger Non-Tissue-Autonomous Tumor Suppressor Response by Adipocytes via Activation of Toll and Eiger/TNF Signaling. Cell Reports 6: 855–867. https://doi.org/10.1016/j.celrep.2014.01.039

Park J. M., H. Brady, M. G. Ruocco, H. Sun, D. Williams, *et al.*, 2004 Targeting of TAK1 by the NF-κB protein Relish regulates the JNK-mediated immune response in Drosophila. Genes Dev. 18: 584–594. https://doi.org/10.1101/gad.1168104

Park Y.-J., S. Kim, H.-P. Shim, J. H. Park, G. Lee, *et al.*, 2021 Phosphatidylserine synthase plays an essential role in glia and affects development, as well as the maintenance of neuronal function. iScience 24: 102899. https://doi.org/10.1016/j.isci.2021.102899

Parvy J.-P., Y. Yu, A. Dostalova, S. Kondo, A. Kurjan, *et al.*, 2019 The antimicrobial peptide defensin cooperates with tumour necrosis factor to drive tumour cell death in Drosophila. eLife 8. https://doi.org/10.7554/eLife.45061

Petrignani B., S. Rommelaere, K. Hakim-Mishnaevski, F. Masson, E. Ramond, *et al.*, 2021 A secreted factor NimrodB4 promotes the elimination of apoptotic corpses by phagocytes in Drosophila. EMBO reports 22: e52262. https://doi.org/10.15252/embr.202052262

Pili-Floury S., F. Leulier, K. Takahashi, K. Saigo, E. Samain, *et al.*, 2004 In vivo RNA interference analysis reveals an unexpected role for GNBP1 in the defense against Gram-positive bacterial infection in Drosophila adults. J Biol Chem 279: 12848–12853. https://doi.org/10.1074/jbc.M313324200

Råberg L., D. Sim, and A. F. Read, 2007 Disentangling Genetic Variation for Resistance and Tolerance to Infectious Diseases in Animals. Science 318: 812–814. https://doi.org/10.1126/science.1148526

Radyuk S. N., K. Michalak, V. I. Klichko, J. Benes, I. Rebrin, *et al.*, 2009 Peroxiredoxin 5 confers protection against oxidative stress and apoptosis and also promotes longevity in Drosophila. Biochem J 419: 437–445. https://doi.org/10.1042/BJ20082003

Raheem N., and S. K. Straus, 2019 Mechanisms of Action for Antimicrobial Peptides With Antibacterial and Antibiofilm Functions. Frontiers in Microbiology 10.

Ramond E., B. Petrignani, J. P. Dudzic, J.-P. Boquete, M. Poidevin, *et al.*, 2020 The adipokine NimrodB5 regulates peripheral hematopoiesis in Drosophila. The FEBS Journal 287: 3399–3426. https://doi.org/10.1111/febs.15237

Ritossa F., 1962 A new puffing pattern induced by temperature shock and DNP in drosophila. Experientia 18: 571–573. https://doi.org/10.1007/BF02172188

Ritossa F., 1996 Discovery of the heat shock response. Cell Stress Chaperones 1: 97–98. https://doi.org/10.1379/1466-1268(1996)001<0097:dothsr>2.3.co;2

Rodrigue-Gervais I. G., K. Labbé, M. Dagenais, J. Dupaul-Chicoine, C. Champagne, *et al.*, 2014 Cellular Inhibitor of Apoptosis Protein cIAP2 Protects against Pulmonary Tissue Necrosis during Influenza Virus Infection to Promote Host Survival. Cell Host & Microbe 15: 23–35. https://doi.org/10.1016/j.chom.2013.12.003

Ross J., H. Jiang, M. R. Kanost, and Y. Wang, 2003 Serine proteases and their homologs in the Drosophila melanogaster genome: an initial analysis of sequence conservation and phylogenetic relationships. Gene 304: 117–131. https://doi.org/10.1016/s0378-1119(02)01187-3

Russo J., S. Dupas, F. Frey, Y. Carton, and M. Brehelin, 1996 Insect immunity: early events in the encapsulation process of parasitoid (Leptopilina boulardi) eggs in resistant and susceptible strains of Drosophila. Parasitology 112 (Pt 1): 135–142. https://doi.org/10.1017/s0031182000065173

Sabin L. R., S. L. Hanna, and S. Cherry, 2010 Innate antiviral immunity in Drosophila. Curr Opin Immunol 22: 4–9. https://doi.org/10.1016/j.coi.2010.01.007

Satyavathi V. V., A. Minz, and J. Nagaraju, 2014 Nodulation: An unexplored cellular defense mechanism in insects. Cellular Signalling 26: 1753–1763. https://doi.org/10.1016/j.cellsig.2014.02.024

Seixas E., R. Gozzelino, Â. Chora, A. Ferreira, G. Silva, *et al.*, 2009 Heme oxygenase-1 affords protection against noncerebral forms of severe malaria. Proceedings of the National Academy of Sciences 106: 15837–15842. https://doi.org/10.1073/pnas.0903419106

Seo M.-D., H.-S. Won, J.-H. Kim, T. Mishig-Ochir, and B.-J. Lee, 2012 Antimicrobial Peptides for Therapeutic Applications: A Review. Molecules 17: 12276–12286. https://doi.org/10.3390/molecules171012276

Seong C.-S., A. Varela-Ramirez, and R. J. Aguilera, 2006 DNase II deficiency impairs innate immune function in Drosophila. Cellular Immunology 240: 5–13. https://doi.org/10.1016/j.cellimm.2006.05.007

Seong C.-S., A. Varela-Ramirez, X. Tang, B. Anchondo, D. Magallanes, *et al.*, 2014 Cloning and Characterization of a Novel Drosophila Stress Induced DNase. PLOS ONE 9: e103564. https://doi.org/10.1371/journal.pone.0103564

Shaukat Z., D. Liu, and S. Gregory, 2015 Sterile Inflammation in Drosophila. Mediators Inflamm 2015. https://doi.org/10.1155/2015/369286

Sheldon I. M., Paula. C. C. Molinari, Thomas. J. R. Ormsby, and John. J. Bromfield, 2020 Preventing postpartum uterine disease in dairy cattle depends on avoiding, tolerating and resisting pathogenic bacteria. Theriogenology 150: 158–165. https://doi.org/10.1016/j.theriogenology.2020.01.017

Shen H.-M., and Z. Liu, 2006 JNK signaling pathway is a key modulator in cell death mediated by reactive oxygen and nitrogen species. Free Radical Biology and Medicine 40: 928–939. https://doi.org/10.1016/j.freeradbiomed.2005.10.056

Silverman G. A., P. I. Bird, R. W. Carrell, F. C. Church, P. B. Coughlin, *et al.*, 2001 The serpins are an expanding superfamily of structurally similar but functionally diverse proteins. Evolution, mechanism of inhibition, novel functions, and a revised nomenclature. J Biol Chem 276: 33293–33296. https://doi.org/10.1074/jbc.R100016200

Sims G. P., D. C. Rowe, S. T. Rietdijk, R. Herbst, and A. J. Coyle, 2010 HMGB1 and RAGE in inflammation and cancer. Annu Rev Immunol 28: 367–388. https://doi.org/10.1146/annurev.immunol.021908.132603

Slavik K. M., B. R. Morehouse, A. E. Ragucci, W. Zhou, X. Ai, *et al.*, 2021 cGAS-like receptors sense RNA and control 3'2'-cGAMP signalling in Drosophila. Nature 597: 109–113. https://doi.org/10.1038/s41586-021-03743-5

Soares M. P., L. Teixeira, and L. F. Moita, 2017 Disease tolerance and immunity in host protection against infection. Nat Rev Immunol 17: 83–96. https://doi.org/10.1038/nri.2016.136

Srinivasan N., O. Gordon, S. Ahrens, A. Franz, S. Deddouche, *et al.*, 2016 Actin is an evolutionarily-conserved damage-associated molecular pattern that signals tissue injury in Drosophila melanogaster, (Z. J. Chen, Ed.). eLife 5: e19662. https://doi.org/10.7554/eLife.19662

Steiner H., D. Hultmark, A. Engström, H. Bennich, and H. G. Boman, 1981 Sequence and specificity of two antibacterial proteins involved in insect immunity. Nature 292: 246–248. https://doi.org/10.1038/292246a0

Steiner H., D. Andreu, and R. B. Merrifield, 1988 Binding and action of cecropin and cecropin analogues: Antibacterial peptides from insects. Biochimica et Biophysica Acta (BBA) - Biomembranes 939: 260–266. https://doi.org/10.1016/0005-2736(88)90069-7

Sun L., J. Wu, F. Du, X. Chen, and Z. J. Chen, 2013 Cyclic GMP-AMP Synthase Is a Cytosolic DNA Sensor That Activates the Type I Interferon Pathway. Science 339: 786–791. https://doi.org/10.1126/science.1232458

Szebenyi A. L., 1969 Cleaning behaviour in Drosophila melanogaster. Animal Behaviour 17: 641–651. https://doi.org/10.1016/S0003-3472(69)80006-0

Takeuchi O., and S. Akira, 2010 Pattern Recognition Receptors and Inflammation. Cell 140: 805–820. https://doi.org/10.1016/j.cell.2010.01.022

Tauszig-Delamasure S., H. Bilak, M. Capovilla, J. A. Hoffmann, and J.-L. Imler, 2002 Drosophila MyD88 is required for the response to fungal and Gram-positive bacterial infections. Nat Immunol 3: 91–97. https://doi.org/10.1038/ni747

Teixeira L., Á. Ferreira, and M. Ashburner, 2008 The Bacterial Symbiont Wolbachia Induces Resistance to RNA Viral Infections in Drosophila melanogaster. PLOS Biology 6: e1000002. https://doi.org/10.1371/journal.pbio.1000002

Tzou P., S. Ohresser, D. Ferrandon, M. Capovilla, J.-M. Reichhart, *et al.*, 2000 Tissue-Specific Inducible Expression of Antimicrobial Peptide Genes in Drosophila Surface Epithelia. Immunity 13: 737–748. https://doi.org/10.1016/S1074-7613(00)00072-8

Uttenweiler-Joseph S., M. Moniatte, M. Lagueux, A. V. Dorsselaer, J. A. Hoffmann, *et al.*, 1998 Differential display of peptides induced during the immune response of Drosophila: A matrix-assisted laser desorption ionization time-of-flight mass spectrometry study. PNAS 95: 11342–11347. https://doi.org/10.1073/pnas.95.19.11342

Veillard F., L. Troxler, and J.-M. Reichhart, 2016 Drosophila melanogaster clip-domain serine proteases: Structure, function and regulation. Biochimie 122: 255–269. https://doi.org/10.1016/j.biochi.2015.10.007

Vlisidou I., and W. Wood, 2015 Drosophila blood cells and their role in immune responses. FEBS J 282: 1368–1382. https://doi.org/10.1111/febs.13235

Vodovar N., M. Vinals, P. Liehl, A. Basset, J. Degrouard, *et al.*, 2005 Drosophila host defense after oral infection by an entomopathogenic Pseudomonas species. Proceedings of the National Academy of Sciences 102: 11414–11419. https://doi.org/10.1073/pnas.0502240102

Wagner C., K. Isermann, H. Fehrenbach, and T. Roeder, 2008 Molecular architecture of the fruit fly's airway epithelial immune system. BMC Genomics 9: 446. https://doi.org/10.1186/1471-2164-9-446

Wang H., O. Bloom, M. Zhang, J. M. Vishnubhakat, M. Ombrellino, *et al.*, 1999 HMG-1 as a Late Mediator of Endotoxin Lethality in Mice. Science 285: 248–251. https://doi.org/10.1126/science.285.5425.248

Weston C. R., and R. J. Davis, 2002 The JNK signal transduction pathway. Current Opinion in Genetics & Development 12: 14–21. https://doi.org/10.1016/S0959-437X(01)00258-1

Yoshida H., Y. Okabe, K. Kawane, H. Fukuyama, and S. Nagata, 2005 Lethal anemia caused by interferon-beta produced in mouse embryos carrying undigested DNA. Nat Immunol 6: 49–56. https://doi.org/10.1038/ni1146

Zughaier S. M., and P. Cornelis, 2018 Editorial: Role of Iron in Bacterial Pathogenesis. Frontiers in Cellular and Infection Microbiology 8.

Curriculum vitae

Education

2021-today **Ph.D in Molecular Life Sciences**
Global Health Institute, Life Sciences, Ecole Polytechnique Fédérale de Lausanne

2017-2019 **Master ès Science in Medical Biology**, specialization "Immunology and Cancer"
Faculty of Biology and Medicine, University of Lausanne - *with the financial support from Hans Wilsdorf Foundation Scholarship*

2014-2017 **Bachelor ès Science in Biology**
Faculty of Biology and Medicine, University of Lausanne

2012-2014 **Bachelor in social and political sciences** (1st and 2nd year)
Faculty of social and political sciences, University of Lausanne

Research

2019-Today **Group of Prof. Bruno Lemaitre, Global Health Institute, EPFL, Lausanne, Switzerland**
"*Investigating the activation of Drosophila melanogaster innate immunity in response to different classes of immune elicitors (PAMPs, DAMPs and abiotic stressors)"*

2019 **Group of Prof. Liliane Michalik, Centre for Integrative Genomics, UNIL, Lausanne, Switzerland**
"Roles of PPAR isoforms in skin cancer progression in response to environmental cues »

2018-2019 **Group of Prof. Nathalie Rosenblatt-Velin, Department "Coeur-Vaisseaux", CHUV, Lausanne, Switzerland**
"Is the cardioprotective effect of LCZ696 linked to increased cardiac regeneration?"

2017-2018 **Group of Prof. Thierry Pedrazzini, Department "Coeur-Vaisseaux", CHUV, Lausanne, Switzerland**
"Promoting cardiomyocytes proliferation in vivo via targeting anti-proliferative long noncoding RNAs using modified antisense oligonucleotides »

Publications

Increasing heart vascularisation after myocardial infarction using brain natriuretic peptide stimulation of endothelial and WT1(+) epicardial cells
N. Li; S. Rignault-Clerc; C. Bielmann; A-C. Bon-Mathier; T. Deglise, **A. Carboni,** M. Ducrest, N. Rosenblatt-Velin , *Elife*. 2020-11-27. Vol. 9, p. e61050. DOI : 10.7554/eLife.61050.

Cecropins contribute to Drosophila host defense against a subset of fungal and Gram-negative bacterial infection
A.L. Carboni ; M. A. Hanson; S. A. Lindsay; S. A. Wasserman; B. Lemaitre, *Genetics*. 2022-01-01. Vol. 220, num. 1, p. iyab188. DOI : 10.1093/genetics/iyab188.

Conferences and Scientific Meetings

2019 European Drosophila Research Conference, **Lausanne, Suisse**

2021 Swiss Drosophila Meeting, **Zurich, Switzerland** – Poster presentation

2022 Annual Drosophila Research Conference, **San Diego and online, USA** – Oral presentation

2022 Phagocytosis of dying cells, Molecules, mechanisms, and therapeutic implications, **Ghent, Belgium** – Poster presentation

Teaching

2019-2022 Immunology (Prof. Lemaitre, **EPFL**)

2020 Biotechnology Lab (Prof. Pick, **EPFL**)

2021 Cellular biology and biochemistry for engineers (Prof. Zufferey, **EPFL**)

Mentoring

Lab immersion of 3rd year Bachelor's students in Life Sciences (**EPFL**): Agatha Hunter, Claire Damery

Language and Other Skills

French (mother tongue), English (C1), Spanish (B2), German (B1)

Basic programming in R, FIJI, QuPath, Geneious

Certificate

2017 2017 : LTK1 certificate – module1 animal experimentation

Leadership / Involvement

2016-2017 Presidency of the Association for students in biology (LAB), University of Lausanne

2017-2019 Student representative for the Master in Medical Biology, University of Lausanne

References

Bruno Lemaitre
EPFL-SV-GHI-UPLEM
Unit of Prof. Lemaitre
Station 19
CH – 1015 Lausanne (VD)
+4121 693 18 31
Bruno.lemaitre@epfl.ch

Roger Clerc
Prof Dr. em Roger G. Clerc PhD PD
University of Basel Biozentrum
Guest professor
c/o EPFL
Life Science Faculty EDOC EDBB EDMS
Room AAB019 Station 19
CH – 1015 Lausanne (VD)
roger.clerc@epfl.ch

Liliane Michalik
Quartier UNIL-Sorge
Bâtiment Génopode
Office : 5024
CH – 1015 Lausanne (VD)
+4121 692 41 47
Liliane.michalik@unil.ch